

May 2014

Hydrochemical Dynamics Under Differing Winter Climate Regimes at the Hubbard Brook Experiment Forest

Colin Fuss
Syracuse University

Follow this and additional works at: <https://surface.syr.edu/etd>



Part of the [Engineering Commons](#)

Recommended Citation

Fuss, Colin, "Hydrochemical Dynamics Under Differing Winter Climate Regimes at the Hubbard Brook Experiment Forest" (2014). *Dissertations - ALL*. 120.

<https://surface.syr.edu/etd/120>

This Dissertation is brought to you for free and open access by the SURFACE at SURFACE. It has been accepted for inclusion in Dissertations - ALL by an authorized administrator of SURFACE. For more information, please contact surface@syr.edu.

Abstract

This dissertation is a two-phase study of the hydrochemical dynamics of drainage waters at the Hubbard Brook Experimental Forest (HBEF) in New Hampshire, USA, that aims to improve understanding of changes in water quality associated with winter climate variation. The first phase was an analysis of the long-term stream and soil water chemistry dataset from Watershed 6, the biogeochemical reference watershed of the HBEF. The second phase was a series of field measurements designed to evaluate variation in the chemistry and hydrology of stream and soil water across a natural gradient of winter climate at the HBEF.

Thirty years (1982-2011) of stream and soil water chemistry data were analyzed to assess the trends of overall recovery from acidification, as well as trends associated with the snowmelt periods of the record, which are characterized by seasonal and episodic acidification of stream runoff. Trends varied by landscape position, but the analysis generally revealed slow increases in the pH and acid neutralizing capacity (ANC) in stream water that were associated with decreases in atmospheric deposition of acid anions, sulfate (SO_4^{2-}) and nitrate (NO_3^-). Trends during snowmelt were similar to the whole-year record, including ANC recovery. Nitrate concentrations in streamwater during snowmelt decreased more rapidly than the whole-year record. Dissolved organic carbon (DOC) concentrations have declined significantly in most forest floor soil waters, apparently driving a small overall decrease in streamwater DOC at the base of the watershed. The DOC concentration decreases in streamwater occurred primarily in the first 15 years of the record.

Soil water chemistry was monitored for two years (2011 and 2012) at a series of 20 plots across the Hubbard Brook valley located to capture variability in winter climate. Variables such as maximum soil frost depth and winter soil temperature variability were positively correlated

with increased leaching of DOC, but not NO_3^- , during the early growing season (May-July). The DOC mobilization was primarily observed in the soil waters draining the forest floor (Oa horizon), and less in the mineral soil (Bs horizon). No effect of winter soil conditions was noted during the late growing season.

Daily streamwater sampling during snowmelt was conducted in two south-facing catchments (Watershed 3 and Watershed 6) for three years (2010-2012), and in one north-facing catchment (Watershed 7) for two years (2011-2012). Streamwater concentrations of NO_3^- and DOC varied among the watersheds and among the years. Nitrate was flushed in high concentration early in snowmelt, prior to dilution. Nitrate was exported in highest concentrations from Watershed 7 during each year, presumably the result of higher microbial nitrogen mineralization and nitrification rates. The highest NO_3^- concentrations in each watershed occurred during snowmelt of 2012, following a winter with low snowpack and above average temperatures. DOC concentrations were largely determined by changes in hydrologic flow, increasing during snowmelt events. The DOC concentration varied among the watersheds and was highly correlated to the winter climate variables for each of the watersheds.

End-member mixing analysis (EMMA) revealed differences in hydrologic flowpaths related to the presence of soil frost. Flow through preferential flowpaths in the forest floor was reduced during days with extensive soil frost. Direct contribution of snow or precipitation water to stream flow water was not markedly increased during times when the soils were frozen, indicating that the soil frost was likely granular and soils retained permeability.

HYDROCHEMICAL DYNAMICS UNDER DIFFERING WINTER CLIMATE REGIMES AT
THE HUBBARD BROOK EXPERIMENTAL FOREST

by

COLIN B. FUSS

B.A., Cornell University, 2004

M.S., Syracuse University, 2009

DISSERTATION

Submitted in partial fulfillment of the requirements for the degree of

Doctor of Philosophy in Civil Engineering

Syracuse University

May 2014

Copyright © Colin B. Fuss 2014
All Rights Reserved

Acknowledgements

My dissertation is a contribution to the Hubbard Brook Ecosystem Study. Hubbard Brook is a National Science Foundation supported Long-Term Ecological Research site. My project was made possible by support from the National Science Foundation (Grants DEB 0949664 – Ecosystem Studies and DEB 1114804 – Long-Term Ecological Research). I am grateful for my financial support from the Syracuse University Fellowship and the Wen-Hsiung and Kuan-Ming Li Fellowship from the Department of Civil and Environmental Engineering.

My advisor, Dr. Charley Driscoll, deserves special thanks. His support, guidance, and commitment have really helped me as pursued my education and research. It has truly been a privilege to work with him. I would like to also give special thanks to the members of my dissertation committee: Dr. Chris Johnson, Dr. Dave Chandler, Dr. Laura Lautz, Dr. Mark Green, and Dr. Peter Groffman. Their insights and expertise have really helped me to expand and advance my work.

I worked with numerous people I have been happy to call colleagues and friends. Mario Montesdeoca, Ed Mason, Mary Margaret Koppers, Jordan Brinkley, and Mike Rice were of great help in running and operating the lab. Kim Driscoll provided me with statistical help that was of great benefit. Joe Denkenberger, Afshin Pourmokhtarian, Brad Blackwell, Jessica Ebert, Qingtao, Zhou, Habib Fakhraei, Svetla Todorova, Dimitar Todorov, Rouzbeh Berton, Sam Fashu Kanu, Amy Sauer, Isaac Allen, and Sam Werner were great people to work with. I am deeply indebted to Maureen Hale, Beth Buchanan, Heather Kirkpatrick, and Linda Lowe for many favors, large and small.

The community of at Hubbard Brook makes it a special place to work. I am especially thankful to our partners from the U.S. Forest Service who keep Hubbard Brook running. Ian

Halm, Nick Grant, and Amey Bailey were of tremendous help. I want to thank the many other researchers and support staff who were critical to my project: John Campbell, Tim Fahey, Pam Templer, Melany Fisk, Myron Mitchell, Lynn Christenson, Jorge Duran, Jen Morse, Don Buso, Tammy Wooster, Nat Cleavitt, and Errin Shoop.

Finally, I wish to give special thanks to my wonderful family. My wife Aude has been an incredible support for me and our son Hugo is the greatest inspiration I could imagine.

TABLE OF CONTENTS

Abstract	i
Acknowledgements.....	v
List of Tables	xii
List of Figures	xiv
1. Introduction	1
2. Literature Review	4
2.1. Acidic deposition in the northeastern United States	4
2.2. Episodic acidification.....	6
2.3. Trends in stream and soil water chemistry	7
2.4. Winter Climate Change.....	8
2.5. Relationship between snowpack depth and soil frost depth	10
2.6. Effects of soil freezing on biogeochemical cycling.....	10
2.7. Effects of soil freezing on hydrologic flow	12
3. Objectives and Hypotheses	14
4. Trends in recovery of stream and soil water chemistry from chronic and snowmelt episodic acidification	18
4.1. Methods.....	18
4.1.1. Site Description.....	18
4.1.2. Sampling and analysis.....	19
4.2. Results.....	21
4.2.1. Soil solution chemistry trends.....	21
4.2.2. Overall stream chemistry trends	22

4.2.3. Snowmelt streamwater chemistry trends	23
4.3. Discussion	23
4.3.1. Overall trends in soil solution and streamwater.....	23
4.3.2. Snowmelt stream chemistry trends	30
4.3.3. Future of recovery and ecosystem health.....	32
4.4. Summary and Conclusions	33
5. Leaching of nitrate and dissolved organic carbon in soil solutions across a natural gradient of winter climate and soil freezing	45
5.1. Methods.....	45
5.1.1. Plot selection and characterization.....	45
5.1.2. Lysimeter installation and sampling	45
5.1.3. Winter climate monitoring.....	46
5.1.4. Laboratory analysis	47
5.1.5. Computative methods and statistics.....	47
5.2. Results.....	48
5.2.1. Characterization of winter climate gradient.....	48
5.2.2. Soil solution NO ₃ ⁻ concentrations.....	48
5.2.3. Soil solution DOC concentrations	49
5.3. Discussion	50
5.3.1. DOC mobilization after soil freezing.....	50
5.3.2. Variable response of NO ₃ ⁻ to soil freezing	52
5.3.3. Winter climate change implications.....	55
5.4. Summary and Conclusions	55

6. Dynamics of streamwater nitrate and dissolved organic carbon during snowmelt with differing winter climatic regimes	69
6.1. Methods.....	69
6.1.1. Site description.....	69
6.1.2. Snowmelt streamwater sampling	69
6.1.3. Stream flow measurements	70
6.1.4. Characterization of winter climatic gradient.....	71
6.1.5. Laboratory analysis	71
6.1.6. Computational methods and statistical analyses.....	72
6.2. Results.....	73
6.2.1. Snowmelt hydrologic response	73
6.2.2. General snowmelt stream hydrochemistry.....	74
6.2.3. Nitrate dynamics across years and watersheds	75
6.2.4. DOC dynamics across years and watersheds.....	76
6.2.5. Snowmelt streamwater nitrate and DOC dynamics in relation to winter climate variation	77
6.2.6. Episodic acidification.....	77
6.3. Discussion.....	78
6.3.1. Nitrate and DOC dynamics during snowmelt.....	78
6.3.2. Episodic acidification.....	81
6.3.3. Winter climate variability and snowmelt stream nitrate and DOC dynamics	83
6.4. Summary and Conclusions	85

7. Hydrological flowpaths during snowmelt in forested headwater catchments under differing winter climatic and soil frost regimes	105
7.1. Methods.....	105
7.1.1. Watersheds for snowmelt hydrologic flowpath study	105
7.1.2. Snowmelt streamwater sampling	106
7.1.3. Stream flow measurements	106
7.1.4. Snowpack and soil frost monitoring	107
7.1.5. Hydrologic flowpath determination.....	107
7.1.6. Laboratory analysis.....	108
7.1.7. End-member mixing analysis	109
7.2. Results.....	110
7.2.1. Interannual and elevational patterns of snow depth and soil frost.....	110
7.2.2. End-member mixing analysis	111
7.2.3. Hydrograph separation.....	111
7.3. Discussion.....	115
7.3.1. Influence of soil frost on infiltration.....	116
7.3.2. Development of different types of soil frost	118
7.3.3. Variability of forest floor preferential flowpaths related to soil frost depth.....	119
7.3.4. Dissolved organic carbon and nitrate as indicators of shifting flowpaths	121
7.3.5. Proposed mechanism of soil frost effect on organic soil flowpaths	123
7.3.6. Implications of climate change for flowpaths and stream chemistry	123
7.4. Summary and Conclusions	124
8. Synthesis and Integration	137

8.1. Overall summary of results	137
8.2. Recommendations for future studies	141
9. References	142
10. Vita.....	158

LIST OF TABLES

Table 4.1. Long-term trends in organic horizon (Oa) soil water chemistry, 1984-2011a.	35
Table 4.2. Long-term trends in mineral horizon (Bs) soil water chemistry, 1984-2011a.....	35
Table 4.3. Long-term trends in stream water chemistry, 1982-2011 ^a	36
Table 4.4. Comparison between trends of overall stream chemistry record and the trends during the snowmelt seasons, 1982-1984.....	37
Table 5.1. Winter climate gradient sites with soil lysimeters.	57
Table 6.1. Study watershed size and topographical characteristics.	87
Table 6.2. Winter climatic measures for the three years of study and the mean of the years 1980-2012.....	87
Table 6.3. Pre-snowmelt and peak early (March) and late (April) snowmelt values by watershed weir sampling site.	88
Table 6.4. Summary of NO ₃ ⁻ and DOC volume-weighted averages and total fluxes by snowmelt months March and April, and totals for the two months for each sampling year.	89
Table 6.5. Concentration-discharge hysteresis loops for NO ₃ ⁻ and DOC by sampling site and hydrologic event.	90
Table 7.1. Catchment and subcatchment information for each snowmelt stream sampling site at the Hubbard Brook Experimental Forest, NH.	126
Table 7.2. Correlation matrix of potential hydrologic flowpath tracers.	126
Table 7.3. Mean concentration values of potential hydrologic flowpath tracers in each end- member. Units for Cl ⁻ , SO ₄ ²⁻ , Na ⁺ , Mg ²⁺ , and H ₄ SiO ₄ are μmol L ⁻¹ . Units for δD and δ ¹⁸ O are ‰. Standard deviations are indicated in parentheses.	126

Table 7.4. Hydrological events during the spring of 2011 and 2012. End-member flow contributions for snow-precipitation, forest floor (FF) soil water, and baseflow-groundwater are estimated through EMMA. Values in parentheses are standard deviations. Soil frost depths are estimated through the linear regression model of soil frost and elevation.127

LIST OF FIGURES

- Figure 4.1. Map of Watershed 6 at the Hubbard Brook Experimental Forest (43°56'N, 71°45'W), showing locations of lysimeter plots and stream sampling points relative to the elevation zones. 38
- Figure 4.2. Precipitation-weighted mean annual wet deposition values for SO_4^{2-} and NO_3^- (top panel), and pH (lower panel) from 1982-2011. Data were obtained from the National Atmospheric Deposition Program (NH02). 39
- Figure 4.3. pH of stream water at the W6 gauging station, 1982-2011. 40
- Figure 4.4. SO_4^{2-} concentration trends (1984-2011) vs. elevation for W6 soil water and stream water. Median trends are estimated by SKT analysis. Vertical bars represent 95% confidence intervals. Transitions between elevation zones are marked with vertical dotted lines. 41
- Figure 4.5. Soil solution and streamwater charge balances represented by annual volume-weighted concentrations of major ions in a) Oa horizon, b) Bs horizon, and c) streamwater. Cation charge is expressed by positive values of $\mu\text{Eq L}^{-1}$, while anion charge is negative. Organic anion concentrations (A^-) were calculated from the charge discrepancy of measured positive and negative species (Driscoll et al. 1989). Soil solution values are weighted by elevation zone to represent the entire watershed; streamwater values are from the gauging station at the base of the watershed. 42
- Figure 4.6. Trends in acid neutralizing capacity, as calculated $C_B - C_A$, from 1982-2011. Trend slope for the overall dataset estimated using SKT. Snowmelt trend is calculated by Mann Kendall analysis. 43

Figure 4.7. Mean monthly NO_3^- concentrations of stream water draining W6 for 1982-1991 and 2002-2011. Vertical bars indicate standard errors.	44
Figure 5.1. Map of the HBEF with winter climate gradient lysimeter sites indicated.	58
Figure 5.2. Boxplots of 2011 and 2012 winter climate variables across all monitoring plots, a) snowpack, b) maximum soil frost depth, and c) SDL winter soil temperature. Statistically significant differences ($p < 0.05$), as analyzed by paired t-test, are marked by *.....	59
Figure 5.3. Relationship between maximum soil frost depth and the <i>Snowpack</i> variable for the winter of a) 2010-2011 and b) 2011-2012 across 20 winter climate gradient monitoring plots.	60
Figure 5.4. Monthly mean concentrations of a) NO_3^- , and b) DOC concentrations in soil solutions. Error bars indicate standard deviations.	61
Figure 5.5. Boxplots of 2011 and 2012 May-July concentrations of DOC in soil solution of the a) Oa horizon and b) Bs horizon, and NO_3^- concentrations in soil solutions of the c) Oa horizon and d) Bs horizon. Statistically significant differences ($p < 0.05$), as analyzed by paired t-test, are marked by *.....	62
Figure 5.6. Scatterplots of soil solution concentrations of NO_3^- during May-July 2011 as related to the previous winter's maximum soil frost depth in a) Oa horizon and b) Bs horizon, and as related to the SDL of winter soil temperature in c) Oa horizon and d) Bs horizon. Vertical bars indicate standard errors.	63
Figure 5.7. Scatterplots of soil solution concentrations of NO_3^- during May-July 2012 as related to the previous winter's maximum soil frost depth in a) Oa horizon and b) Bs horizon,	

and as related to the SDL of winter soil temperature in c) Oa horizon and d) Bs horizon. Vertical bars indicate standard errors.	64
Figure 5.8. Scatterplots of soil solution concentrations of DOC during May-July 2011 as related to the previous winter's maximum soil frost depth in a) Oa horizon and b) Bs horizon, and as related to the SDL of winter soil temperature in c) Oa horizon and d) Bs horizon. Vertical bars indicate standard errors.	65
Figure 5.9. Scatterplots of soil solution concentrations of DOC during May-July 2012 as related to the previous winter's maximum soil frost depth in a) Oa horizon and b) Bs horizon, and as related to the SDL of winter soil temperature in c) Oa horizon and d) Bs horizon. Vertical bars indicate standard errors.	66
Figure 5.10. Scatterplots of soil solution concentrations of DOC during August-September 2011 as related to the previous winter's maximum soil frost depth in a) Oa horizon and b) Bs horizon, and as related to the SDL of winter soil temperature in c) Oa horizon and d) Bs horizon. Vertical bars indicate standard errors.....	67
Figure 5.11. Scatterplots of soil solution concentrations of DOC during August-September 2012 as related to the previous winter's maximum soil frost depth in a) Oa horizon and b) Bs horizon, and as related to the SDL of winter soil temperature in c) Oa horizon and d) Bs horizon. Vertical bars indicate standard errors.....	68
Figure 6.1. Map of Hubbard Brook Experimental Forest with study watersheds, sampling and monitoring sites indicated.....	91
Figure 6.2. Snowmelt season hydrochemical dynamics in Watershed 3 based on discrete daily samples from 1 March 2010 to 30 April 2010, with a) stream flow, b) NO ₃ ⁻ , c) DOC,	

d) SO ₄ ²⁻ , and e) ANC indicated. Low elevation samples collected at the W3 weir (W3-L, 527 m). High elevation samples collected at 635 m (site W3-H).	92
Figure 6.3. Snowmelt season hydrochemical dynamics in Watershed 6 (site W6-L) based on discrete daily samples from 1 March 2010 to 30 April 2010, with a) stream flow, b) NO ₃ ⁻ , c) DOC, d) SO ₄ ²⁻ , and e) ANC indicated.	93
Figure 6.4. Snowmelt season hydrochemical dynamics in Watershed 3 based on discrete daily samples from 1 March 2011 to 30 April 2011, with a) stream flow, b) NO ₃ ⁻ , c) DOC, d) SO ₄ ²⁻ , and e) ANC indicated. Low elevation samples collected at the W3 weir (W3-L, 527 m). High elevation samples collected at 635 m (site W3-H).	94
Figure 6.5. Snowmelt season hydrochemical dynamics in Watershed 6 (site W6-L) based on discrete daily samples from 1 March 2011 to 30 April 2011, with a) stream flow, b) NO ₃ ⁻ , c) DOC, d) SO ₄ ²⁻ , and e) ANC indicated.	95
Figure 6.6. Snowmelt season hydrochemical dynamics in Watershed 3 based on discrete daily samples from 1 March 2011 to 30 April 2011, with a) stream flow, b) NO ₃ ⁻ , c) DOC, d) SO ₄ ²⁻ , and e) ANC indicated. Low elevation samples collected at the W3 weir (site W7-L, 619 m). High elevation samples collected at 720 m (site W7-H).	96
Figure 6.7. Snowmelt season hydrochemical dynamics in Watershed 3 based on discrete daily samples from 1 March 2012 to 30 April 2012, with a) stream flow, b) NO ₃ ⁻ , c) DOC, d) SO ₄ ²⁻ , and e) ANC indicated. Low elevation samples collected at the W3 weir (W3-L, 527 m). High elevation samples collected at 635 m (site W3-H).	97
Figure 6.8. Snowmelt season hydrochemical dynamics in Watershed 6 (site W6-L) based on discrete daily samples from 1 March 2012 to 30 April 2012, with a) stream flow, b) NO ₃ ⁻ , c) DOC, d) SO ₄ ²⁻ , and e) ANC indicated.	98

Figure 6.9. Snowmelt season hydrochemical dynamics in Watershed 3 based on discrete daily samples from 1 March 2012 to 30 April 2012, with a) stream flow, b) NO_3^- , c) DOC, d) SO_4^{2-} , and e) ANC indicated. Low elevation samples collected at the W3 weir (site W7-L, 619 m). High elevation samples collected at 720 m (site W7-H).	99
Figure 6.10. Concentration-discharge relationships for NO_3^- in streamwater at W3-L, W6-L, and W7-L during a) early snowmelt 2011 and b) early and peak snowmelt 2012.	100
Figure 6.11. Concentration-discharge relationships for NO_3^- at site W3-L during a) March and b) April sampling dates of the 2010, 2011, and 2012 snowmelt seasons.	101
Figure 6.12. Concentration-discharge relationships for DOC at site W3-L by sampling year...	102
Figure 6.13. Relationship of ΔANC with a) ΔNO_3^- , b) ΔDOC , and c) ΔCa^{2+} by watershed and year.....	103
Figure 6.14. 2012 Mean volume-weighted DOC concentration by month as a function of preceding winter maximum soil frost depth.	104
Figure 7.1. Map of Hubbard Brook's south-facing experimental watersheds, indicating locations of stream sampling sites, soil water lysimeters, and snow and soil frost monitoring sites.	128
Figure 7.2. Relationship of snowpack (a,b) and soil frost depth (c,d) with elevation for each of the two study winters. Regression statistics shown for mid-winter (open circles) and early snowmelt (closed circles).....	129
Figure 7.3. Snowpack and soil frost evolution during the winters of 2011 and 2012 at high elevation (766 m) and low elevation (536 m) monitoring sites.	130
Figure 7.4. Mixing diagrams generated with principal component analysis for streamwater collected at the three sampling sites during the winters of 2011 and 2012.	131

Figure 7.5. Watershed 6 hydrograph separation (W6-L) with EMMA for snowmelt during a two month period in a) 2011 and b) 2012. Lower panels indicate fraction of flow through flowpaths during an approximately two week period of early season snowmelt. 132

Figure 7.6. Watershed 3 fractional separation of flowpaths from EMMA for a two week period early in the snowmelt season in 2011 (left column) and 2012 (right column). The top panels of each column show the W3 hydrograph. The proportional flow at the W3-H site is indicated in the middle set of panels and the lower panels show the proportional flow at the W3-L site..... 133

Figure 7.7. Detail of mean daily soil temperatures at 5 cm depth for three high elevation sites (688 m, 698 m, and 766 m) and three low elevation sites (487 m, 536 m, and 601 m) during peak snowmelt in March 2012. Error bars represent standard deviations..... 134

Figure 7.8. Concentration-discharge relationships in W6 for a) DOC, and b) NO_3^- during early snowmelt periods of minimal soil frost and extensive soil frost to the depth of the Oa horizon. Dates for 2011 data are 5-20 March 2011. The 2012 dates with soil frost are 5-15 March, and without soil frost are 18-26 March. 135

Figure 7.9. Conceptual model of potential granular soil frost effects on Oa soil horizon preferential flowpaths, in which a) frost granules block preferential flowpaths, slowing flow and promoting deeper percolation into mineral soil, and b) preferential flowpaths are maintained but frost presence prevent chemical exchange with soil matrix. 136

1. Introduction

Upland forest ecosystems in the northeastern United States are important in the regulation of the quantity and quality of water downstream. Northern forest ecosystems generally have tight biogeochemical cycles with little loss of nutrients and elements to runoff. Environmental perturbations can alter the manner in which vegetation and soils effectively work to maintain element cycles and conserve drainage water losses. The Hubbard Brook Experimental Forest (HBEF) in the White Mountains of New Hampshire has been the site of research for a half century on the basic functions of the northern hardwood forest ecosystem and the effects of disturbances to this environment. The wide-scale anthropogenic disturbances impacting these forest ecosystems include harvesting and other forest disturbances, acidic deposition resulting from air pollution, and most recently global climate change driven by increased concentrations of greenhouse gases.

The first documentation of acidic deposition in North America was made at the Hubbard Brook Experimental Forest (HBEF) based on precipitation collections dating from the early 1960s (Likens et al. 1972). Acidic deposition is a regional problem in the northeastern United States and primarily results from emissions of SO₂ and NO_x in the Midwest (Driscoll et al. 2001). The effects of acidic deposition include both chronic acidification of stream and soil waters and increased susceptibility to episodic acidification during hydrologic events such as rain storms and especially snowmelt (Driscoll et al. 2001).

Climate change has been well documented and the observed changes include a 0.75°C increase in global mean temperatures during the last 100 years, as well as shifts in precipitation patterns (IPCC 2007). In the northeastern United States, the climatic and hydrological data are

consistent with global trends. Hayhoe et al. (2007) found that surface air temperature has increased in the northeastern USA by 0.8°C during the 20th century, and variable changes in annual precipitation have averaged to an increase of nearly 100 mm. Future projections, depending on which emissions scenario is followed, indicate that temperatures will continue to increase during the 21st century by between 2.1 and 5.3°C, with increases in annual precipitation of 7-14% (Hayhoe et al. 2008). Coupled with a declining proportion of winter precipitation falling as snow (Huntington et al. 2004), these trends have led to decreasing winter snowpacks and associated shifts in hydrology (Burakowski et al. 2008; Campbell et al. 2010).

Ecological and biogeochemical processes in northern forests are expected to change with climate-induced changes in forest species composition, growing season length, and forest hydrology (Campbell et al. 2009; Groffman et al. 2012). Tree species composition is expected to change as cold-tolerant conifer species are reduced and hardwood species move their range northward (Iverson and Prasad 1998). Species composition of northern hardwood forests is an important factor in biogeochemical cycling. For example, nitrification and N export from watersheds is higher in forests dominated by sugar maple compared to oak or beech (Lovett et al. 2004). The growing season, as defined by the period between the last spring freeze to the first hard freeze in autumn, has increased across the United States during the last half century (Schwartz et al. 2006) and is expected to continue increasing in the future (Tebaldi et al. 2006). The increased growing season length in the northern forest will impact ecological and hydrological processes such as annual productivity, nutrient uptake, evapotranspiration, soil moisture, and stream flow (Campbell et al. 2009). In addition to the hydrological changes based on increased water demand by vegetation, climate change is expected to impact the quantity and temporal distribution of precipitation. Wet-dry cycles in the soil can be affected by changes in

the temporal distribution of precipitation and rainfall events can markedly alter the release of solutes such as NO_3^- , DOC, and Al to drainage waters (Mitchell et al. 2006). Expected hydrological changes also include increases in rain on snow events, which can lead to episodic acidification (Maclean et al. 1995).

Recent research has acknowledged the importance of winter ecological processes (e.g. Campbell et al. 2005) as well as the relatively rapid rate of climate change during winter months (Hayhoe et al. 2007). The changing winter temperature and snow regime is hypothesized to result in “colder soils in a warmer world” due to decreased insulation of soils with reduced snowpacks (Groffman et al. 2001a). This pattern, accompanied by increases in soil frost, has been shown to likely have effects on ecological and biogeochemical processes, including root mortality and reduced nutrient uptake during the growing season (Tierney et al. 2001, Cleavitt et al. 2008) and consequent nutrient loss (Fitzhugh et al. 2001). Although hypothesized to affect microbial activity or biomass, no changes have been detected (Groffman et al. 2001b). Additionally, winter climate change is likely to have significant impacts on the timing and magnitude of snowmelt events. Soil frost is also hypothesized to affect the hydrologic flowpaths of melt waters. Given that the snowmelt period is responsible for a large portion of annual hydrologic and element fluxes (Likens et al. 1977), changes in the factors influencing the timing, magnitude, and composition of snowmelt runoff can be expected to have consequences for the overall biogeochemical budgets of northern hardwood forests. My dissertation research seeks to assess the chemistry of drainage waters at Hubbard Brook in the context of historical acidic deposition and current and projected winter climate change, with a particular focus on the dynamics of spring snowmelt events.

2. Literature Review

2.1. Acidic deposition in the northeastern United States

Acidic deposition is the transfer of strong acids and acid-forming materials from the atmosphere to Earth's surface, including ions, gases, and particles derived from gaseous emissions of sulfur and nitrogen oxides, ammonia, and particulate emissions of acidifying compounds (Driscoll et al. 2001). Acidic deposition developed as an environmental issue in the 1960s and 70s. Acidic precipitation and acidification of surface waters were initially reported at several Swedish and other Scandinavian sites by Oden (1968). The first documentation of acidic deposition in North America was at the Hubbard Brook Experimental Forest in New Hampshire based on precipitation collections begun in the early 1960s (Likens et al. 1972). Acidic deposition in the northeastern United States has primarily resulted from prevailing winds carrying SO_x and NO_x pollutant emissions from atmospheric source areas in the Midwest (Driscoll et al. 2001).

The ecological effects of acidic deposition are numerous and diverse (Driscoll et al. 2001). Acidic deposition has been directly linked to widespread dieback of red spruce trees during the 1970s and 1980s (Craig and Friedland 1991) and sugar maple (Duchesne et al. 2002). Strong acids can mobilize dissolved inorganic aluminum from soils to surface waters, which at elevated concentrations ($>2 \mu\text{mol L}^{-1}$) can be highly toxic to fish (Baker and Schofield 1982). Additionally, acidified surface waters has been shown to promote mercury accumulation in fish (Driscoll et al. 1994). Deposition of anthropogenic nitrogen has been shown to lead to eutrophication of coastal waters (Jaworski et al. 1997).

The identification of acidic deposition as an environmental problem in the United States led to a series of pollution controls enacted through federal legislation. The amendments to the Clean Air Act (CAAA) were passed in 1970 and were the first legal limitations on sulfur dioxide (SO₂) emissions. In 1990 the U.S. Congress enacted further amendments to the CAAA by passing Title IV of the Acidic Deposition Control Program, which imposed further limitations on SO₂ emissions and began controls on nitrogen oxides (NO_x) emissions from electric utilities. In 2003 the NO_x Budget Trading Program (NBP) was passed to initiate a cap-and-trade approach to controlling emissions of NO_x from power plants and other large combustion sources in the eastern U.S. In 2005 the U.S. EPA implemented the Clean Air Interstate Rule (CAIR), which was ultimately vacated by the U.S. District Court, but EPA was allowed to continue to implement CAIR while they developed an alternative rule.

The cumulative effects of the CAAA, NBP, and CAIR on acidic deposition have been substantial. At the Hubbard Brook Experimental Forest, Likens et al. (2005) showed that the deposition of SO₄²⁻ and NO₃⁻ are strongly related to the emissions of SO₂ and NO_x in air mass back-trajectory source areas. Emissions of SO₂ in those source areas have declined steadily since peaking in 1970 and have translated into significant declines in SO₄²⁻ deposition at Hubbard Brook (Likens et al. 2001). This trend is similar to SO₄²⁻ deposition declines across much of the U.S., especially in the northeastern region (Lehmann et al. 2005). Nitrate deposition, after having shown little change between 1980 and 2000 (Baumgardner et al. 2002), has decreased more rapidly since the early 2000s (Greaver et al. 2012; Likens and Buso 2012).

2.2. Episodic acidification

Episodic acidification is the short term decrease in the acid neutralizing capacity of surface waters during periods of high hydrologic flow. The phenomenon is widespread throughout regions of North America and Europe (Wigington et al. 1990). Episodic acidification can have deleterious effects for downstream water quality, as the associated mobilization of dissolved inorganic aluminum can be toxic to fish and other aquatic biota (Baker and Schofield 1982; Baker et al. 1996).

Acidification events can result from both natural processes and atmospheric deposition. Changes in hydrologic flowpaths during high-flow events can determine the nature and extent of these acidification events. During base flow, the dominant flowpaths are through deeper mineral soil horizons, contributing flow from groundwater storage. During hydrologic events, the flowpaths contributing most to stream water are routed through shallower soil, which tend to be more acidic because of natural processes and acidic deposition (Chen et al. 1984; Potter et al. 1988). Four major natural processes have been shown to contribute to acidification episodes: (1) dilution, (2) nitrification, (3) organic acid production, and (4) sea salt (Wigington et al. 1996).

The main control on episodic acidification across regions in the United States has been shown to be the dilution of base cation concentrations (Wigington et al. 1990). Additionally, atmospheric deposition of anthropogenically derived acids can cause or exacerbate acidification events in surface waters. Atmospheric deposition can contribute to episodic acidification by (1) providing direct inputs of acids to surface waters, (2) providing SO_4^{2-} , NO_3^- , NH_4^+ , and H^+ , which accumulate in the upper soil horizons during relatively dry periods, and (3) lowering the chronic ANC of surface waters, which leads to even lower ANC during episodes (Galloway et al. 1987).

Pulses of increased nitrate concentrations concurrent with hydrologic events have been noted to be especially important contributors to decreased ANC values in the catchments of the northeastern USA (Wellington et al. 1990; Sullivan et al. 1997). Increases in SO_4^{2-} have been shown to significantly contribute to acidification in streams of Pennsylvania (DeWalle and Swistock 1994) and throughout the mid-Atlantic region (O'Brien et al. 1993). Wellington and Driscoll (2004) showed that organic acids can contribute significantly to acidification events in streams with already relatively high DOC concentrations.

2.3. Trends in stream and soil water chemistry

Widespread increases of DOC concentrations in surface waters across many parts of Europe and North America have been reported in recent decades (Driscoll et al. 2003; Evans et al. 2005; Skjelkvåle et al. 2005). The underlying causes of increased DOC concentrations are not well understood. A number of studies have suggested decreases in acidic deposition (Evans et al. 2006; Monteith et al. 2007) as the driver leading to increased DOC concentrations, while others point to climate-related changes (Hongve et al. 2004; Worrall and Burt 2007; Lepistö et al. 2008), or land management changes (Yallop and Clutterbuck 2009). Clark et al. (2010) attempted to link the hypotheses while considering different spatial and temporal scales. Hubbard Brook, the site of this dissertation research, has been shown to be somewhat of an outlier by defying the trends of increasing DOC concentrations in surface waters. Stream water DOC concentration has shown a long-term decline at Hubbard Brook, apparently driven by a decrease in DOC leaching in soil waters (Palmer et al. 2004).

While numerous studies have published trends in surface water chemistry (e.g. Stoddard et al. 1999; Driscoll et al. 2003; Skjelkvåle et al. 2005; Warby et al. 2005) in the context of

recovery from acidification, comparatively few studies have examined long-term trends in soil water chemistry. Palmer et al. (2004) examined soil water chemistry trends with 15 years of data at the Hubbard Brook Experimental Forest in New Hampshire. The Swedish Throughfall Monitoring Network (SWETHRO) monitors soil water chemistry across many sites with three sampling times each year (Löfgren et al. 2010; Pihl Karlsson et al. 2011; Akselsson et al. 2013). Akselsson et al. (2013) analyzed the trends of soil water chemical recovery from acidification across nine sites in southern Sweden and found generally slow recoveries from acidification and sensitivity to sea salt deposition during the study period 1996-2008.

2.4. Winter Climate Change

Across the northeastern United States and eastern Canada, the temperatures have increased more during winter months than summer (1.2 and 0.7°C, respectively) during the 20th century (Hayhoe et al. 2007). Climate projections for the northeastern U.S. suggest that during the 21st century, the temperature could increase by 2.1-5.3°C, depending on the greenhouse gas emission scenario followed (Hayhoe et al. 2008). Winter precipitation projections are less certain, but the projections indicate increases of 12-30%, with an increasing proportion falling as rain instead of snow.

The Hubbard Brook Experimental Forest has a number of comprehensive long-term climatic datasets dating back as far as 1956 from weather stations located throughout the forest. Campbell et al. (2010) reported significant long-term mean annual temperature increases across the Hubbard Brook valley ranging from 0.017 to 0.028°C per year. Similar to the study by Hayhoe et al. (2007) for the northeastern U.S. as a whole, winter temperatures increased faster at Hubbard Brook than during other seasons, with different weather stations across the valley

showing average winter temperature increases of 0.029 to 0.036°C per year. Ice cover duration at Mirror Lake at the HBEF has been measured each winter from 1968. The duration of ice cover has been shortening by an average of approximately 0.5 days per year, and the earlier melt dates are most correlated with warmer spring temperatures (Likens 2000).

Total annual precipitation has increased significantly at the majority of weather stations located within the HBEF, including at all stations with more than 48 years of data (Campbell et al. 2010). The increase in precipitation at these stations ranges from 3.5 to 6.7 cm per decade (Campbell et al. 2007). Winter precipitation, on the other hand, did not change at any of the measuring stations. Regional studies have reported snow is a decreasing proportion of winter precipitation (Huntington et al. 2004; Burakowski et al. 2008). This trend has not been observed in the Hubbard Brook data, but the reporting of snow versus rain in precipitation measurements only dates back to 1979 (Campbell et al. 2010).

A combined lack of change in winter precipitation and warmer winter air temperatures has the effect of decreasing snowpack accumulation and duration. The long-term record of weekly snowpack measurements at the HBEF, initialized in 1959, shows that maximum snow depth has decreased by 0.47 cm per year (0.13 cm per year in snow-water equivalence), and snow cover duration has decreased by 0.40 days per year (Campbell et al. 2010). Changing patterns of precipitation and snowpack accumulation are altering the stream flow dynamics at Hubbard Brook. Snowmelt is occurring earlier (Hamburg et al. 2013) and the peak spring snowmelt flows are decreasing (Campbell et al. 2011). The reduced winter snowpacks, coupled with warmer temperatures, has led increased stream flow throughout the winter prior to the peak of snowmelt (Campbell et al. 2011).

2.5. Relationship between snowpack depth and soil frost depth

Reduced snowpacks, even in the presence of warmer air temperatures, are hypothesized to lead to increased instances and severity of soil freezing with climate change (Isard and Schaetzl 1998; Groffman et al. 2001a). Snow cover provides an insulation of the soils in northern latitudes that protects them from severe freezing during outbreaks of cold temperatures. Soil frost depth typically varies inversely with snow depth, and lack of snow and late developing snowpacks have been correlated with deeper and more persistent soil frost compared to years in which the snowpack developed early in winter (Stadler et al. 1996; Shanley and Chalmers 1999). A number of manipulation studies have shown increases in soil frost depth with snow removal in experimental plots (Boutin and Robitaille 1995; Groffman et al. 2001a; Decker et al. 2003)

2.6. Effects of soil freezing on biogeochemical cycling

In a study using natural variation in snowdepth at Niwot Ridge in Colorado, Brooks et al. (1998) found higher export of N from soils with shallow or inconsistent snow cover. Using long-term soil water chemistry data from a Norway Spruce stand in southeastern Germany, Callesen et al. (2007) found that extreme soil freezing led to increased concentrations of inorganic nitrogen. This response was most pronounced in the mineral soil. In a study of 16 forested watersheds in south-central Ontario over a 16-year period, Watmough et al. (2004) found soil freezing to be a significant factor contributing to increased nitrate export. In a study of mesocosms with Swedish tundra soils, Grogan et al. (2004) found that moderate freezing had minimal influence on the dynamics of soluble N and C pools. Results of laboratory experiments conducted by Herrmann and Witter (2002) on Swedish agricultural soils led them to conclude that freeze-thaw cycles had little influence on annual N and C budgets.

Boutin and Robitaille (1995) manipulated snow depth in sugar maple stands in Québec and found induced soil freezing resulted in significantly elevated concentrations of NO_3^- and NH_4^+ in soil solutions during the following growing season. Though they did not measure fine-root dynamics, the authors speculated that the leaching of nutrients may have been caused by extensive fine-root mortality and subsequent canopy dieback. Similarly, Fitzhugh et al. (2001) found increased NO_3^- leaching in soil solutions from snow removal plots in a sugar maple stand at Hubbard Brook, especially solutions draining the organic soil horizon.

At Hubbard Brook, the long term record of stream water chemistry and soil frost survey has been used to analyze the impact on soil frost on watershed NO_3^- runoff. Soil frost was considered rare at the HBEF prior to 1970 (Hart et al. 1962). Widespread soil freezing occurred during the winters of 1969-1970 and 1973-1974 and was linked with episodes of high streamwater NO_3^- loss from watersheds during 1970 and 1974 (Likens and Bormann 1995). Mitchell et al. (1996) observed increased NO_3^- losses in stream water at Hubbard Brook and several other sites across the northeastern U.S. during snowmelt in 1990 following extensive soil freezing that developed during a severe cold outbreak in December 1989. Fitzhugh et al. (2003) found that soil freezing was a significant predictor of stream nitrate concentrations during the period 1970-1989, explaining 47% of the short-term variability. They also noted, however, that the relationship between soil freezing and stream NO_3^- disappeared during later years, 1990-1997. Hubbard Brook experienced widespread soil freezing during the winter of 2005-2006 and Judd et al. (2011) predicted it would lead to high NO_3^- runoff, but they observed that watershed NO_3^- export in 2006 was among the lowest on record. While the mobilization of NO_3^- reported by Fitzhugh et al. (2001) was quite large ($> 250 \mu\text{Eq L}^{-1}$), the authors did not find substantial mobilization of DOC resulting from the induced frost treatment.

2.7. Effects of soil freezing on hydrologic flow

The reported hydrological effects of soil frost are varied. Commonly, increased surface runoff during snowmelt or rain events is observed under conditions of frozen soil (e.g. Dunne and Black 1971; Kane and Stein 1983). Large amounts of surface runoff over frozen soil has been implicated in widespread flooding events, including in the Sierra Nevada Mountains (Haupt 1967), and New England (Diebold 1938). A number of other studies, however, have shown that infiltration can be high in frozen soil (e.g. Munter 1986), or is variable (Stadler et al. 1996; Shanley and Chalmers 1999; Bayard et al. 2005).

The hydrological effects of soil frost appear to depend strongly on the nature and development of the soil frost. Soil frost can broadly be categorized into either concrete frost or granular frost. Concrete frost tends to develop in soils in open or agricultural areas (Sartz 1957; Pierce et al. 1958; Shanley and Chalmers 1999), but can also occur in forested areas (Fahey and Lang 1975). The development of concrete soil frost is favored in higher moisture content and finely textured soils (Kane and Stein 1983), including tilled soils with disrupted aggregate structure (USDA NRCS 2009). Concrete frost has been shown to reduce water infiltration and lead to greater surface runoff. Granger et al. (1984) and Johnsson and Lundin (1991) showed that the infiltration capacity of soils in agricultural systems was inversely related to the total soil moisture contents at the onset of freezing. Conversely, granular frost tends to occur in unsaturated soils (Hardy et al. 2001). Infiltration capacity is preserved in these soils as granular frost does not completely bridge the pore spaces (USDA NRCS 2009).

Mid-winter climatic factors such as early melt events followed by refreezing are likely to affect infiltration characteristics. Bayard et al. (2005) studied the effects of frozen soil on runoff

dynamics in southern Switzerland and found that snowmelt water infiltration was reduced to 65-75% under conditions of deep and persistent soil frost, compared with 90-100% during the previous season when a deeper snowpack prevented development of soil frost. They attributed the reduced soil infiltration capacity to a basal ice sheet which formed following mid-winter melt events.

3. Objectives and Hypotheses

The research for this dissertation was divided into two phases. The first was an evaluation of hydrochemical trends in stream and soil water at Hubbard Brook over the past 30 years, including an examination of trends during snowmelt. The second phase was a set of field-based experiments to assess the variability in stream and soil water chemistry and hydrology as they relate to natural variability in winter climate and snowmelt conditions.

The first phase involved a data analysis of the long-term records of streamwater and soil water chemistry at Watershed 6, Hubbard Brook's biogeochemical reference watershed. Previous research has shown a long-term trend of recovery from acidification at this site (Palmer et al. 2004). My data analysis was conducted to determine whether and at what rate the recovery from acidification has continued in the overall record of stream and soil water chemistry. I also conducted an additional focused analysis to detect hydrochemical trends only during the snowmelt season. Snowmelt is the highest flow period of the annual cycle and when the watersheds are most prone to episodic acidification. These sets of analyses allowed me to make a comparison between the trends overall and those during snowmelt, thereby determining if the snowmelt episodic acidification is changing differently from the overall trends.

The second phase was a series of field studies to determine the variability of soil water chemistry, stream water chemistry and hydrology during snowmelt under differing winter climatic conditions, especially the variability in snowpack and soil frost depth. This was accomplished by setting up study sites across the Hubbard Brook valley to characterize the winter conditions along a natural climatic gradient, using variations in elevation and aspect.

My dissertation was organized and focused by developing overarching hypotheses, as well as a set of specific objectives and hypotheses for each of the phases. These are listed below.

Overarching hypotheses: The chemistry of drainage waters at the Hubbard Brook Experimental Forest is recovering in response to several decades of reduced atmospheric acid deposition, though snowmelt episodic acidification remains severe. Winter climate variation affects hydrochemical dynamics during snowmelt, with areas more prone to shallower snowpacks and greater soil frost development experiencing the greatest leaching of NO_3^- , DOC, and overall acidity.

Objective 1 (Phase 1): Assess the recovery of drainage waters from acidic deposition, including a determination if the trends during the snowmelt season, when episodic acidification is of greatest concern, differ from the overall rate of recovery.

Hypothesis 1: The recovery of stream and soil water chemistry will be diminished during the snowmelt season relative to the overall baseflow trends. Over the past three decades atmospheric N deposition has not decreased to the same extent as SO_4^{2-} deposition, and NO_3^- becomes relatively more important to acidification during hydrologic events, especially snowmelt. The decreased base status of the upper soil horizons resulting from years of chronic acidic deposition will contribute to greater dilution of base cations in streamwater associated with source waters from shallow flowpaths during hydrologic events.

Objective 2 (Phase 2): Evaluate the response of soil solution chemistry to soil frost across a natural gradient of winter climate and associated soil frost development.

Hypothesis 2: Soil freezing will result in changes in soil solution chemistry that will vary by landscape position. At plots relatively low in elevation and those with south-facing aspects, snow depth will be lower and soils will incur more frost during winter. During snowmelt and into the growing season soil solutions draining the forest floor at plots with relatively severe soil freezing will leach more NO_3^- and DOC and be more acidic than the sites at higher elevation and on north-facing slopes with less soil frost. The effects of soil frost on solution chemistry will be weaker or nonexistent in the mineral soils, which have a greater capacity to buffer acidity and retain nutrients.

Objective 3 (Phase 2): Assess the variability of stream chemistry during snowmelt in watersheds with differing winter climatic regimes.

Hypothesis 3: Soil freezing will lead to increased flushing of NO_3^- and DOC in watersheds and years with more severe frost during winter relative to those with less. The chemistry of stream runoff will vary by landscape position, with greater flushing of NO_3^- and DOC at higher elevations where the soils are shallower but have relatively more organic matter. However, higher elevations will be less susceptible to soil freezing disturbance, so patterns will be less affected by changes in winter climate. Episodic acidification will be more severe in streams with larger increases in NO_3^- concentrations during snowmelt.

Objective 4 (Phase 2): Evaluate differences in hydrologic flowpaths utilized during snowmelt under differing soil frost conditions

Hypothesis 4: Soil frost penetrating the depth of the forest floor will alter the hydrologic flowpaths of snowmelt while the frost persists. The frost which develops will be granular

rather than concrete and will therefore not prevent infiltration of melt waters, although routing of runoff through preferential forest floor flowpaths will be diminished. The granular frost will block these flowpaths and force more water through deeper, slower flowpaths. Catchments and subcatchments will vary in their soil frost characteristics based on elevation and aspect. Deeper soil frost will develop in areas at lower elevation and those with south-facing aspects, where snowpack accumulation will be less.

4. Trends in recovery of stream and soil water chemistry from chronic and snowmelt episodic acidification

4.1. Methods

4.1.1. Site Description

The Hubbard Brook Experimental Forest (HBEF) is located in the White Mountain National Forest in central New Hampshire, USA (43°56' N, 71°45' W). This study was conducted in and near Watershed 6 (W6), the HBEF biogeochemical reference watershed (13.2 ha, elevation 549-792 m, slope 16°, southeasterly aspect; Figure 4.1) The HBEF has a cool-temperate, humid-continental climate, with mean July and January temperatures of 18.8 and -8.5°C respectively (at 450 m elevation). Annual precipitation averages approximately 140 cm and is distributed nearly evenly throughout the year. Roughly 30% of the annual precipitation occurs as snow (Federer et al. 1989). The landscape of the HBEF is generally covered with glacial till derived largely from local bedrock with a depth ranging from zero along the ridge tops to several meters at the lower elevations (Palmer et al. 2004). The most common soils are well-drained Spodosols, primarily Haplorthods (Johnson et al. 2000), which contain a well-developed organic horizon (3-15 cm; Likens et al. 1977) and are underlain by relatively impervious bedrock (Rangeley Formation, a pelitic schist). Higher-elevation soils tend to be shallowest and soil depth is greater at lower elevations (Lawrence et al. 1986). The vegetation of W6 is dominated by northern hardwood species, including American beech (*Fagus grandifolia* Ehrh.), sugar maple (*Acer saccharum* Marsh.), and yellow birch (*Betula alleghaniensis* Britt.). At higher elevations, balsam fir (*Abies balsamea* (L.) Mill), red spruce (*Picea rubens* Sarg.), and paper birch (*Betula papyrifera* var. *cordifolia* Marsh.) are prominent.

4.1.2. Sampling and analysis

Soil solutions were collected monthly from tension-free lysimeters. These lysimeters are installed in the Oa, Bh and Bs horizons at three sites located adjacent to W6 at elevations of 600m (low elevation hardwood zone, LH), 730m (high elevation hardwood zone, HH), and 750m (spruce-fir-white birch zone, SFB) (Figure 4.1). Three replicate lysimeters were installed beneath the Oa and Bh horizons and within the Bs horizon at each elevation zone site. Samples have been collected approximately monthly from these lysimeters since their installation in 1983. Stream samples were collected from six longitudinal sites from the headwaters draining the SFB zone to the gauging station at the base of the watershed. Wet deposition chemistry data are available through the National Atmospheric Deposition Program (NADP) (NH02) (NADP 2013).

The pH of all samples was measured potentiometrically with a glass electrode. Calcium (Ca), magnesium (Mg), potassium (K), and sodium (Na) were analyzed using atomic absorption spectroscopy (AAS) for samples prior to 2004 and with inductively coupled plasma mass spectrometry (ICP-MS) for samples after 2004. The major anions sulfate (SO_4^{2-}), nitrate (NO_3^-), and chloride (Cl^-) were analyzed using ion chromatography. Fluoride (F^-) was analyzed using an ion selective electrode until 2002, and ion chromatography for samples after 2002. Total base cations (C_B ; $\mu\text{Eq L}^{-1}$) are the sum of $2[\text{Ca}^{2+}] + 2[\text{Mg}^{2+}] + [\text{K}^+] + [\text{Na}^+]$; total strong acid anions (C_A ; $\mu\text{Eq L}^{-1}$) are the sum of $2[\text{SO}_4^{2-}] + [\text{NO}_3^-] + [\text{Cl}^-] + [\text{F}^-]$. Acid neutralizing capacity (ANC) in this study was calculated as the difference between the sum of base cations and the sum of strong acid anions ($\text{ANC} = C_B - C_A$). DOC was measured using infrared detection of CO_2 following UV-persulfate oxidation. For samples prior to 1989, total monomeric Al (Al_m) was determined by extraction with 8-hydroxy-quinoline in methyl isobutyl ketone (MIBK) in the field and analysis

by graphite furnace AAS; for samples after 1989, Al_m was determined colorimetrically following chelation with pyrocatechol violet. Organic monomeric aluminum (Al_o) was determined by the same method as Al_m , after samples passed through a resin ion exchange column. Inorganic monomeric aluminum (Al_i) was calculated as the difference between Al_m and Al_o . I estimate concentrations of organic anions (A^-) as the difference in measured concentrations of solutes with positive charge and negative charge (in $\mu Eq L^{-1}$).

Statistical trend analysis was conducted using the non-parametric modified seasonal Kendal Tau test (SKT, Hirsch et al. 1982; Hirsch and Slack, 1984). This analysis is stronger than simple regression models for data which exhibit seasonal patterns and are autocorrelated. The trends were analyzed for the entire dataset to assess the overall changes in each solute's concentration. The trend analysis for the spring snowmelt period was performed with a Mann-Kendall test using a single annual value from the sampling that occurred most closely to the peak snowmelt of each year. The date of stream sampling most closely associated with peak snowmelt was identified from Hubbard Brook's long-term stream flow record. Hubbard Brook's snow-water equivalency dataset was consulted to identify the lysimeter sampling date that included the greatest input from melting snow during the month preceding sample collection. Though not included in statistical trend analyses, we also present data as volume-weighted annual values. For soil and stream solutions, volume-weighted solute concentrations were calculated by multiplying each monthly concentration by the percentage annual of stream flow occurring during a given month. The volume-weighted concentrations in soil water of each elevation zone were subsequently multiplied by the relative area of each elevation zone (LH=0.5, HH=0.3, SFB=0.2; Johnson et al. (2000) to calculate area-weighted concentration for the whole watershed.

4.2. Results

4.2.1. Soil solution chemistry trends

The pH of soil waters draining the Oa horizon did not change significantly at either the LH or HH zones, but did increase slightly at the SFB site ($0.004 \text{ units y}^{-1}$; $p = 0.05$) over the course of the sampling record 1984-2011 (Table 4.1). Within the Bs horizon, only the soil water of the HH zone has experienced a modest upward trend in pH ($0.006 \text{ units y}^{-1}$; $p = 0.02$). The ANC of soil water increased significantly in the Oa soil water only at the SFB zone, but increased in the Bs soil water of both the HH and SFB zones. In the Bs soil waters that significantly increased in ANC, the C_A concentrations declined at a faster rate than C_B . These C_A declines were driven by rapidly decreasing SO_4^{2-} concentrations. The negative trend in SO_4^{2-} concentration was more pronounced in the Bs soil horizon solutions than the Oa horizon, with more rapid decreases in the higher elevation zones (Table 4.1; Table 4.2). Conversely, the decrease in C_B concentrations followed an opposite pattern with respect to elevation; faster declines were observed at lower elevation. This was especially evident in the Bs solutions, where the C_B concentration decline in the LH zone ($-2.13 \text{ } \mu\text{Eq L}^{-1} \text{ y}^{-1}$) was relatively rapid compared to the trends in the HH ($-0.70 \text{ } \mu\text{Eq L}^{-1} \text{ y}^{-1}$) and SFB ($-0.92 \text{ } \mu\text{Eq L}^{-1} \text{ y}^{-1}$).

Decreasing concentrations of NO_3^- and DOC occurred to a greater extent in soil waters draining the forest floor relative to the Bs mineral soil. NO_3^- decreased significantly in Oa soil water in both the LH and HH zones (Table 4.1). In the Bs solutions a statistically significant decline in NO_3^- concentrations was detected only in the LH zone, and at a rate of decline that was lower than Oa soil solutions in the LH zone (-0.34 versus $-1.55 \text{ } \mu\text{Eq L}^{-1} \text{ y}^{-1}$). The DOC concentrations showed statistically significant declines in the Oa soil solutions of all three elevation zones, ranging from $-15.8 \text{ } \mu\text{mol C L}^{-1} \text{ y}^{-1}$ in the HH zone, to $-25.1 \text{ } \mu\text{mol C L}^{-1} \text{ y}^{-1}$ in the

LH zone (Table 4.1; Table 4.2). For the Bs solutions, only the HH zone soil waters had a significant decrease in DOC ($-3.68 \mu\text{mol C L}^{-1} \text{y}^{-1}$).

4.2.2. Overall stream chemistry trends

The streamwater of Watershed 6 at Hubbard Brook has become less acidic over the sampling period (1982-2011). The overall change in the pH of stream water at the W6 gauging station (site W6-7) was 0.01 units y^{-1} . The pH increased significantly at all longitudinal stream sampling sites and did not decrease at any stream location during the study period (Table 4.3). The most significant increases in pH occurred in the lower reaches of the watershed. Conversely, the greatest increases in ANC were in the higher elevation reaches of W6. This resulted from marked declines in C_A concentrations, driven by SO_4^{2-} , relative to C_B trends, which were consistently negative and did not vary appreciably with elevation (Table 4.3). The NO_3^- concentrations in streamwater declined to a lesser extent than SO_4^{2-} . There was not a clear elevational pattern to the magnitude of NO_3^- trends, but the most significant ($p < 0.05$) declines were observed at lower elevation sites. Monomeric Al concentrations generally decreased in streamwater, though Al_i and Al_o trends differed depending on elevation. At the highest elevation stream sites, Al_o decreased faster than Al_i , while the reverse was true at the lower elevation sites (Table 4.3). The DOC concentration decreased slightly at the watershed outlet (W6-7, Figure 4.1), but no significant trends were observed at the other five longitudinal stream sampling sites (Table 4.3).

4.2.3. Snowmelt streamwater chemistry trends

Streamwater in W6 during the snowmelt exhibited generally similar trends to the overall data record (Table 4.4). Snowmelt streamwater has become slightly less acidic in recent years; the pH increased at a rate of 0.009 unit y^{-1} ($p = 0.02$), and ANC increased by 0.91 $\mu\text{Eq L}^{-1} y^{-1}$ ($p < 0.01$). The small increase in ANC results from decreased concentrations of C_A ($-2.00 \mu\text{Eq L}^{-1} y^{-1}$, $p < 0.01$) and a slightly slower decline in C_B ($-1.21 \mu\text{Eq L}^{-1} y^{-1}$, $p < 0.01$). The decreased C_A trend resulted from a steady SO_4^{2-} decline ($-1.44 \mu\text{Eq L}^{-1} y^{-1}$, $p < 0.01$) and a substantial NO_3^- decline ($-0.28 \mu\text{Eq L}^{-1} y^{-1}$, $p = 0.01$). Congruent with the decreased acidity, monomeric Al species declined, with Al_i decreasing 0.25 $\mu\text{mol L}^{-1} y^{-1}$ ($p < 0.01$) and Al_o decreasing 0.04 $\mu\text{mol L}^{-1} y^{-1}$ ($p = 0.03$). The DOC concentration in snowmelt streamwater did not change over the sampling period ($p = 0.98$), though the overall trend was significant.

4.3. Discussion

4.3.1. Overall trends in soil solution and streamwater

The previous analysis of Hubbard Brook soil water chemistry trends over the period 1984-1998 by Palmer et al. (2004) showed that the soil water drainage was generally becoming more acidic. The current long-term analysis shows that the previous pattern of acidification is no longer evident and has reversed in recent years. This change in the pH of soil water appears to be consistent with an increase in stream water pH. While the overall rate of increase in the pH of stream water at the W6 gauging station has been 0.01 units y^{-1} from 1982-2011, much of this increase has occurred since 1999 (Figure 4.3). Palmer et al. (2004) found no significant changes in pH from 1982-2000 at Hubbard Brook despite other indicators of recovery from acidification such as increases in the ANC. The authors, however, postulated that the deprotonation of organic

acids and the hydrolysis of aluminum were important factors buffering against increases in pH. These effects could be expected to be temporary as capacity for continued dissociation of organic acids is limited and the concentration of Al_i continues to decrease.

I observed consistent significant decreasing trends in the concentration of SO_4^{2-} at all soil water (Table 4.1; Table 4.2) and stream sampling sites (Table 4.3). The declines in stream and soil water SO_4^{2-} are driven by changes atmospheric deposition during the study period. The SO_4^{2-} concentration in bulk deposition peaked at Hubbard Brook in the late 1960s and has decreased steadily since (Likens et al. 2001), including the 30 year record used in my analysis (Figure 4.2). The rate of change in stream SO_4^{2-} concentration from 1982-2011 ($-1.54 \mu\text{Eq L}^{-1} \text{y}^{-1}$) at the base of W6 is greater than the rate observed in wet deposition ($-0.98 \mu\text{Eq L}^{-1} \text{y}^{-1}$) during the same time frame. This discrepancy suggests there are additional factors influencing SO_4^{2-} dynamics in the watershed. Indeed, previous watershed input-output budgets (Likens et al. 2002), and biogeochemical modeling (Gbondo-Tugbawa et al. 2002), have shown there is a missing source of S at Hubbard Brook that would explain higher export of SO_4^{2-} relative to atmospheric deposition. Mitchell et al. (2011) observed similar imbalances in 15 watersheds across the northeastern U.S. and southeastern Canada, and attributed them to net mineralization of organic S that had been stored from years of chronic excess SO_4^{2-} deposition. Furthermore, Mitchell and Likens (2011) showed that the release of internally stored S has become relatively more important to streamwater SO_4^{2-} export with time at Hubbard Brook, and that the overall export of SO_4^{2-} is shifting from control by atmospheric deposition to climatic regulation. While the SO_4^{2-} concentration declines observed in stream and soil water are undoubtedly contributing to an overall modest recovery from acidification, the mineralization of legacy S pools in the soil and release as SO_4^{2-} are likely slowing the rate of recovery. This is further demonstrated in our

analysis of SO_4^{2-} trends longitudinally in streamwater, which shows that the higher elevation portion of W6 has experienced nearly double the rate of SO_4^{2-} decline as the base of the watershed (Table 4.3; Figure 4.4). The soil depth of W6 is inversely related to elevation (Johnson et al. 2000), suggesting that the deeper soils in the lower portion of the watershed have more stored S available for mineralization to SO_4^{2-} . I would expect that as this S pool decreases with time the rate of recovery from acidification will increase, leading to more rapid increases in pH and ANC.

In soils with low base saturation, the deposited strong acid anions are typically neutralized in drainage waters by a combination of base cations and Al (Figure 4.5; Cronan and Schofield, 1990). As would be expected, the leaching of C_B has declined steadily throughout the course of the soil water chemistry record, especially in relation to decreasing SO_4^{2-} deposition. Monomeric Al concentrations have also generally declined in stream and soil water. In the Oa soil solutions the decreasing monomeric Al concentrations have mostly been in the Al_o form. Al_i has actually shown a slight increase in the Oa soil water in the LH and SFB zones. As the solutions draining the Oa horizon are typically rich in DOC, it is not surprising that the decrease in monomeric Al has been predominantly been in the organically-complexed Al_o fraction. Additionally, studies of Al dynamics in acidic soils have suggested that formation of organic matter-Al complexes can be more important to overall Al solubility than pH-dependent mineral phase solubility (Berggren and Mulder 1995; Skyllberg 1999). Palmer et al. (2004) hypothesized that changes in organic-Al complex formation could explain the moderate decreases in Al_i concentrations of soil waters despite their unchanged or even decreasing pH.

The Al_i concentration in stream water has declined from an average of $7.6 \mu\text{mol L}^{-1}$ during the first five years of monitoring (1982-1985) to $2.0 \mu\text{mol L}^{-1}$ during the five most recent

years of our data analysis (2007-2011). The concentration of Al_i mobilized is an important measure of surface water quality as Al_i has been shown to be a primary factor affecting fish in acid-impacted waters (Baker and Schofield, 1982). Organically-complexed Al (Al_o) is considered to be nontoxic to fish in comparison to Al_i . The results show that while Al_o concentrations in stream water have decreased, the portion of total monomeric Al as Al_o has increased from an average 26% during the first five years of the study (1982-1986) to 69% during the most recent five years (2007-2011). The current low concentrations of Al_i would suggest that hydrolysis of Al is not contributing nearly the acidity to stream water as in past years.

I report highly significant decreases in DOC concentration in the Oa soil solutions of all elevation zones during the period 1984-2011 (Table 4.1), as well as for the Bs soil solution in the HH zone (Table 4.2). The DOC concentration has also decreased significantly in the streamwater measured at the base of the watershed (Site W6-7), although I observed non-significant declines at the upstream longitudinal stream sampling sites (Table 4.3). The results are surprising considering the widespread phenomenon of increasing DOC in surface waters across Europe and eastern North America (Stoddard et al. 1999; Worrall et al. 2004; Skjelkvåle et al. 2005; Driscoll et al. 2007). Although fewer studies have long-term measurements of soil water DOC concentrations, the DOC in surface water is generally derived from soils so it would be expected that soil water trends should be concurrent with surface water trends. Indeed, increases in streamwater DOC concentrations were linked to increasing concentrations in soil waters in two forested catchments in the western Czech Republic (Hruška et al. 2009). In contrast, several Scandinavian studies have reported trends of decreasing soil water DOC concentrations. Löfgren and Zetterberg (2011) analyzed DOC trends at sites across southern Sweden during the period

1987-2008. Using records from 68 sites with at least 10 years of data, the authors found that DOC concentrations were decreasing at 31 sites, while increasing at only five sites. Similarly, Akselsson et al. (2013) found that DOC concentrations were decreasing in soil water at seven out of nine Swedish sites with at least 19 years of data. Wu et al. (2010) also found largely negative trends in soil water DOC in conifer plots across Norway during the period 1996-2006. Hubbard Brook has characteristics—such as soil type, climate, and historical acid deposition—similar to the Scandinavian sites, so it may not be surprising to find comparable DOC trends in Hubbard Brook soil waters. Löfgren et al. (2010) used the Stockholm Humic Model to investigate DOC solubility in soil water and concluded that DOC trends could be either positive or negative depending on changes in pH, ionic strength, and soil Al pools. They concluded that decreasing ionic strength was driving trends of decreasing DOC in soil water. The Hubbard Brook charge balance (Figure 4.5) clearly shows substantial declines in the major anions and cations in soil water over the past three decades. Hruška et al. (2009), on the other hand, suggested decreasing ionic strength led to DOC increases in soil water at the Czech sites. Löfgren and Zetterberg (2011) indicated that differences in soil sampling depth could influence the DOC concentrations and trends, as the increasing DOC reported at the Czech sites by Hruška et al. (2009) were for samples collected just beneath the forest floor, while the decreasing DOC reported for Swedish sites by Löfgren et al. (2010) were for samples collected at 50 cm depth. My results, however, indicate that DOC in the soil water draining the forest floor has decreased at a more rapid rate than in the mineral soil solutions. It is not clear why DOC trends in forest floor soil solutions at Hubbard Brook would differ so markedly from those measured by Hruška et al. (2009). One potential explanation is the elevated dissolved Al concentrations in Czech sites—as reported for streamwater—relative to values observed at Hubbard Brook. As the model results from Löfgren

et al. (2010) suggest, higher concentrations of dissolved aluminum oxyhydroxides promote higher DOC solubility. Laboratory studies of organic soils show a positive relationship between pH and DOC concentration (Tipping and Hurley 1988; Kennedy et al. 1996). The Hubbard Brook dataset showed invariant pH until the last 10-15 years, after which values have increased significantly (see above). This timeframe appears to coincide with a tapering off of declines in DOC concentrations. I also have not observed increases in soil water concentrations of organic anions, but the marked decreases in concentrations of SO_4^{2-} and NO_3^- have increased the relative importance of organic anions in soil solutions (Figure 4.5).

Similar to the soil waters, DOC concentrations in stream water at Hubbard Brook W6 have previously been reported by Palmer et al. (2004) to decrease during the period 1982-2000 ($-1.40 \mu\text{mol C L}^{-1} \text{ y}^{-1}$; $p = 0.02$). My updated analysis of the period 1982-2011 shows that the DOC concentrations have continued to decline, but at a much slower overall rate ($-0.53 \mu\text{mol C L}^{-1} \text{ y}^{-1}$; $p = 0.04$). Over the most recent 15 years of our dataset, 1997-2011, the DOC concentration of streamwater did not change significantly ($p = 0.41$). This trend in streamwater mirrors soil water observations (see above). Although DOC concentrations have leveled off in recent years, The Hubbard Brook results still contrast with many other sites that show increases in DOC concentration in streams. Burns et al. (2006) observed significant increases in DOC concentrations in 80% of the streams they analyzed in New York's Catskill Mountains. Similar increases have been reported in upland streams in Finland, where eight forested catchments were monitored for 15-29 years (Sarkkola et al. 2009). However, not all studies point to increases in stream DOC concentrations. Worrall and Burt (2007) analyzed the trends in DOC concentrations of 315 sites located across the U.K. with at least 10 continuous years of data. They found that while most had increasing DOC, 55 sites exhibited significant decreasing trends, primarily in

southwestern England. Clair et al. (2008) found decreasing TOC concentrations in the streams of two forested catchments in southwestern Nova Scotia with chemistry records from 1982-2004. Similar to my results, the authors noted that the bulk of the decrease occurred during the 1980s before leveling off in later years. It is difficult to determine the underlying cause of the decline of DOC concentration of W6 streamwater during the 1980s and 1990s, as Hubbard Brook has many characteristics in common with other surface water sites that are experiencing increasing DOC concentrations. The DOC decline in W6 streamwater appears to be driven by the changes in soil solution chemistry described above. It is not clear whether the leveling of DOC concentration I have noted for approximately the past 15 years indicates a long-term steady-state, or potentially the beginning of a reversal toward the increasing DOC trends experienced by many other sites. Continued long-term measurements should answer this question.

The concentrations of NO_3^- in stream water have declined in the lower portion of the watershed (Table 4.3), apparently driven by the particularly pronounced decreasing NO_3^- trends in the soil solutions of the LH zone (Table 4.1; Table 4.2). Atmospheric N deposition has decreased, although I do not directly attribute the decreased NO_3^- leaching in soil solutions and stream water to decreased atmospheric deposition. The decline of NO_3^- export in stream water began in the late 1970s, relatively early in Hubbard Brook's record, after having initially increased from the early 1960s through the mid-1970s (Bernhardt et al. 2005; Yanai et al. 2013). The trend of declining stream NO_3^- is evident throughout the entire annual cycle (Figure 4.7). While concentration decreases have been most marked in the winter and spring, there also has been a distinct lengthening of low NO_3^- during the summer-fall period. The NO_3^- concentration in bulk deposition was relatively constant from approximately 1970 until 2003, after which it has declined (Likens and Buso 2012). The decline in watershed losses of NO_3^- is puzzling, as it runs

counter to the long-standing theories of forest development and nutrient cycling, which suggest that as biomass accumulation slows, N losses should increase if N inputs remain unchanged (Vitousek and Reiners 1975). In fact, predictions have been made that continuous excess N deposition on previously N-limited northern forest systems would lead to a state of “nitrogen saturation,” which should be accompanied by marked increases in stream NO_3^- losses (Aber et al. 1989). Biogeochemical models employed at Hubbard Brook have consistently over-predicted stream NO_3^- compared to measured data since the early 1980s (e.g. Aber and Driscoll, 1997; Gbondo-Tugbawa et al. 2001; Pourmokhtarian et al. 2012). Yanai et al. (2013) found that the recent low streamwater export of N at Hubbard Brook—relative to inputs—could not be explained by measured accumulation of N in the forest floor or vegetation, and the watershed mass balance indicated a missing sink for N. The authors suggested the N budget imbalance could be explained by either increased gaseous loss through denitrification, or increased storage in the mineral soil, for which a statistically significant change is difficult to detect. Indeed, measurements of soil water N species do support the suggestion that NO_3^- is being immobilized in the mineral soil, as fluxes from the Oa horizon are significantly greater than from the Bs horizon (Johnson et al. 2000; Dittman et al. 2007; Yanai et al. 2013). Moreover, Bernal et al. (2012) used isotopic evidence to suggest that denitrification was an unlikely explanation of decreases in stream NO_3^- .

4.3.2. *Snowmelt stream chemistry trends*

My results showed very similar trends between the overall monthly sampling record and observations for snowmelt. Increases in pH and ANC are remarkably similar between the snowmelt record and the overall record. The spring snowmelt is still markedly more acidic than

the remainder of the year ($\sim 10 \mu\text{Eq L}^{-1}$; Figure 4.6), but appears to be recovering from acidification at the same rate as observed for the entire annual cycle. The spring season is prone to episodic acidification as snowmelt waters are often transported via preferential flowpaths in the shallow organic soil where base cations are dilute relative to strong acid anions (Schaefer et al. 1990; Wigington et al. 1990). The results of the Hubbard Brook trend comparison are notable because results suggest that chronic acid deposition may not have depleted base cations in the forest floor to an extent that makes the watershed permanently more susceptible to severe episodic acidification during high flow events. However, the snowmelt samplings did not necessarily coincide with the absolute highest discharge events during snowmelt. Rather, monthly sampling during snowmelt is assumed to be generally representative of the seasonal characteristics.

For most solutes, the changes in stream snowmelt concentrations from 1982-2011 did not significantly differ from the trends in the overall record (Table 4.4). The only exception we found was for NO_3^- , which has been decreasing more rapidly during the snowmelt period ($-0.28 \mu\text{mol L}^{-1} \text{y}^{-1}$) than for the overall record ($-0.03 \mu\text{mol L}^{-1} \text{y}^{-1}$). The relatively rapid long-term decline in stream NO_3^- concentrations observed during snowmelt was likely driven by decreased atmospheric deposition of NO_3^- . Sebastyen et al. (2008) used isotopic evidence at Sleeper's River, Vermont to show that during baseflow conditions, stream NO_3^- is almost exclusively derived from nitrification in the soil, while during early and peak snowmelt, atmospheric inputs account for a considerable portion of the NO_3^- in stream water. During snowmelt, NO_3^- derived from atmospheric deposition that had accumulated in the snowpack can be transported directly to the streams via overland or shallow subsurface flowpaths with little transformation. The decreased NO_3^- deposition that has occurred over approximately the past 10 years would be

expected to disproportionately affect the trend during the snowmelt seasons, as this is the period of the annual cycle when stream NO_3^- is most likely to be sourced most directly from deposition.

DOC concentrations, somewhat in contrast to NO_3^- , are decreasing overall ($-0.53 \mu\text{mol C L}^{-1} \text{ y}^{-1}$; $p = 0.04$), but show no significant trend during the snowmelt season ($p = 0.98$). The overall declines in DOC concentrations of stream water seem to be primarily driven by decreased leaching of DOC from the Oa soil horizons. The unchanged concentrations of DOC observed in stream water during snowmelt are puzzling, as I also observed highly significant declines in DOC concentrations in Oa soil water during snowmelt that were similar in magnitude to those observed throughout the year. Furthermore, snowmelt is the period of the year when the Oa horizon would be expected to be the most hydrologically connected to the stream due to high flows and I would therefore have anticipated the hydrochemical trends of streamwater and Oa soil water to more closely match.

4.3.3. Future of recovery and ecosystem health

While these results suggest that base cations have not been depleted from the forest floor to such a degree as to inhibit recovery from acidification during the high flow (and relative acidic) snowmelt period, it is likely that a depletion of exchangeable base cations from the soil is slowing the overall recovery and affecting forest health. In acid-sensitive soils, deposition of strong acid anions displaces base cations faster than they can be replaced through mineral weathering processes or atmospheric cation deposition. This alteration of the soil base status has limited recovery in surface water ANC at Hubbard Brook and across the northeastern U.S., despite marked reductions in acidic deposition (Likens et al. 1996; Lawrence et al. 1999; Palmer et al. 2004). A watershed-scale calcium silicate addition was conducted at Hubbard Brook's

Watershed 1 (W1) in 1999 as an experiment to test the effects of replacing Ca lost due to acidic deposition. Indeed, this Ca manipulation at W1 has resulted in mitigation of acidification and is supplying ANC to drainage waters (Cho et al. 2012).

Acidic deposition can permanently affect the composition and health of forest ecosystems. Red spruce has been severely impacted by acidic deposition across the northeastern U.S., including growth declines and mortality. Acidic deposition affects red spruce directly by leaching Ca from the needles (DeHayes et al. 1999), and indirectly by changing underlying soil chemistry (Cronan and Grigal 1995). Acid-impacted soils were found to be a factor explaining impaired growth of sugar maple (Duchesne et al. 2002). The highest incidences of sugar maple dieback in Pennsylvania were found to be at sites with low supply of Ca and Mg to soil and foliage and where stress from drought and insect defoliation was highest (Horsley et al. 2000). Studies of sugar maple health and seedling survivorship at Hubbard Brook have shown that the species has fared significantly better since the Ca amendment in W1 relative the reference W6 (Juice et al. 2006; Battles et al. 2014).

4.4. Summary and Conclusions

Drainage waters at Hubbard Brook are slowly recovering from acidic deposition, including small increases in pH and ANC, as well as decreases leaching of base cations and mobilization of Al_j . I also observed a pattern of long-term decreases in snowmelt acidification that were largely similar to the overall trends. Hydrologic conditions make snowmelt the most acidic period of the annual cycle and results suggest that the susceptibility to high flow-driven episodic acidification is slowly improving.

The observed recovery has been driven in part by declines in the atmospheric deposition of acidic compounds. Deposition of SO_4^{2-} has declined steadily throughout the 30 years of monitoring due to regulations on emissions through the Amendments to the Clean Air Act, and the deposition of NO_3^- has declined over the past decade due to emissions controls put in place through the NO_x Budget Trading Program. While a sustained decline in SO_4^{2-} deposition and subsequent leaching in drainage waters has occurred, the overall recovery of stream and soil water from acidification is slowed by SO_4^{2-} exports that exceed inputs due to mobilization of SO_4^{2-} stored in the soil as a legacy of decades of elevated deposition. The recent decrease in NO_3^- deposition has contributed to the decreased acidity of precipitation and likely has further reduced leaching of base cations, but the decline in streamwater NO_3^- concentrations began prior the trend of lower deposition, reflecting the complex dynamics of nitrogen in the ecosystem that are not completely understood. I also observed overall negative trends in DOC concentrations, which make Hubbard Brook somewhat of an anomaly considering many similar systems have experienced increased DOC concentrations. These trends, however, appear to have flattened over approximately the past 15 years and it is possible they will reverse to mirror the patterns seen elsewhere. These shifts are changing the character of soil and stream solutions at Hubbard Brook, from waters previously dominated by strong acid anions (i.e., SO_4^{2-} , NO_3^-), to solutions increasingly dominated by naturally occurring organic matter. Continued monitoring should provide insight into the future of DOC and NO_3^- dynamics, both of which directly and indirectly influence acid-base conditions. I also anticipate sustained monitoring to resolve the rate at and the extent to which all recovery trends continue. Recovery from acidification in drainage water could accelerate if the deposition of acidic compounds continues to decline and the legacy SO_4^{2-} stored in soil is gradually depleted.

Table 4.1. Long-term trends in organic horizon (Oa) soil water chemistry, 1984-2011a.

		pH	C _B	C _A	ANC	Ca	SO ₄ ²⁻	NO ₃ ⁻	Al _i	Al _o	DOC
Low Hardwood	slope	-0.003	-3.64	-3.20	-0.33	-2.05	-1.18	-1.55	+0.04	-0.20	-25.09
	P	0.58	<0.01	<0.01	0.40	<0.01	<0.01	<0.01	0.07	<0.01	<0.01
High Hardwood	slope	+0.000	-2.51	-3.13	+0.80	-1.40	-1.54	-1.22	-0.09	-0.28	-15.81
	P	0.97	<0.01	<0.01	0.16	<0.01	<0.01	<0.01	0.06	<0.01	0.02
Spruce-Fir-Birch	slope	+0.004	-1.80	-2.71	+0.93	-0.94	-2.25	-0.13	+0.05	-0.37	-23.79
	P	0.05	<0.01	<0.01	0.01	<0.01	<0.01	0.12	0.05	<0.01	<0.01

^aSlope units for C_B, C_A, ANC, Ca, SO₄²⁻, and NO₃⁻ are $\mu\text{Eq L}^{-1} \text{y}^{-1}$. Units for DOC are $\mu\text{mol C L}^{-1} \text{y}^{-1}$.

Table 4.2. Long-term trends in mineral horizon (Bs) soil water chemistry, 1984-2011a.

		pH	C _B	C _A	ANC	Ca	SO ₄ ²⁻	NO ₃ ⁻	Al _i	Al _o	DOC
Low Hardwood	slope	-0.002	-2.13	-2.48	+0.43	-1.56	-1.74	-0.34	+0.01	-0.05	-0.67
	P	0.56	<0.01	<0.01	0.12	<0.01	<0.01	<0.01	0.85	<0.01	0.15
High Hardwood	slope	+0.006	-0.70	-2.59	+2.04	-0.34	-2.37	-0.09	-0.48	-0.19	-3.68
	P	0.02	<0.01	<0.01	<0.01	<0.01	<0.01	0.19	<0.01	<0.01	<0.01
Spruce-Fir-Birch	slope	+0.000	-0.92	-3.25	+2.46	-0.51	-2.97	-0.03	-0.68	-0.18	+3.33
	P	0.99	<0.01	<0.01	<0.01	<0.01	<0.01	0.38	<0.01	<0.01	0.22

^aSlope units for C_B, C_A, ANC, Ca, SO₄²⁻, and NO₃⁻ are $\mu\text{Eq L}^{-1} \text{y}^{-1}$. Units for DOC are $\mu\text{mol C L}^{-1} \text{y}^{-1}$.

Table 4.3. Long-term trends in stream water chemistry, 1982-2011^a.

Site	Elevation (m)		pH	C _B	C _A	ANC	Ca	SO ₄ ²⁻	NO ₃ ⁻	Al _i	Al _o	DOC
W6-1	751	slope	+0.004	-1.30	-2.97	+1.79	-0.50	-2.48	-0.01	-0.10	-0.37	-1.54
		P	0.04	<0.01	<0.01	<0.01	<0.01	<0.01	0.01	0.14	<0.01	0.79
W6-2	732	slope	+0.005	-1.08	-2.86	+1.94	-0.58	-2.54	0.00	-0.22	-0.18	+1.20
		P	<0.01	<0.01	<0.01	<0.01	<0.01	<0.01	0.68	<0.01	<0.01	0.54
W6-3	701	slope	+0.004	-0.97	-2.54	+1.74	-0.58	-2.14	-0.13	-0.39	-0.10	+1.48
		P	0.02	<0.01	<0.01	<0.01	<0.01	<0.01	0.06	<0.01	<0.01	0.22
W6-4	663	slope	+0.004	-0.92	-2.29	+1.48	-0.53	-1.84	-0.16	-0.40	-0.08	-0.77
		P	0.02	<0.01	<0.01	<0.01	<0.01	<0.01	<0.01	<0.01	<0.01	0.18
W6-5	602	slope	+0.009	-0.87	-2.18	+1.37	-0.61	-1.76	-0.08	-0.36	-0.06	-0.08
		P	<0.01	<0.01	<0.01	<0.01	<0.01	<0.01	<0.01	<0.01	<0.01	0.88
W6-7	544	slope	+0.010	-1.13	-1.94	+0.88	-0.80	-1.54	-0.04	-0.19	-0.04	-0.53
		P	<0.01	<0.01	<0.01	<0.01	<0.01	<0.01	<0.01	<0.01	<0.01	0.04

^aSlope units for C_B, C_A, ANC, Ca, SO₄²⁻, and NO₃⁻ are $\mu\text{Eq L}^{-1} \text{y}^{-1}$. Units for DOC are $\mu\text{mol C L}^{-1} \text{y}^{-1}$.

Table 4.4. Comparison between trends of overall stream chemistry record and the trends during the snowmelt seasons, 1982-2011, at site W6-7.

Parameter		Overall trend	Snowmelt trend
pH	slope	+0.010	+0.009
	P	<0.01	0.02
C _B	slope	-1.13	-1.21
	P	<0.01	<0.01
C _A	slope	-1.94	-2.00
	P	<0.01	0.01
ANC	slope	+0.88	+0.91
	P	<0.01	<0.01
Ca	slope	-0.80	-0.82
	P	<0.01	<0.01
SO ₄ ²⁻	slope	-1.54	-1.44
	P	<0.01	<0.01
NO ₃ ⁻	slope	-0.03	-0.28
	P	<0.01	0.01
Ali	slope	-0.19	-0.25
	P	<0.01	<0.01
Alo	slope	-0.04	-0.04
	P	<0.01	0.04
DOC	slope	-0.53	+0.08
	P	0.04	0.98

^aSlope units for C_B, C_A, ANC, Ca, SO₄²⁻, and NO₃⁻ are $\mu\text{Eq L}^{-1} \text{y}^{-1}$. Units for DOC are $\mu\text{mol C L}^{-1} \text{y}^{-1}$.

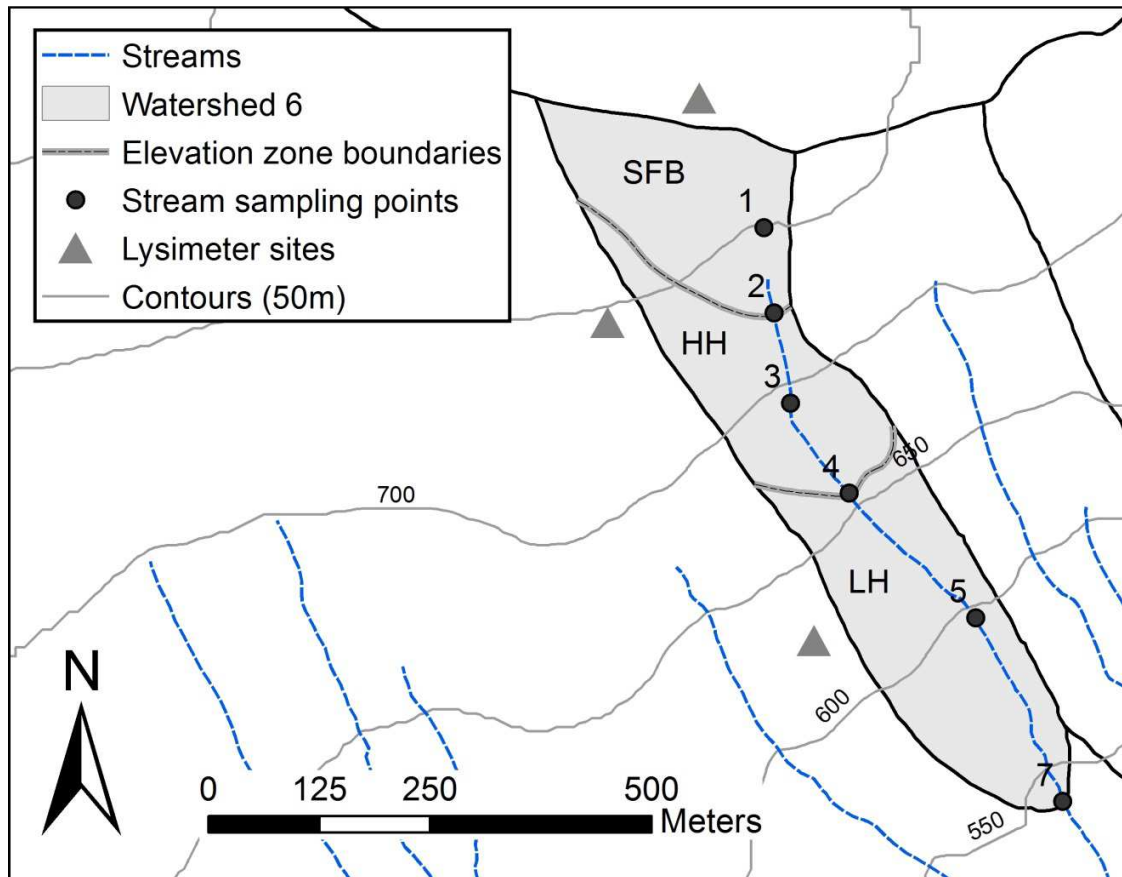


Figure 4.1. Map of Watershed 6 at the Hubbard Brook Experimental Forest (43°56'N, 71°45'W), showing locations of lysimeter plots and stream sampling points relative to the elevation zones.

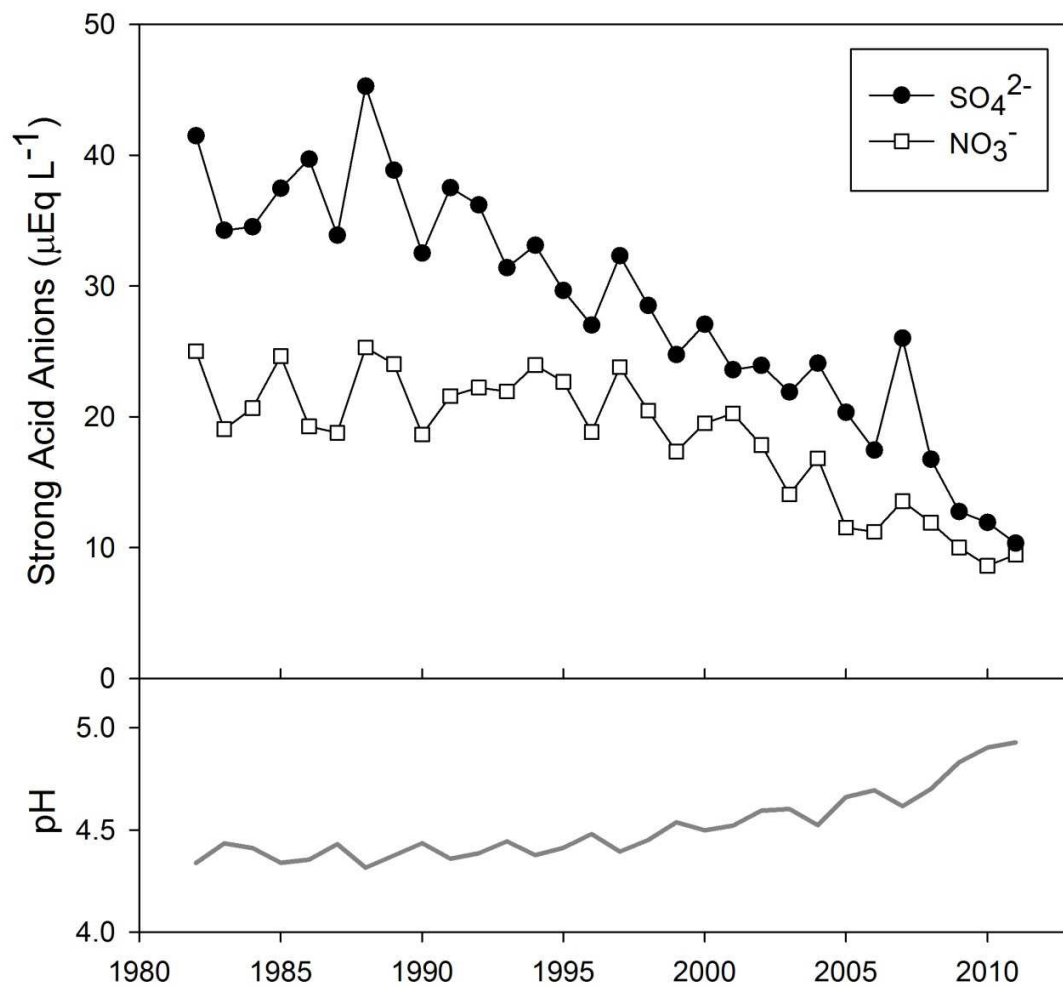


Figure 4.2. Precipitation-weighted mean annual wet deposition values for SO_4^{2-} and NO_3^- (top panel), and pH (lower panel) from 1982-2011. Data were obtained from the National Atmospheric Deposition Program (NH02).

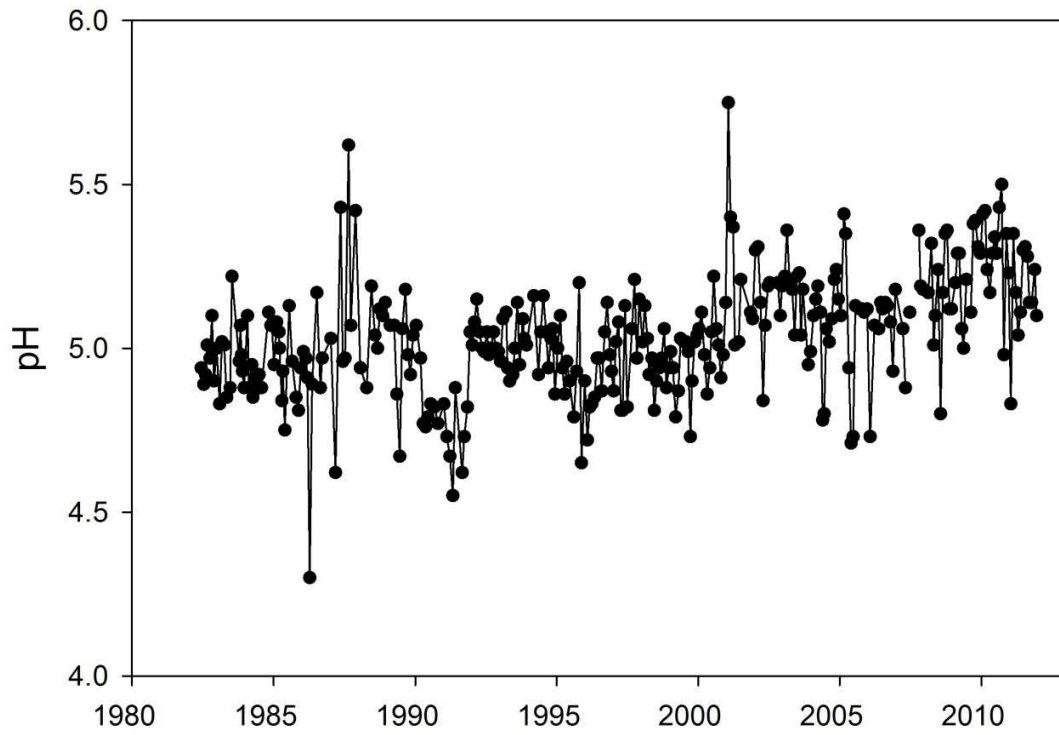


Figure 4.3. pH of stream water at the W6 gauging station, 1982-2011.

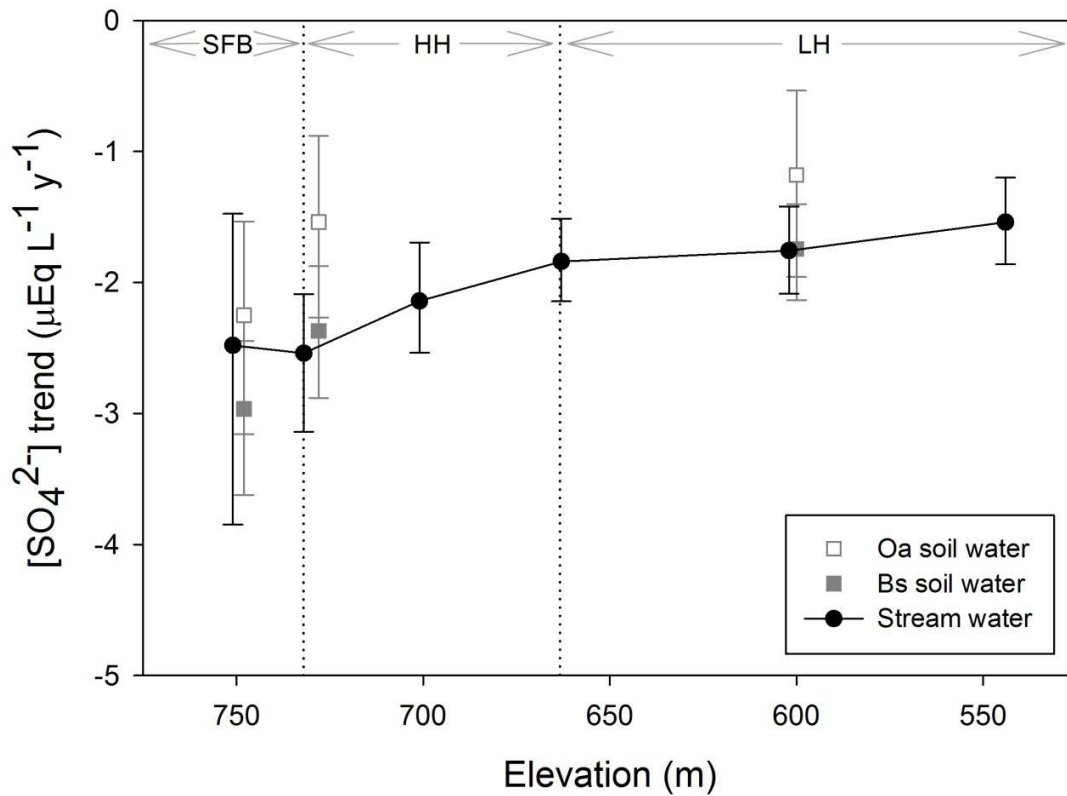


Figure 4.4. SO_4^{2-} concentration trends (1984-2011) vs. elevation for W6 soil water and stream water. Median trends are estimated by SKT analysis. Vertical bars represent 95% confidence intervals. Transitions between elevation zones are marked with vertical dotted lines.

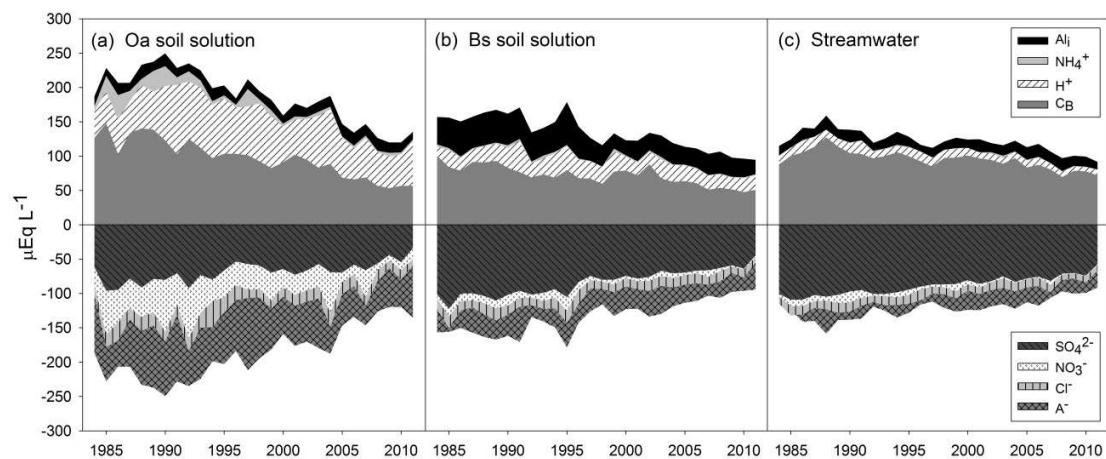


Figure 4.5. Soil solution and streamwater charge balances represented by annual volume-weighted concentrations of major ions in a) Oa horizon, b) Bs horizon, and c) streamwater. Cation charge is expressed by positive values of $\mu\text{Eq L}^{-1}$, while anion charge is negative. Organic anion concentrations (A^-) were calculated from the charge discrepancy of measured positive and negative species (Driscoll et al. 1989). Soil solution values are weighted by elevation zone to represent the entire watershed; streamwater values are from the gauging station at the base of the watershed.

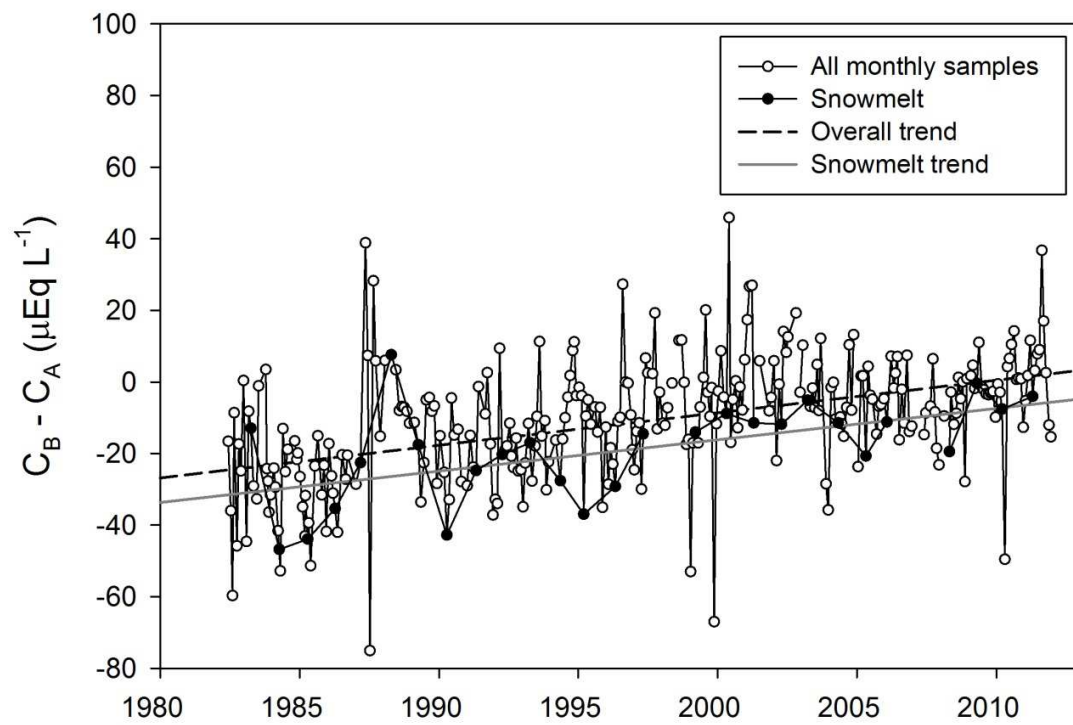


Figure 4.6. Trends in acid neutralizing capacity, as calculated $C_B - C_A$, from 1982-2011. Trend slope for the overall dataset estimated using SKT. Snowmelt trend is calculated by Mann Kendall analysis.

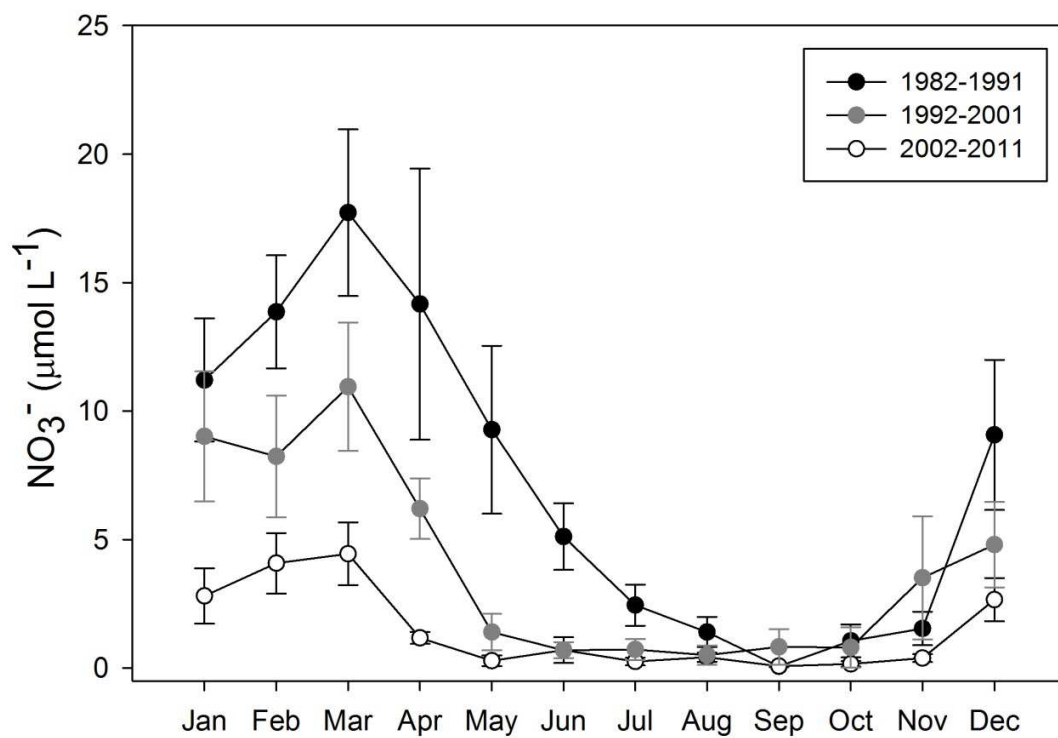


Figure 4.7. Mean monthly NO_3^- concentrations of stream water draining W6 for 1982-1991 and 2002-2011. Vertical bars indicate standard errors.

5. Leaching of nitrate and dissolved organic carbon in soil solutions across a natural gradient of winter climate and soil freezing

5.1. Methods

5.1.1. Plot selection and characterization

Twenty individual plots were set up during the fall of 2010 at Hubbard Brook along an elevation gradient from 375 to 775 m to evaluate the role of climatic variation in controlling NO_3^- and DOC leaching in soil solutions. The plots were selected to capture the variability of winter climate across the valley and were located on both north and south-facing slopes throughout the elevation range (Figure 5.1). The climate gradient encompasses a 2.0°C variation in winter air temperature, approximately the same as predicted temperature changes due to climate change across the northeastern U.S. during the next 50-100 years (Hayhoe et al. 2007). Plots were selected to have the same forest composition. Specifically the presence of dominant canopy sugar maples was chosen because previous soil freezing manipulations have shown most consistent biogeochemical responses in sugar maple stands (Fitzhugh et al. 2001; Groffman et al. 2001b, 2011). The plots were each 10 m in diameter and located a minimum 300 m from each other.

5.1.2. Lysimeter installation and sampling

Of the 20 plots used in the gradient study, four had pre-existing zero tension lysimeters: one located west of Watershed 6 (Driscoll et al. 1988), two located in Watershed 1 (Cho et al. 2010), and one located near the Mt. Kineo trail (Groffman et al. 2011). At each of the 16 other plots tension-free lysimeters were installed during September and October of 2010. One plot was

moved following the spring of 2011 (Table 5.1) to improve accessibility to the plot and expand the elevational range on the south-facing slopes. Lysimeter cups were constructed from angled cross sections of 4 inch diameter PVC pipes, which drain via PVC tubing to 2-L polyethylene reservoirs. A soil pit was excavated at each site and the lysimeter collectors were inserted in the upslope face of the soil pit just beneath the forest floor (Oa horizon), and within the Bs horizon. The soil pits were backfilled to prevent water accumulation and to ensure thermal conditions of the soil were not disturbed.

The tension-free lysimeters collected soil water continually and were evacuated approximately monthly following installation. Roughly six months following installation were allowed for the disturbance effects on chemistry to subside; NO_3^- concentrations were used as an indicator of soil disturbance. Sampling for data collection commenced in March 2011 and continued approximately monthly through September 2012, providing two years of data for the snowmelt period and growing season.

5.1.3. Winter climate monitoring

Each plot was monitored approximately biweekly with measurements of snow depth and soil frost depth during the winters of 2010-2011 and 2011-2012. The snow depth was recorded as the mean of three locations in each plot. Snow depth and snow-water equivalence was measured using Federal (Mt. Rose) snow tubes. Three replicate soil frost tubes were installed during the fall of 2010 at each plot according to the methods outlined by Hardy et al. (2001). These consisted of removable PVC tubes filled with methylene blue dye, which turns a purple color when frozen and thus allows personnel to visually measure the depth of frozen water. Soil

temperature and volumetric water content were continuously recorded at 5 cm depth with Decagon 5TM combination probes connected to Decagon EM50 dataloggers.

5.1.4. Laboratory analysis

Soil solution samples were measured for NO_3^- concentrations using ion chromatography (Dionex, Sunnyvale, CA). Dissolved organic carbon (DOC) was analyzed through persulfate oxidation followed by infrared CO_2 detection (Teledyne Tekmar, Mason, OH).

5.1.5. Computative methods and statistics

Soil solution chemistry data were compared with variables representative of the winter climate gradient encompassed by the 20 plots for each of the two winters. The maximum frost depth from the biweekly measurements was selected as an indicator of frost intensity variation. The SDL coefficient of variation (standard deviation of log-transformed soil temperature observations) was chosen as a measure of winter soil temperature variability and an indicator of frequency of freeze and thaw events during the winter. Snowpack variation between sites was characterized by creating a 'snowpack' variable, the area under the curve when snow depth is plotted against time.

Regression analysis was used to explore the relationship between concentrations of soil solution DOC and NO_3^- and winter climatic variables. Previous research on soil frost effects on soil solution chemistry have reported differing effects between early and late summer (Fitzhugh et al. 2001; Haei et al. 2010). Therefore, the soil solution chemistry data were grouped as mean concentrations for each plot for both the early growing season (May through July) or late

growing season (August and September). Paired t-tests were used to compare mean DOC and NO_3^- concentrations between the two years of the study.

5.2. Results

5.2.1. *Characterization of winter climate gradient*

Across the 20 monitoring plots, snowpack accumulation was markedly higher during the winter of 2010-2011 compared to 2011-2012 (Figure 5.2), while maximum soil frost depths and SDL of winter soil temperature were generally greater during the winter of 2011-2012. The relationship between snow depth and soil frost was significant and negative during the second winter, but no significant relationship was observed during the first winter (Figure 5.3).

5.2.2. *Soil solution NO_3^- concentrations*

Soil solution NO_3^- concentrations varied greatly among sites, but were consistently higher in the Oa compared to the Bs horizon. Nitrate varied seasonally in both horizons, with the highest concentrations found in the spring and winter, and a marked decrease during the summer months (Figure 5.4). Comparison between the two years of study revealed that concentrations of NO_3^- in Oa-horizon soil solutions during the early growing season months were higher in 2011 compared to 2012 ($p < 0.01$), while the Bs solution concentrations were higher in 2012 ($p = 0.03$) (Figure 5.5).

Analysis of NO_3^- concentrations in soil solutions as a function of the winter climate variable for snow and soil freezing revealed no significant relationships across the gradient of plots (Figure 5.6, Figure 5.7). High variation was noted for NO_3^- concentrations among sites,

with mean values in the Oa horizon ranging from 5.7 to 245 $\mu\text{Eq L}^{-1}$, and from less than 0.1 up to 29.5 $\mu\text{Eq L}^{-1}$ in the Bs horizon during the early growing season of 2011.

5.2.3. Soil solution DOC concentrations

In contrast to NO_3^- concentrations, soil solution DOC was highest in the summer and lowest in the winter. Markedly lower concentrations were measured in the Bs horizons compared to the Oa horizon (Figure 5.4). The DOC concentrations in soil solutions were similar overall between the growing seasons of 2011 and 2012 (Figure 5.5). Mean concentrations in the Oa horizon were modestly greater during the early growing season in 2012 relative to 2011 ($p = 0.11$), but the Bs solutions showed no sign of difference ($p = 0.93$).

Positive relationships ($p < 0.10$) between DOC concentrations in soil solutions and the winter soil variable *SDL winter soil temperature* were found in the solutions of the Oa horizon during May-July 2011 (Figure 5.8), and between *maximum frost depth* and *SDL winter soil temperature* in the Oa horizon solutions in 2012 (Figure 5.9). Generally these relationships were not found in the solutions of the Bs horizon, though a modest positive relationship between DOC and soil frost depth existed in the Bs horizon during the early growing season of 2012 (Figure 5.9). A significant relationship also existed between Oa soil water DOC and *SDL winter soil temperature* during the snowmelt of 2012 ($p = 0.04$). By the late growing season (August-September) of both years, no relationship between DOC concentration in soil solution and the previous winters' soil freezing variables was evident (Figure 5.10 and Figure 5.11)

Soil solution DOC concentrations were generally unrelated to corresponding NO_3^- concentrations. A weak positive relationship in the Oa horizon was noted for the early growing

season of 2011, although less than 10% of the variation in NO_3^- concentrations could be explained by DOC.

5.3. Discussion

A positive relationship between maximum soil frost depth and the SDL of winter soil temperature was observed for the winter of 2011-2012, but not for 2010-2011. This reflects the lower snowpack accumulation during the second winter, which exposed the soil to greater temperature variability, including greater soil freezing intensity during particularly cold days. During the winter of 2010-2011 the snowpack was relatively deep across all sites. This insulated the soil well throughout most of the winter, though early in the winter soils were exposed to freezing at some sites. Overall these results suggest that a more pronounced soil frost gradient would be observed during years with lower overall snowpack accumulation, ranging from reasonably well-insulated soils with little frost at higher elevations and on north-facing slopes to more exposed soils with deeper frost at the lower elevations and the south-facing side of the valley. Using a natural gradient of winter climate, as opposed to a snow removal manipulation, has the advantage of capturing the dynamics of snow-soil frost interactions under actual ambient soil temperature variations.

5.3.1. *DOC mobilization after soil freezing*

The results presented in the chapter suggest a positive relationship between soil freezing (and freeze/thaw cycles, as indicated by SDL of winter soil temperature) and the concentration of DOC in soil solutions, especially those draining the Oa horizon. The relationship was much more distinct during the second year of the study when soil frost was more pronounced. This likely

reflects the marked overall differences between the two winters. The winter of 2011-2012 had a much lower average snowpack than the winter of 2010-2011, which exposed the soil both to greater frost depths at most sites, as well as greater susceptibility to freezing and thawing as air temperatures changed (Figure 5.2). The results presented here corroborate other field or laboratory studies that link soil frost, and freeze/thaw cycles, to increased DOC leaching in soil solutions (e.g. Hentschel et al. 2008; Haei et al. 2010; Campbell et al. 2014).

In a long-term soil frost manipulation experiment in northern Sweden, Haei et al. (2010) found that soil solution DOC concentrations during the spring and summer were positively related to the duration of soil frost during the previous winter. Kalbitz et al. (2000) noted that previous studies have shown freeze and thaw cycles increase DOC release from soils and speculated that a physical disruption of the soil matrix could make previously stabilized soil organic matter more available for leaching. Campbell et al. (2014) observed a pulse of DOC in leachate from Hubbard Brook soils treated under severe frost (-15°C) conditions in the laboratory and noted that the quality of DOC (as indicated by SUVA_{254}) also increased. They speculated that the pulse of DOC could have originated from microbial cells lysed during the severe frost treatment. Haei et al. (2012) also found increased lability of DOC leached from laboratory freeze experiments with Swedish boreal soils and speculated a microbial origin. However, in a laboratory experiment with German forest soils, Hentschel et al. (2008) found a pulse of DOC following initial freezing and thawing, but they noted that the DOC quality did not change as a treatment effect and that soil freezing had mobilized DOC with lignin content too high to be derived from microbial lysis.

The DOC results I present here are consistent with soil frost causing a physical disruption of the soil matrix which results in the prolonged release of DOC for several months following

snowmelt rather than one pronounced pulse. Furthermore, the somewhat stronger relationship between DOC mobilization and SDL of winter soil temperature compared to maximum frost depth also suggests that higher frequency freezing and thawing of the organic soil is more disruptive to the soil matrix than simply maximum frost intensity, though the biweekly monitoring of frost depth may have been insufficient to capture the true extent of maximum soil frost depths. The lack of relationship between DOC concentrations and previous winter soil frost during the later sampling dates (August-September) indicates that the soils had stabilized after several months or the most easily leachable DOC had been depleted.

5.3.2. Variable response of NO_3^- to soil freezing

The results presented here showed no clear relationship between the winter climate variables investigated and the concentrations of NO_3^- in soil solutions for either winter. Previous investigations into the response of NO_3^- leaching to soil freezing events have shown varying results. A snowpack manipulation (reduction by shoveling) study at the HBEF during the winters of 1997-1998 and 1998-1999 showed a strong treatment effect in the NO_3^- leaching response to induced soil frost. Fitzhugh et al. (2001) found NO_3^- concentrations in soil solutions greater than $400 \mu\text{mol L}^{-1}$ during the growing season in the Oa horizon of treatment plots with sugar maple, compared to less than $100 \mu\text{mol L}^{-1}$ in the non-manipulated reference plots. They also found treatment effects in the Bs horizons. Boutin and Robitaille (1995) found similar results following a snow removal experiment in a sugar maple stand in Québec. However, Groffman et al. (2011) found little treatment effect on NO_3^- in soil solution to a snow manipulation study conducted in sugar maple stands at the HBEF during the winters of 2002-2003 and 2003-2004.

Discrepancies have also been noted when looking for changes in streamwater export of NO_3^- following widespread soil freezing events. Fitzhugh et al. (2003) investigated the deviations in streamwater chemistry in Hubbard Brook's W6 long-term record and found significantly increased annual fluxes of stream NO_3^- following soil freezing events only during the earlier years of the record, the 1970s. The later years (1990s) of the record showed no conclusive relationship between soil freezing and NO_3^- response at the watershed level. Similarly, Judd et al. (2011) predicted widespread soil freezing during the winter of 2005-2006 would lead to increased NO_3^- runoff, but found the concentrations in 2006 at W6 to be the lowest on record. Studies at other sites have also produced variable results. Laboratory freeze treatments of soil cores from a Norwegian heathland produced increased leaching of NH_4^+ and decreased leaching of NO_3^- (Austnes and Vestgarden 2008), while severe frost treatment of HBEF soil cores by Reinmann et al. (2012) led to lower losses of both NO_3^- and NH_4^+ .

These variable and apparently contradictory results suggest that the response of NO_3^- leaching to soil freezing is subject to more complex controls than simply the presence of soil frost. The marked increases in soil solution NO_3^- reported by Fitzhugh et al. (2001) were attributed to reduced growing season N uptake by sugar maple fine roots, which had been damaged by the soil freezing. Tierney et al. (2001) observed significantly increased fine-root mortality resulting from those soil freeze treatments. The response of NO_3^- leaching to soil freezing events may be regulated by the degree to which fine roots are damaged. The soil temperatures experienced during soil freezing events are typically not cold enough to directly kill roots ($>4^\circ\text{C}$), so a physical disruption of the soil matrix, such as frost heaving, may be responsible for fine-root mortality. Cleavitt et al. (2008) however found no relationship between measured frost heaving and fine-root mortality at the Hubbard Brook snow manipulation plots

studied in the winters of 2002-2003 and 2003-2004 and suggested cellular damage caused fine-root mortality.

Groffman et al. (2011) hypothesized that the differing responses of NO_3^- leaching to soil freezing events could be driven by interactions between C and N responses or interannual variability of C and N dynamics in the forest. Indeed, the results I found indicated a moderate DOC mobilization in response to soil freezing (and especially freezing and thawing cycles) but no NO_3^- response. This supports the hypothesis (Groffman et al. 2011) that when soil freezing mobilizes DOC, the increased DOC availability can suppress losses of NO_3^- . These results are also consistent with soil-freezing manipulation studies that found opposite or differing responses of DOC. The earliest freeze treatment study at Hubbard Brook produced marked increases in NO_3^- leaching and no significant effect on DOC (Fitzhugh et al. 2003). In contrast, a field snow manipulation in Norway resulted in increased DOC leaching but no increases in NO_3^- (Austnes et al. 2008; Kaste et al. 2008). However, the laboratory treatments by Austnes and Vestgarden (2008) found increased DOC and decreased NO_3^- mobilization following freezing of soil cores. These often opposing responses of DOC and NO_3^- are consistent with the theory that if and when DOC is mobilized as a response to soil freezing disturbance, a corresponding response of NO_3^- may be prevented by increased microbial N immobilization or denitrification as an effect of freshly mobilized DOC becoming available as a labile carbon source. Mørkved et al. (2006) noted pulses of N_2O following soil freeze and thaw and attributed them to increases in denitrification resulting from increased availability of DOC to fuel microbial denitrifiers. Experimental additions of labile DOC have been shown to dramatically reduce NO_3^- runoff losses through increased microbial N immobilization or denitrification (e.g. Bernhardt and Likens 2002; Sobczak et al. 2003). Also, increased DOC availability has been hypothesized to

underlie the widespread trend of decreasing NO_3^- concentrations in streams across the northeastern U.S. (Goodale et al. 2005).

5.3.3. *Winter climate change implications*

The contrasting winter conditions in the two years of this study, and gradients of winter variables within the HBEF, illustrate that changes in snowpack accumulation can have marked effects on soil freezing intensity and frequency. Campbell et al. (2010) have shown that the winter climate at Hubbard Brook has been warming and that snowpacks have been decreasing, especially at lower elevations and on the south-facing side of the valley. Continued warming should be expected to decrease winter snowpack accumulation further and in more widespread areas, exposing soils to greater temperature variability and frost development. My results show that the sites with the thinnest snow cover and greatest soil freezing are the most likely to respond with leaching of DOC during the months following winter. This finding has implications for the carbon balance of soils and nutrient cycling under future climate scenarios, suggesting a potential for increased loss of soil organic carbon following soil freezes. It also underscores the need to investigate how climate-driven changes in DOC mobilization may be affect long-term trends in surface water DOC concentrations.

5.4. Summary and Conclusions

The results of this chapter demonstrate that reduced insulation of soil associated with decreased winter snowpack accumulation can lead to increased soil frost formation and greater susceptibility to midwinter freeze and thaw cycles. Increases in soil frost intensity and soil freeze/thaw events can, in turn, lead to changes in the soil solution chemistry. Increased DOC

mobilization was found in soils most affected by freezing. The effect persisted for several months into the growing season before stabilizing, indicating a likely soil matrix disruption which exposed more readily leachable DOC. I observed the strongest response in the Oa horizon, consistent with the greater exposure of the upper soil horizons to freeze disturbance and greater concentrations of organic matter. I found no relationship between soil freezing measures and soil solution NO_3^- concentrations. Other studies have shown conflicting responses of NO_3^- leaching and the results presented here are consistent with the hypothesis that a mobilization of labile DOC in soils may prevent a NO_3^- increase by stimulating microbial N immobilization. These results are important considerations for the future of C and N dynamics in forest ecosystems which are likely to experience more frequent or severe soil freezing events as climate change results in decreased snowpack accumulation.

Table 5.1. Winter climate gradient sites with soil lysimeters.

Plot	Elevation (m)	Aspect	Experimental watershed
IL1	375	S	None
IL2	401	S	None
IL3	511	S	None
IH1	539	N	None
IH2	555	N	None
IH3	595	N	None
E1	588	N	None
E2	687	N	None
E3	770	N	None
E4	632	N	W7
E5	724	N	W7
E6	536	S	W3
E7	609	S	W3
E8	630	S	W3
E9	670	S	W3
E10 ¹	698	S	W1
E11A	706	S	West of W6
E11B	766	S	West of W6
E12	688	S	West of W6
E13	601	S	West of W6
E14 ¹	487	S	W1

Plot names designated with “IL” or “IH” indicate “intensive low” or “intensive high” elevation, and were subject to additional research activities by collaborators (results not presented here). Plots with designation “E#” are categorized as “extensive.” Soil water lysimeter setup was identical across all plots.

¹Plots E10 and E14 were not included in study of soil solution chemistry due to location in W1, which was experimentally treated with an addition of calcium silicate in 1999 to mitigate acidification.

²Plot E11B was added to replace E11A during summer 2011. E11A is used in the 2011 analysis. E11B was used in the 2012 analysis.

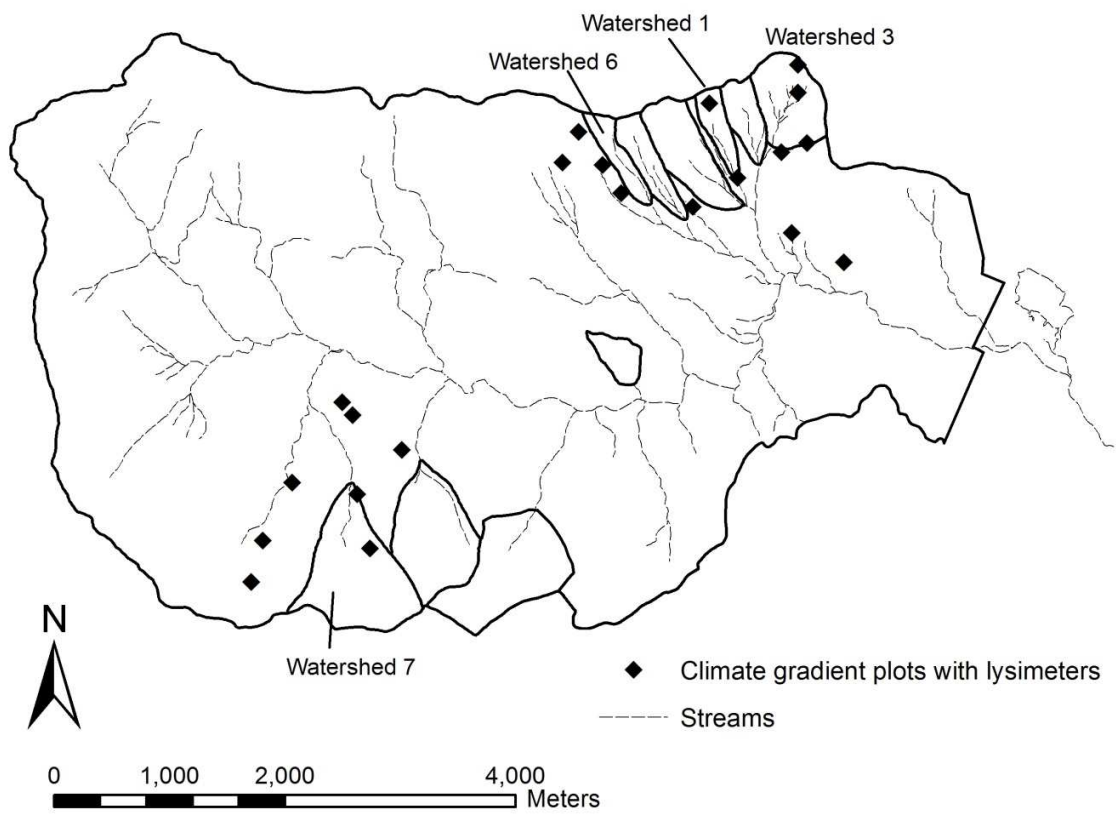


Figure 5.1. Map of the HBEF with winter climate gradient lysimeter sites indicated.

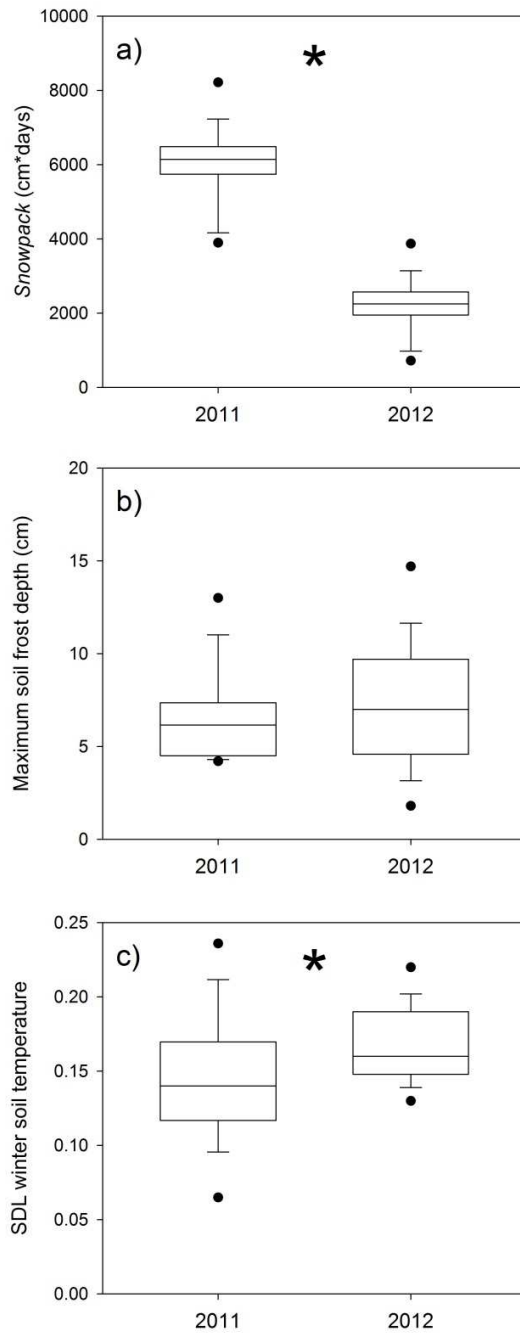


Figure 5.2. Boxplots of 2011 and 2012 winter climate variables across all monitoring plots, a) snowpack, b) maximum soil frost depth, and c) SDL winter soil temperature. Statistically significant differences ($p < 0.05$), as analyzed by paired t-test, are marked by *.

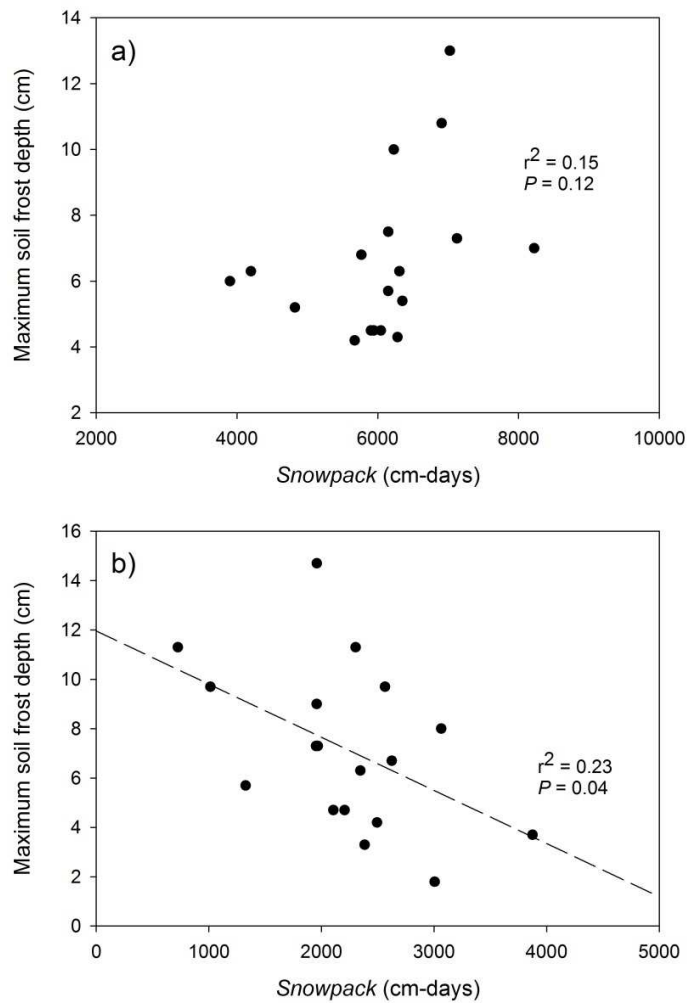


Figure 5.3. Relationship between maximum soil frost depth and the *Snowpack* variable for the winter of a) 2010-2011 and b) 2011-2012 across 20 winter climate gradient monitoring plots.

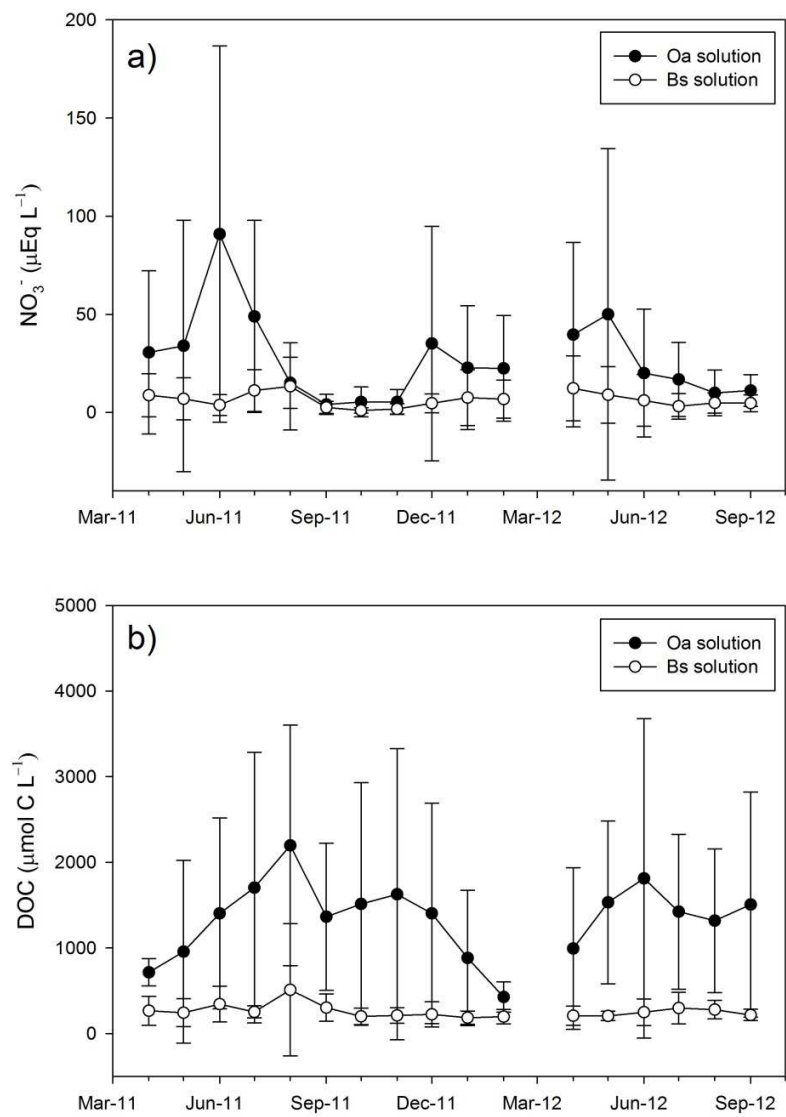


Figure 5.4. Monthly mean concentrations of a) NO₃⁻, and b) DOC concentrations in soil solutions. Error bars indicate standard deviations.

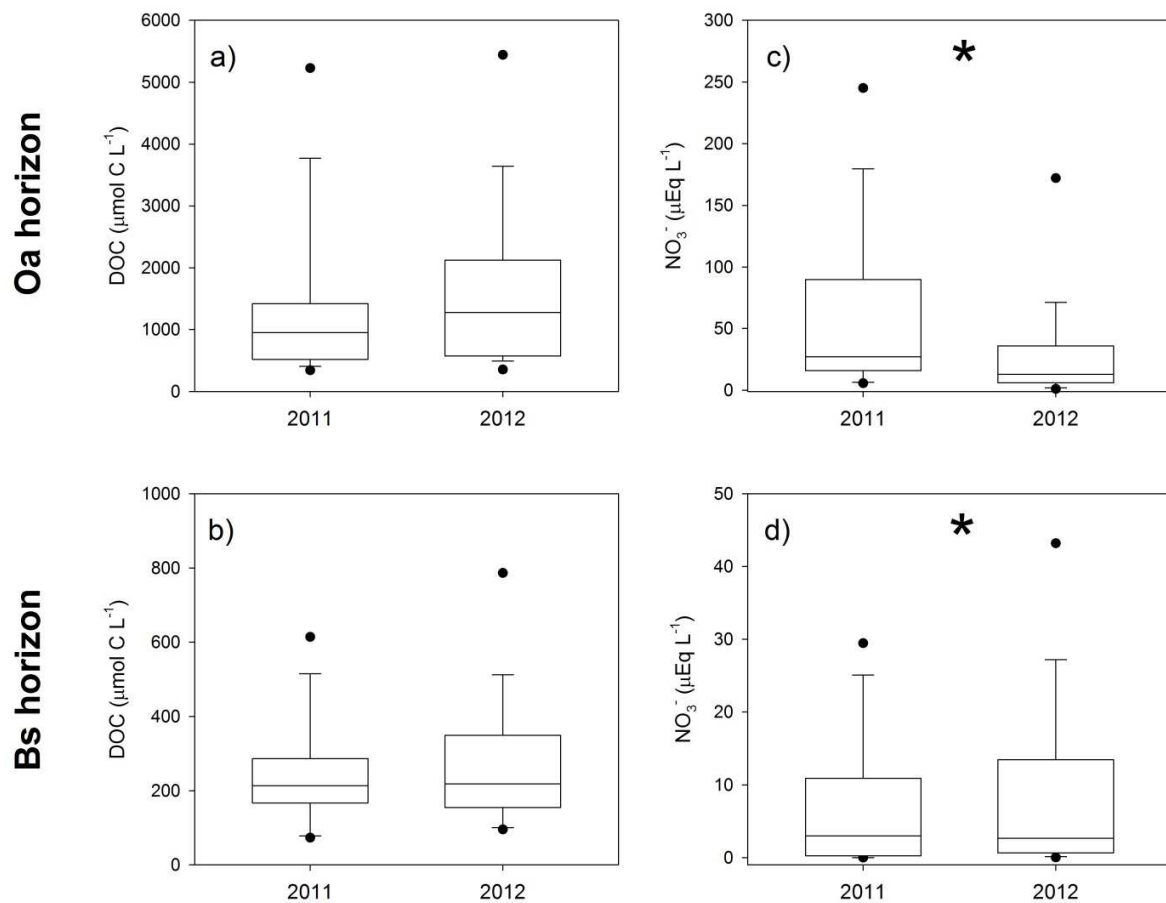


Figure 5.5. Boxplots of 2011 and 2012 May-July concentrations of DOC in soil solution of the a) Oa horizon and b) Bs horizon, and NO_3^- concentrations in soil solutions of the c) Oa horizon and d) Bs horizon. Statistically significant differences ($p < 0.05$), as analyzed by paired t-test, are marked by *.

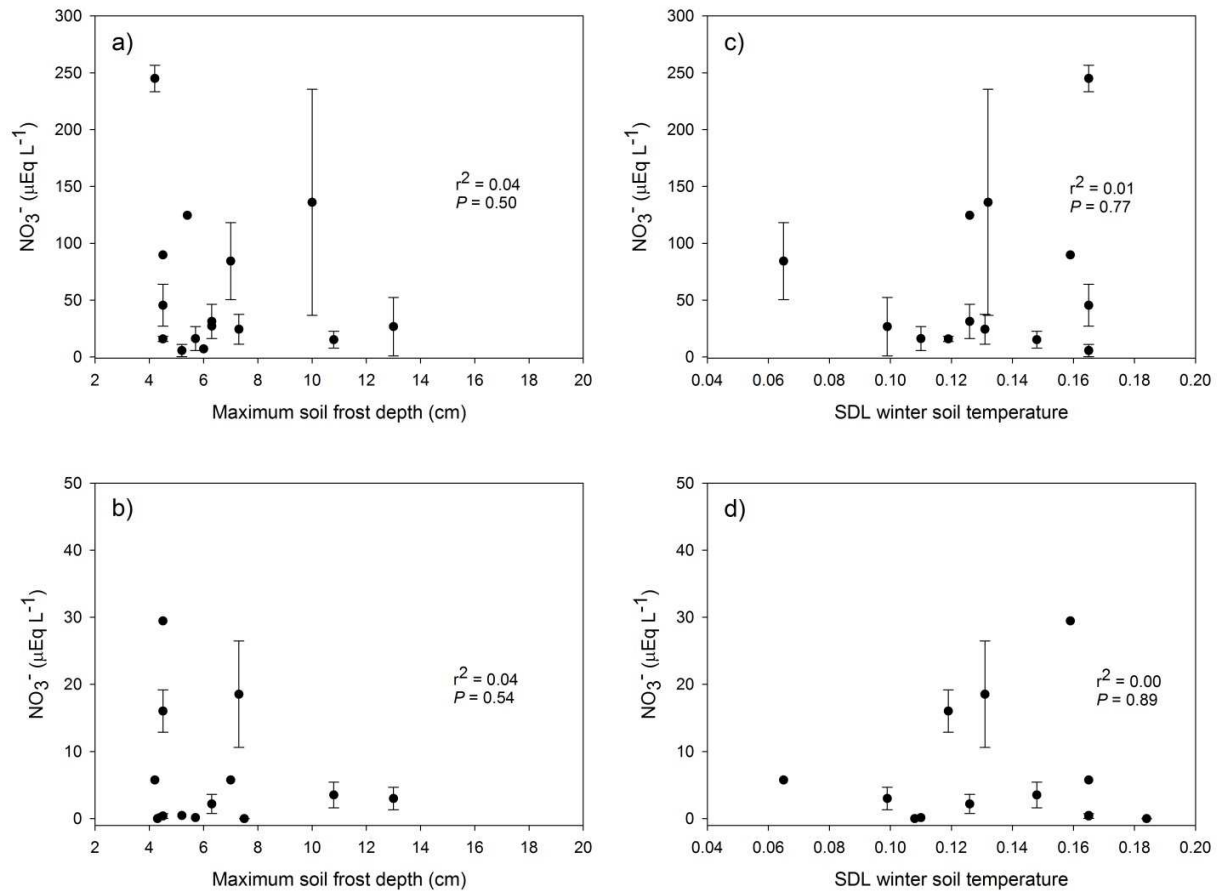


Figure 5.6. Scatterplots of soil solution concentrations of NO_3^- during May-July 2011 as related to the previous winter's maximum soil frost depth in a) Oa horizon and b) Bs horizon, and as related to the SDL of winter soil temperature in c) Oa horizon and d) Bs horizon. Vertical bars indicate standard errors.

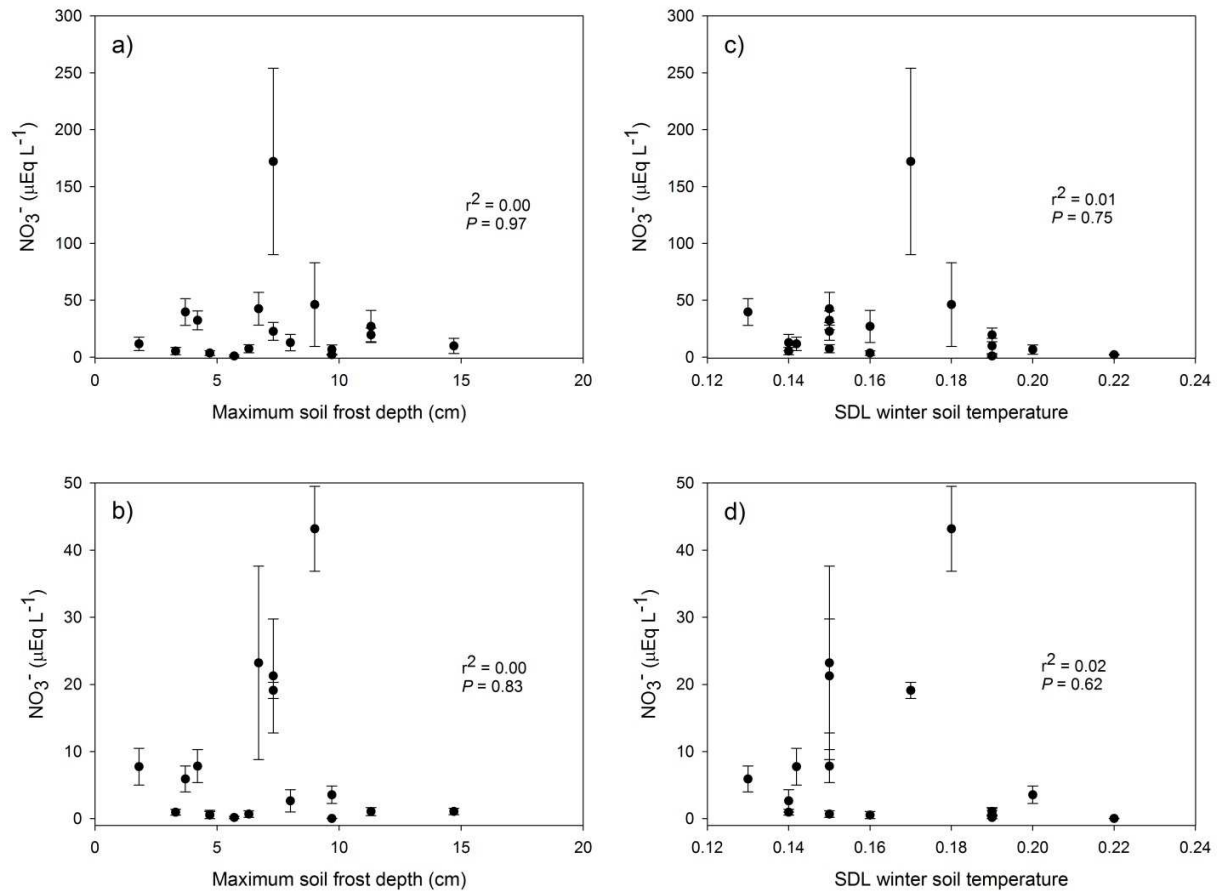


Figure 5.7. Scatterplots of soil solution concentrations of NO_3^- during May-July 2012 as related to the previous winter's maximum soil frost depth in a) Oa horizon and b) Bs horizon, and as related to the SDL of winter soil temperature in c) Oa horizon and d) Bs horizon. Vertical bars indicate standard errors.

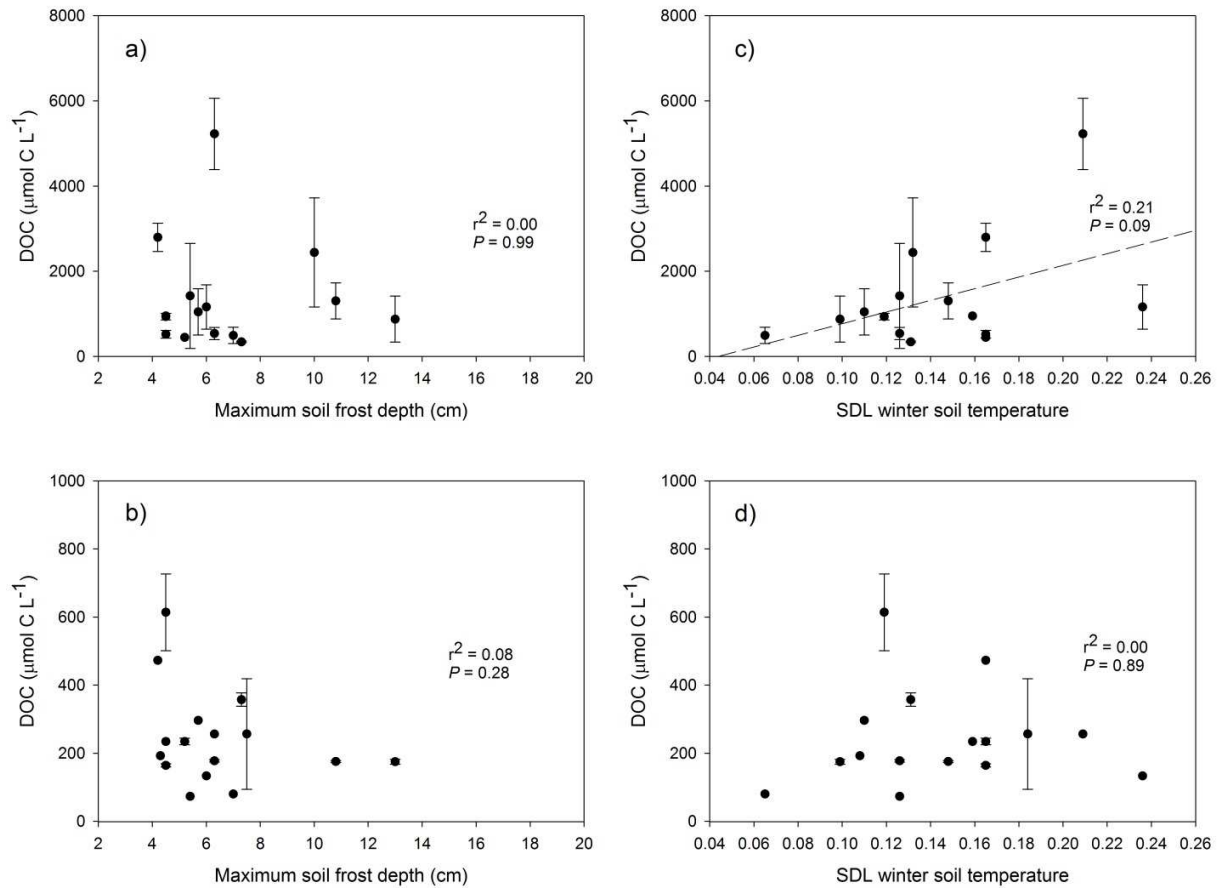


Figure 5.8. Scatterplots of soil solution concentrations of DOC during May-July 2011 as related to the previous winter's maximum soil frost depth in a) Oa horizon and b) Bs horizon, and as related to the SDL of winter soil temperature in c) Oa horizon and d) Bs horizon. Vertical bars indicate standard errors.

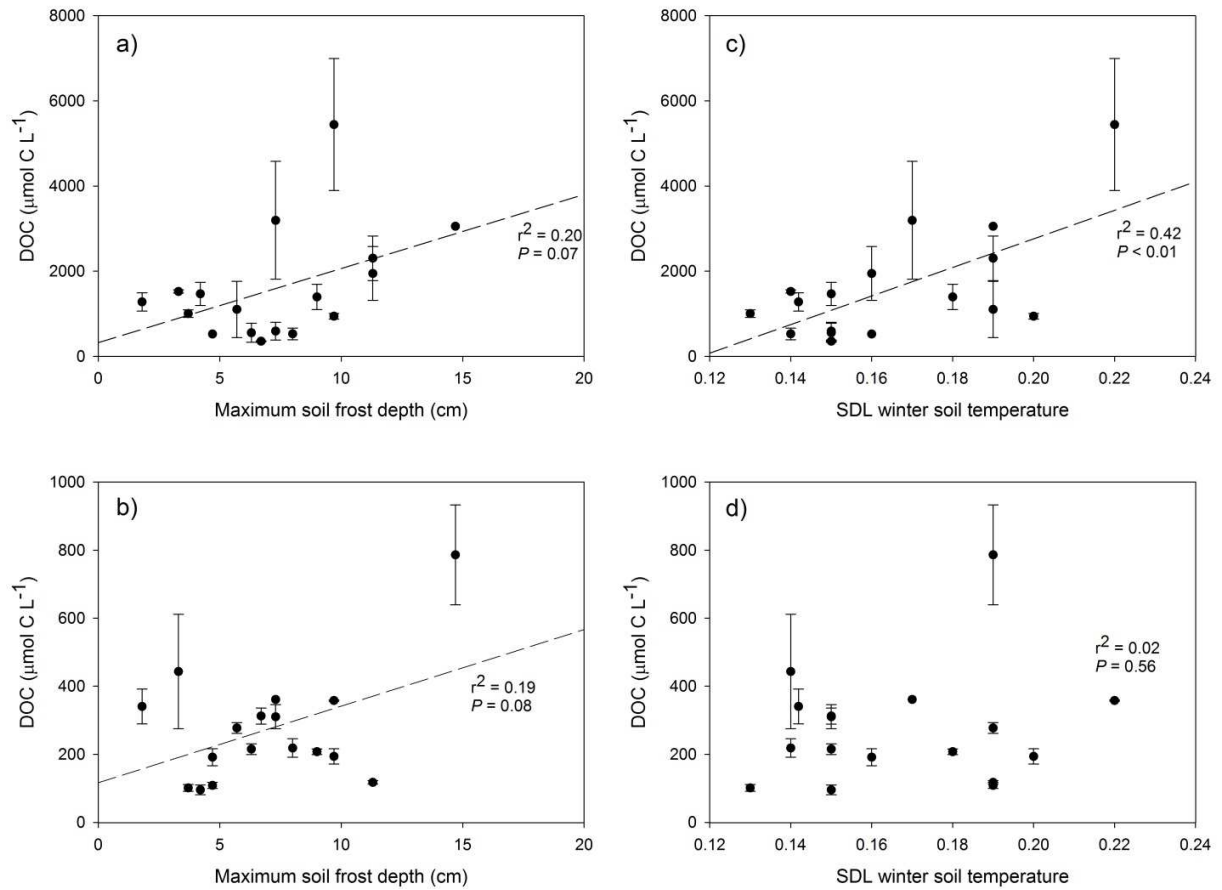


Figure 5.9. Scatterplots of soil solution concentrations of DOC during May-July 2012 as related to the previous winter's maximum soil frost depth in a) Oa horizon and b) Bs horizon, and as related to the SDL of winter soil temperature in c) Oa horizon and d) Bs horizon. Vertical bars indicate standard errors.

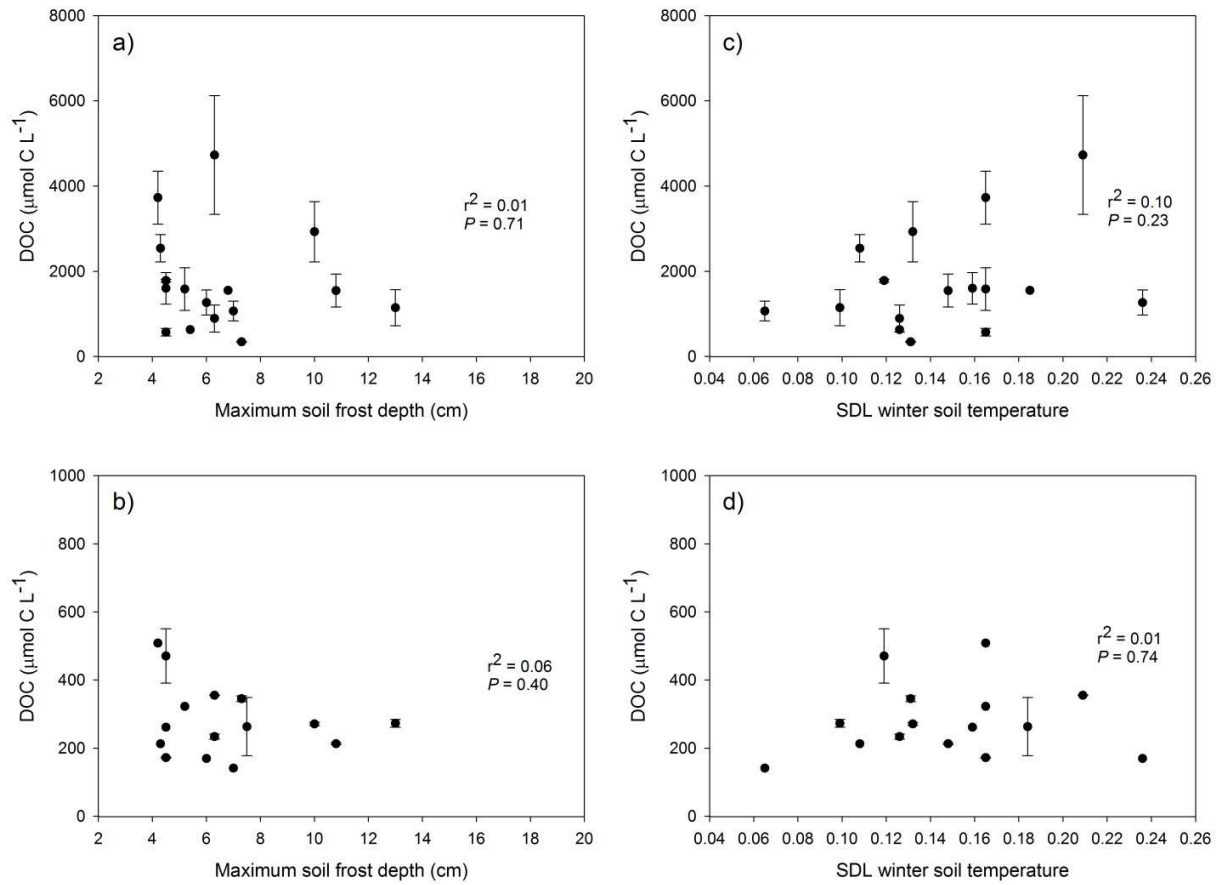


Figure 5.10. Scatterplots of soil solution concentrations of DOC during August-September 2011 as related to the previous winter's maximum soil frost depth in a) Oa horizon and b) Bs horizon, and as related to the SDL of winter soil temperature in c) Oa horizon and d) Bs horizon. Vertical bars indicate standard errors.

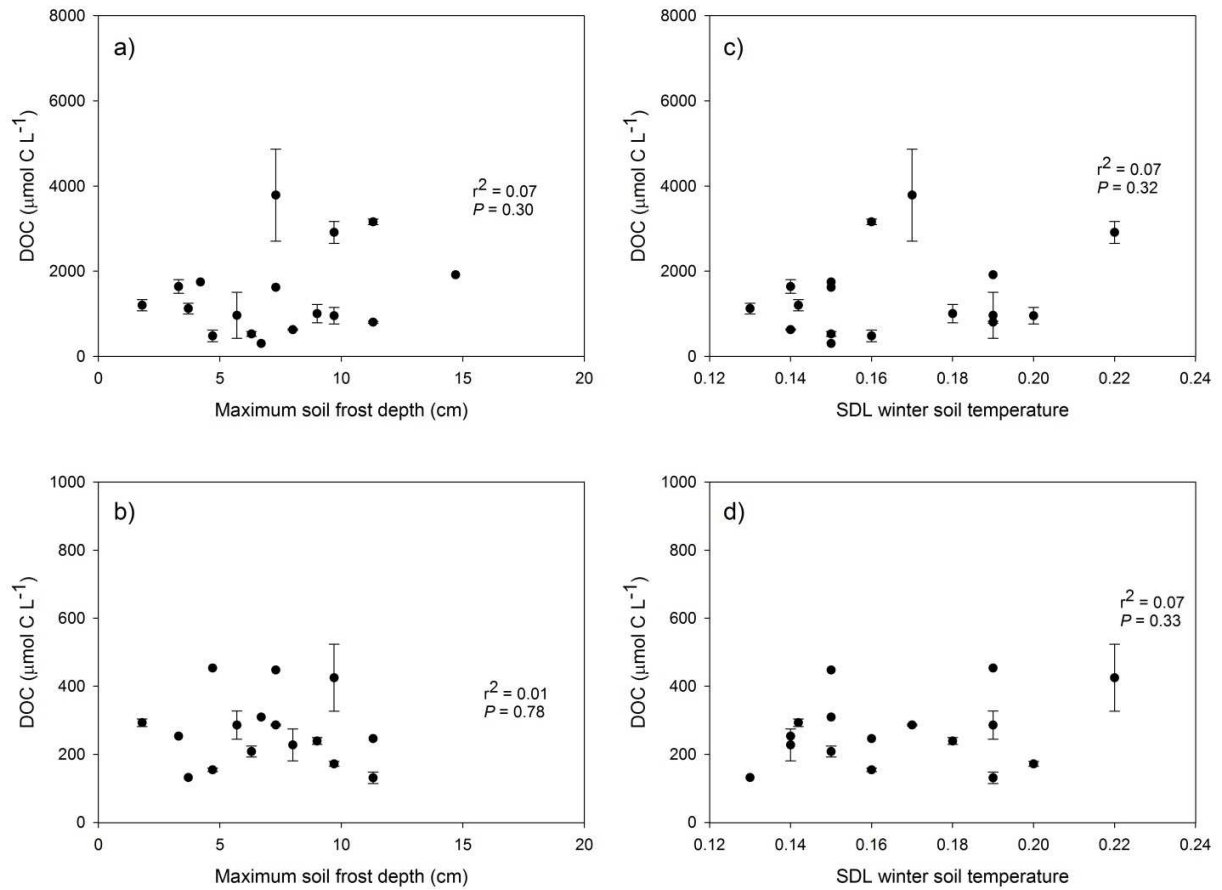


Figure 5.11. Scatterplots of soil solution concentrations of DOC during August-September 2012 as related to the previous winter's maximum soil frost depth in a) Oa horizon and b) Bs horizon, and as related to the SDL of winter soil temperature in c) Oa horizon and d) Bs horizon. Vertical bars indicate standard errors.

6. Dynamics of streamwater nitrate and dissolved organic carbon during snowmelt with differing winter climatic regimes

6.1. Methods

6.1.1. Site description

This study was conducted at three gauged experimental watersheds at the HBEF: Watershed 3 (W3), Watershed 6 (W6), and Watershed (W7). Watershed 3 and W6 are south-facing catchments and W7 is located on the north-facing slope of the Hubbard Brook valley (Figure 6.1). These watersheds have not undergone experimental treatments. The forests are of even age, having last been commercially logged in the early 20th century. Forest composition varies across the valley (Schwarz et al. 2003) based on aspect and elevation, but is similar across the three study watersheds. Mixed northern hardwood forest is the dominant pattern at lower elevations, comprised of American beech (*Fagus grandifolia* Ehrh.), sugar maple (*Acer saccharum* Marsh.), and yellow birch (*Betula alleghaniensis* Britt.). Balsam fir (*Abies balsamea* (L.) Mill), red spruce (*Picea rubens* Sarg.), and paper birch (*Betula papyrifera* var. *cordifolia* Marsh.) are prominent at the highest elevations. Given its higher overall elevation and north-facing aspect, the species composition in W7 is characterized by greater densities of white birch, spruce and fir at the higher elevations of the watershed compared to the south-facing W3 and W6.

6.1.2. Snowmelt streamwater sampling

Streamwater was sampled during the snowmelt period of 2010, 2011, and 2012. The sites in the south-facing watersheds (W3-L, W3-H, and W6-L) were sampled in each of the three

years, while the sites in W7 (W7-L and W7-H) were sampled only during the snowmelts of 2011 and 2012. The 2010 snowmelt sampling was initiated as an exploratory year of data collection to gauge the variation between two watersheds and elevational differences. The snowmelt sites were expanded in 2011 to include W7 following selection and instrumentation of climate gradient monitoring sites (described below). Streamwater sampling was started the first week of March each year and continued until early or mid-May, once the stream flow appeared to return to baseflow conditions. Samples were collected daily using Teledyne ISCO (Lincoln, NE) 3700 or 6712 automated samplers. The samplers were programmed to collect samples simultaneously from each site once each day. Collections occurred in the middle of the afternoon (15:00 EST or 16:00 EDT) when stream flow and air temperature were expected to be highest, in order to minimize the likelihood of sampling problems due to low flow or ice formation in the sampling lines and/or pump mechanisms. The samples were removed from the autosamplers within 14 days from the time of collection. Samples were subsequently stored at 4°C until laboratory analysis. Prior to removal from the ISCO autosamplers, the samples were at ambient field temperatures, which were comparable to laboratory refrigeration, although water samples did freeze and thaw during the early weeks of the sampling.

6.1.3. Stream flow measurements

Continuous stream flow measurements are made at the outlet of each watershed, by gauging stage heights with either a V notch weir (W3) or a V notch weir coupled with a San Dimas flume (W6 and W7) (Reinhart and Pierce 1964). Stream flow is expressed in millimeters per day, which is derived from integrating instantaneous measurements over time and normalizing by the watershed area.

6.1.4. Characterization of winter climatic gradient

To characterize the winter climatic variations in the study watersheds, 14 independent monitoring plots were set up in October 2010. Nine pots were located across the elevation range of the south-facing watersheds to characterize the climatic gradients in W3 and W6, and five plots were located on the north-facing slope of the valley in and near W7 (Figure 6.1). Each plot was monitored approximately biweekly for measurements of snow depth and soil frost depth. The snow depth was recorded as the mean of three locations in each plot. Snow depth and snow water equivalence were measured using Federal (Mt. Rose) snow tubes. Three replicate soil frost tubes were installed during the fall of 2010 at each plot according to the methods outlined by (Hardy et al. 2001). These consisted of removable PVC tubes filled with methylene blue dye, which turns a purple color when frozen and thus allows personnel to visually measure the depth frozen water. Soil temperature and volumetric water content were continuously recorded at 5 cm depth with Decagon 5TM combination probes connected to Decagon EM50 dataloggers.

6.1.5. Laboratory analysis

Streamwater samples were measured for total concentrations of Mg, Na, Ca, and K with inductively coupled plasma mass spectrometry (ICP-MS; Perkin Elmer, Waltham, MA). These concentrations were assumed to equal their ionic counterparts: Mg^{2+} , Na^+ , Ca^{2+} , and K^+ Anions (F^- , Cl^- , NO_3^- , and SO_4^{2-}) were measured using ion chromatography (Dionex, Sunnyvale, CA). Dissolved organic carbon was analyzed through persulfate oxidation followed by infrared CO_2 detection (Teledyne Tekmar, Mason, OH).

6.1.6. Computational methods and statistical analyses

The acid neutralizing capacity (ANC) in this study was calculated as the difference between the sum of base cations and the sum of strong acid anions ($ANC = C_B - C_A$). The total base cation concentration (C_B ; $\mu\text{Eq L}^{-1}$) was calculated as the sum of $2[\text{Ca}^{2+}] + 2[\text{Mg}^{2+}] + [\text{K}^+] + [\text{Na}^+]$; the total strong acid anion concentration (C_A ; $\mu\text{Eq L}^{-1}$) are the sum of $2[\text{SO}_4^{2-}] + [\text{NO}_3^-] + [\text{Cl}^-] + [\text{F}^-]$. The episodic acidification of snowmelt events was defined as the difference between the pre-event ANC value and the minimal ANC value during the event, with the episodic acidification term as ΔANC . Solute fluxes over the entire snowmelt period and the early (March) and later (April) snowmelt were calculated as the product of daily solute observations and mean daily discharge summed over the interval of interest. Volume-weighted concentrations were calculated by dividing solute fluxes by the cumulative flow over the time period of interest. Missing daily stream chemistry values were estimated as the average of the prior and following discrete sample values.

Concentration-discharge relationships for solutes during snowmelt events were evaluated by linear regression analysis. Comparisons between concentration-discharge slopes were conducted through general linear models including dummy variables to test for the interactive effect of categorical variables, such as snowmelt year or watershed, on the dependent variable (solute concentration) in the regression model. Significance for all analyses was determined at $\alpha \leq 0.05$.

A series of variables were derived from the snowpack, soil frost, and soil temperature measurements in order to compare the winter climate factors with stream hydrochemical dynamics. The winter climate variables were generated to characterize snowpack and soil conditions that varied with elevation. Linear regression models were developed to estimate

values for the variable at given elevations. Separate models were developed for the north-facing and south-facing watersheds using the monitoring sites associated with the study watersheds as described above. The elevation-climate gradient models were applied against the mean elevation of each of the study watersheds in order to estimate the climatic variables for each watershed for each winter. The mean elevation for each watershed was calculated from a 10-meter digital elevation model (DEM) using ArcGIS (ESRI) spatial analyst.

6.2. Results

6.2.1. *Snowmelt hydrologic response*

In each of the three years of study, snowmelt commenced in early to mid-March, although the winter meteorological conditions resulted in contrasting snowmelt magnitude and duration (Figure 6.2-Figure 6.9). Both 2010 and 2012 were warmer than average winters with lower than normal snowpack accumulation (Table 6.1). In contrast, the winter of 2011 was marked by relatively cold temperatures and high snowpack accumulation. The 2011 snowmelt was characterized by an initial large rain-on-snow event on 6-7 March 2011, followed by an extended cold period with little melt before peak snowmelt was initiated by rain events and warmer temperatures in the middle and later periods of April. The shallow snowpacks which had developed in 2010 and 2012 melted over the course of 2-3 weeks, with peak stream flows both years markedly lower than the value observed in 2011 (e.g., Figure 6.2, Figure 6.7). The snowmelt of 2012 proceeded quickly—concluding by the end March—and was followed by a dry period of approximately three weeks with low stream flow before rainfall events generated a marked stream discharge response beginning 21 April and returning to baseflow by 30 April.

The variation in snowmelt hydrology among years was greater than among watersheds, although flow magnitude and timing were related to variations in the meteorological conditions of each watershed. Watershed 3 and W6 are both located on the south-facing slope of the Hubbard Brook valley with mostly overlapping elevation ranges (Table 4.1). The meteorological conditions were similar between W3 and W6 for each of the three years of study. W7—on the north-facing slope—was studied for only 2011 and 2012. Both of these snowmelt years demonstrated differences between the north-facing and south-facing aspect. Cooler temperatures and lower solar radiation resulted in later snowmelt on W7.

6.2.2. *General snowmelt stream hydrochemistry*

Stream NO_3^- and DOC showed the greatest variation in concentrations in response to changes in flow during snowmelt. Streamwater NO_3^- and DOC dynamics followed a consistent overall pattern during snowmelt in each watershed and each year of sampling. The pre-snowmelt baseflow was characterized by low concentrations of NO_3^- and DOC. At the onset of snowmelt in early March, when stream discharge increased rapidly above baseflow conditions, the concentrations of NO_3^- and DOC increased coincidentally with flow rate. Throughout the snowmelt season, DOC concentrations responded to changes in flow. In contrast NO_3^- concentrations responded by marked increases with flow early during snowmelt, but increases in NO_3^- became more muted as snowmelt progressed (e.g. Figure 6.5).

Streamwaters during baseflow prior to snowmelt had the highest concentrations of base cations and SO_4^{2-} during the sampling period (Table 6.3). The concentrations of these solutes were subsequently diluted during snowmelt, exhibiting a negative correlation with increases in stream flow.

6.2.3. Nitrate dynamics across years and watersheds

Pre-snowmelt baseflow NO_3^- concentrations were significantly higher in 2012 compared to 2011 (paired t-test, $p = 0.02$). The lowest concentrations were found in W6 and the highest in W7 (Table 6.3). Similar to the premelt concentrations, the NO_3^- concentration increases associated with the initial snowmelt pulse in March were highest in W7 and lowest in W6. During the April high-flow events—peak snowmelt in 2011 and rain-on-bare ground in 2012—W7 also had the highest NO_3^- concentrations and the lowest were observed in W6. The April high flow was generally associated with lower peak NO_3^- concentration relative to the March peak flow (Table 6.3). The exception was in W7 in April 2012. The NO_3^- concentration in W7-L streamwater on 23 April 2012 was $47.2 \mu\text{Eq L}^{-1}$, the highest of any streamwater sample measured during the study. The difference in flushing of NO_3^- with high flow was confirmed through regression analysis of the concentration-discharge relationships for each watershed (Figure 6.10). The slope of the NO_3^- -discharge fit was significantly higher in W7 compared to W3 or W6 ($p < 0.01$, Figure 6.10), although data for the date with highest discharge were missing for W7-L.

Three years of data collected in W3 and W6 and two years in W7 showed the interannual variability of NO_3^- dynamics. NO_3^- during snowmelt was strongly controlled by hydrology, though not completely. The highest concentration-discharge slope was found in 2012 (for W3-L), while the lowest was for the 2010 data (Figure 6.11). Both 2010 and 2012 were years of low snowmelt; much higher flows were observed in 2011. While the volume-weighted concentrations of NO_3^- for the entire snowmelt were highest in 2012, the total flux of NO_3^- from each of the three watersheds was highest in 2011 (Table 6.4).

At the W3-H sampling site, the concentrations of NO_3^- were consistently higher than at the corresponding downstream site (W3-L). The concentration difference was typically highest early in snowmelt, with NO_3^- values 5-15 $\mu\text{Eq L}^{-1}$ higher at W3-H than W3-L. As depletion of NO_3^- pools progressed during snowmelt flushing, the difference between watershed sites declined. By the peak snowmelt high flows in mid to late April 2011, NO_3^- concentrations at W3-H were only 2-3 $\mu\text{Eq L}^{-1}$ higher than W3-L. In W7, there was almost no variation in stream NO_3^- concentrations between the upper site (W7-H) and the downstream site at the weir (W7-L) during the 2011 snowmelt. Differences were generally less than 2 $\mu\text{Eq L}^{-1}$ between the sites. During the 2012 snowmelt, the NO_3^- concentrations were somewhat higher at W7-H compared to W7-L during the early melt events (by 3-10 $\mu\text{Eq L}^{-1}$) and were slightly lower during the later dates of the March snowmelt (difference of 2-8 $\mu\text{Eq L}^{-1}$). At the time of the 23 April rain event the concentration increase of NO_3^- in W7-H streamwater was markedly less than what was observed at W7-L (21.2 $\mu\text{Eq L}^{-1}$ vs. 47.2 $\mu\text{Eq L}^{-1}$).

6.2.4. DOC dynamics across years and watersheds

Dissolved organic carbon concentrations in streamwater were similar in each year of the study. Fluxes and concentrations of DOC during snowmelt were strongly driven by differences in hydrology. Consequently, the volume-weighted mean concentrations were similar across time for a given watershed (Table 6.4). Among the three watersheds, the concentrations and fluxes of DOC were lowest in the north-facing W7. The DOC dynamics in W3 and W6 were similar.

In contrast to the patterns of NO_3^- concentrations, DOC did not undergo a seasonal dilution. Concentrations consistently increased with increases in hydrologic flow throughout the season suggesting that the source pool of DOC was not limited, except during the high flows of

April 2011. (Figure 6.12), although during the very high flow dates in late April 2011 some dilution effect may have limited peak DOC concentrations at increases in flow above 20 mm day⁻¹.

Dissolved organic carbon concentrations in streamwater varied by elevation to differing degrees in the two study watersheds with higher elevation sampling sites. In W3 at site W3-H, the streamwater DOC concentration was typically at least 300 $\mu\text{mol C L}^{-1}$ greater than the downstream site (W3-L) (Figure 6.2, Figure 6.4, Figure 6.7). At the W7-H site, DOC concentrations in streamwater exceeded the values at W7-L by a much smaller amount, typically 50-100 $\mu\text{mol C L}^{-1}$ (Figure 6.6 and Figure 6.9).

6.2.5. Snowmelt streamwater nitrate and DOC dynamics in relation to winter climate variation

Across the watersheds, the volume-weighted mean streamwater DOC concentrations during March and April were positively correlated with the following variables: maximum soil frost depth, snow depth duration, and soil temperature variability. There was a strong positive relationship between the maximum soil frost depth and the corresponding mean volume-weighted DOC concentrations (Figure 6.14). NO_3^- concentrations showed no relationship with any of the climatic factors analyzed.

6.2.6. Episodic acidification

Episodic acidification associated with high-flow conditions during snowmelt was observed across each of the experimental watersheds in each year. The episodic acidification—

Δ ANC, the change in the balance between base cations and strong acid anions—was most pronounced at the commencement of snowmelt when the largest pulsed increases in NO_3^- concentrations occurred coincident with dilution of base cations. The magnitude of Δ ANC varied by watershed and snowmelt year (Figure 6.13). The most acute episodic acidification occurred in W7 in both years, where Δ ANC was -40.5 and $-35.8 \mu\text{Eq L}^{-1}$ in 2011 and 2012, respectively. The magnitude of Δ ANC was similar in both of the south-facing watersheds, ranging from $-12.4 \mu\text{Eq L}^{-1}$ in W6 in 2011 to $-23.8 \mu\text{Eq L}^{-1}$ for the snowmelt of 2012 in W3. Paired t-test results indicated no differences between the two years in terms of Δ ANC ($p = 0.63$). Increased NO_3^- concentrations contribute to decreases in ANC, and Δ ANC values were negatively correlated with the concurrent change in NO_3^- concentrations across watersheds, although ΔNO_3^- did not significantly explain the variation in Δ ANC ($p = 0.08$, Figure 6.13). Increased concentrations of DOC under high-flow conditions would be expected to be accompanied by higher concentrations of organic anions in streamwater. No relationship was found however between Δ DOC and Δ ANC ($p = 0.86$). The decline of Ca^{2+} concentrations during high flow was found to significantly explain variation in Δ ANC ($p = 0.02$) across the watersheds during the two sampling years. Despite the more negative Δ ANC observed at W7 relative to W3 and W6, the absolute ANC values did not differ markedly among watersheds. This reflects the higher C_B concentrations in W7 during premelt conditions (Table 6.3).

6.3. Discussion

6.3.1. Nitrate and DOC dynamics during snowmelt

Nitrate dynamics during snowmelt followed similar flushing patterns of accumulated soil NO_3^- pools as have been observed previously in northeastern U.S. forested watersheds (Ohte et al. 2004; Christopher et al. 2008; Sebestyen et al. 2008; Pellerin et al. 2012). I observed this general pattern in each of the three years and in each watershed, but the patterns and concentrations differed based on hydrological and biogeochemical factors. While 2010 and 2012 were similar in terms of low snowpack development and relatively low stream discharge during peak snowmelt, the NO_3^- concentrations were markedly higher in 2012 than 2010. The high concentrations likely are the result of greater rates of mineralization and nitrification in the soils preceding snowmelt. The low snowpack also exposed soils to frost development, and high temperature variability in 2012. These factors could explain the lack of immobilization of NO_3^- by soil microbes during the winter of 2012. Additionally, the peak in NO_3^- concentration during the April rain event following several weeks of dry conditions support the mechanism that soil NO_3^- pools accumulated due to higher rates of nitrification associated with the relatively warm spring season following snowmelt. It is not clear why NO_3^- concentrations in 2010 were low under seemingly similar conditions to 2012. The detailed climate monitoring data were not available for the winter of 2010, but the long-term meteorological data indicates it was also warmer than average (Table 6.2). Rain on snow events occurred several times between December 2009 and February 2010. These events likely flushed away soil NO_3^- accumulations, leaving a smaller pool at the start of the March snowmelt compared to conditions in 2012.

Contrary to NO_3^- dynamics over the course of the snowmelt seasons, DOC did not undergo the declining concentrations that would be expected from depletion of a finite pool. However, during the April 2011 peak snowmelt DOC concentrations did not increase with increases in flow above approximately 20 mm day^{-1} (Figure 6.12). This appears to be a

temporary dilution effect resulting from previous flushing of DOC from the forest floor. Similar flushing of DOC from upper soil horizons led to decreasing concentrations in runoff during prolonged snowmelt in an alpine catchment in Colorado (Boyer et al. 1997).

Hysteresis loops in the concentration/discharge relationship can be used to evaluate sources of solutes during hydrologic events (Hinton et al. 1998; McGlynn and McDonnell 2003). Over the course of several events during the 2011 and 2012 snowmelt seasons, I observed generally counter-clockwise hysteresis in DOC and NO_3^- concentrations with flow (Table 6.5.). Pellerin et al. (2012) found counter-clockwise hysteresis relationships for chromophoric dissolved organic matter fluorescence (FDOM, a surrogate for DOC) at Sleepers River, Vermont. They hypothesized that this relationship was the result of delayed contributions of DOC from surface and shallow subsurface flowpaths on the hillslope. This hypothesis is supported by previous results from Sleepers River that showed a counter-clockwise hysteresis between hillslope groundwater levels and streamflow (Kendall et al. 1999). While most of my observed hysteretic relationships were counter-clockwise, there were several exceptions. During an early season event 16-21 March 2011, the hysteresis loops were generally clockwise or non-existent. Clockwise hysteresis can be indicative of source areas that are temporarily depleted of solutes (Hornberger et al. 1994; Boyer et al. 2000). This explanation fits well with the early 2011 snowmelt season at Hubbard Brook, when the large rain event (6-7 March 2011) likely flushed available DOC and NO_3^- from the riparian areas. The snowmelt event with predominantly clockwise hysteresis (16-21 March 2011) was relatively small (maximum daily flows 5-13 mm day^{-1} by watershed) and would have likely sourced streamflow primarily from riparian areas. Overall, the general similarities between the DOC and NO_3^- hysteresis patterns indicate that not

only are they mobilized from the shallow organic soil through preferential flowpaths, but they also are sourced from similar areas within the watersheds during events.

6.3.2. Episodic acidification

The patterns of snowmelt-associated acidification presented here are notable due to the relatively similar magnitude of ΔANC between the two years of intensive snowmelt study, despite the greater snowmelt runoff occurring during 2011. Greater variation in ΔANC among the watersheds was found than among years, suggesting watershed characteristics are more important to patterns of snowmelt episodic acidification than maximum discharge rates. In both 2011 and 2012, the ΔANC associated with snowmelt was more negative in W7, the north-facing study catchment, than in the south-facing watersheds, W3 and W6. The more acute episodic acidification in W7 was a result of two factors—higher flushing of NO_3^- at a given discharge (Figure 6.10), and greater dilution of base cations than occurred in the south-facing watersheds. The upper-elevation stream water in W7 (collected at site W7-H) had consistently lower ANC values than the downstream site (W7-L). While NO_3^- flushes were somewhat greater in W7 than W3 and W6, the ΔNO_3^- coincident with episodic acidification did not fully explain the ΔANC differences among the watersheds.

As stream discharge shifts from low baseflow to high flow during snowmelt events, the relatively high concentrations of groundwater SO_4^{2-} are diluted by flow derived from the snowpack or soil water. The degree of dilution of SO_4^{2-} is substantial in each of the watersheds studied. DeWalle and Swistock (1994) found that SO_4^{2-} concentrations increased and were important contributors to ANC depression, in four of five streams they studied in central Pennsylvania in the late 1980s and early 1990s. Across the northeastern U.S. changes in SO_4^{2-}

concentrations during hydrologic events have been found to be a significant contributor to ANC decreases in Pennsylvania and the New York Adirondacks (Wigington et al. 1996), and in Maine (Kahl et al. 1992). In a coastal plain stream system of the mid-Atlantic U.S., O'Brien et al. (1993) found increased stream SO_4^{2-} concentrations in Reedy Creek, Virginia during a storm event. These studies were conducted at locations and times with high SO_4^{2-} deposition. Therefore, high concentrations of SO_4^{2-} in precipitation, and presumably in shallow soils, led to high transport to surface waters during precipitation events or snowmelt. The relative dilution of SO_4^{2-} noted here in Hubbard Brook streams during snowmelt events underscores the importance of the long-term trends of decreasing concentrations of SO_4^{2-} in wet deposition and soil leachate. The long-term data analysis presented in Chapter 4 show that during snowmelt over 30 years, SO_4^{2-} has been declining faster than C_B , which suggests that the greater dilution of SO_4^{2-} relative to C_B has reduced the severity of snowmelt episodic acidification.

Increases in stream DOC concentration during snowmelt pulses did not appear to affect the magnitude of ΔANC , though this may be in part because I used ANC as calculated by $C_B - C_A$ rather than measured ANC. Kramer et al. (1990) showed that in northeastern U.S. watersheds at high elevation (>530m), organic acids were predominantly strongly acidic. Each of the watersheds studied here are high enough in elevation to meet this classification. Any acidification effects of increased mobilization of organic strong acid anions during snowmelt are masked by the more important factors of NO_3^- and base cation dilution. Concentrations of DOC are relatively low in the watershed sampled here and organic acids would likely play more of a role in episodic acidification in streams with higher DOC concentrations. Among Hubbard Brook's north-facing experimental watersheds, Watershed 9 (W9) has significantly higher DOC concentrations (>500 $\mu\text{mol L}^{-1}$ at baseflow) than the other catchments (McDowell 1982).

Wellington and Driscoll (2004) studied episodic acidification during snowmelt and summer storms at W9 and found that during the summer storms increases in organic anion concentrations were a major contributor to short-term decreases in ANC. However, similar to the results presented here, they found that during snowmelt in W9, episodic acidification was dominated by a combination of NO_3^- mobilization and base cation dilution. Given the importance of NO_3^- during snowmelt, it seems likely that DOC would play a larger role in episodic acidification associated with summer non-snowmelt hydrologic events when the pool of soil NO_3^- available for flushing is lower, due to plant and microbial retention.

6.3.3. Winter climate variability and snowmelt stream nitrate and DOC dynamics

The DOC concentrations measured across the three watersheds were highly correlated with the estimated mean maximum soil frost depth of the individual watersheds. This result suggests that the winter climate is strongly influencing DOC mobilization to streamwater during snowmelt, although it is possibly there are variables among these three watersheds that covary with the winter climate differences. That is, that factors not accounted for are influencing DOC concentrations in streamwater differently in each watershed. Unfortunately there are not long-term stream DOC concentration observations outside of W6 that could be used for comparison. However, results suggesting that DOC concentration in streamwater during snowmelt responds positively with the depth of maximum soil frost during the preceding winter are consistent with the findings of other studies using long-term data or manipulations. Haei et al. (2010) found that colder winter soils are linked to higher DOC concentrations in boreal headwater streams in the Nyänget subcatchment in the Krycklan watershed of northern Sweden, where a long-term soil freezing manipulation was conducted. In the same area, Ågren et al. (2010) also found soil frost

duration among several variables indicative of long, cold winter soil conditions that explained increased DOC stream concentrations during snowmelt. Austnes and Vestgarden (2008) conducted laboratory experiments using montane heathland soils from Norway and found that prolonged frost can increase leaching of DOC. At Hubbard Brook, a field snow manipulation study by Groffman et al. (2011) found that induced soil frost promotes mobilization of DOC, although a prior study (Fitzhugh et al. 2001) did not find a treatment effect on DOC concentrations in soil solutions from experimentally induced soil frost.

Stream NO_3^- concentrations during snowmelt exhibited considerable differences among years and watersheds. However, the winter climatic variables used in the analysis did not explain the variation in NO_3^- concentrations. This finding is not necessarily surprising given the complexity of explaining NO_3^- responses to soil-frost development. While several studies have shown that soil frost can induce NO_3^- leaching in soils (Boutin and Robitaille 1995; Fitzhugh et al. 2001), others have shown little effect (Kaste et al. 2008). Inconsistencies have been especially noted for studies at the catchment scale. Mitchell et al. (1996) found significantly higher than average stream NO_3^- concentrations during the snowmelt of 1990 at several watershed across the northeastern U.S., including W6 at Hubbard Brook, and linked it to widespread severe soil frost development the previous winter. Fitzhugh et al. (2003) analyzed the long-term chemistry record for W6 and found soil-frost disturbance was linked to increased NO_3^- export early in the record, during the 1970s, but had inconsistent responses in later decades. Hubbard Brook experienced a severe soil frost event during the winter of 2006 but the following annual NO_3^- export was low (Judd et al. 2011). Watmough et al. (2004) did not find soil frost to be a significant predictor of stream NO_3^- across 16 forested catchments in South Central Ontario, Canada between 1982 and 1999. Finding a response of NO_3^- to soil frost during snowmelt is complicated by the observation

that effects on NO_3^- leaching often appear strongest during the growing season (Fitzhugh et al. 2001; Hentschel et al. 2009), presumably a result of reduced plant uptake due to frost-damaged fine roots (Tierney et al. 2001).

The results I present in this study indicate that NO_3^- concentrations were highest in W7 during both snowmelt seasons. W7 is the north-facing watershed of the study and had the deepest winter snowpacks. Given that NO_3^- exported during snowmelt is primarily the product of soil nitrification (Piatek et al. 2005; Campbell et al. 2006; Sebestyen et al. 2008), this observation is suggestive that W7 had higher overwinter nitrification rates and/or lower immobilization rates than either of the south-facing watersheds. Snowpacks of increased depth and duration have been shown to elevate microbial activity relative to shallow and discontinuous snow cover (Brooks et al. 1998; Groffman et al. 2009). At the HBEF Groffman et al. (2009) found higher rates of nitrification at high elevation plots which had greater snow cover. The lower DOC availability in W7 may account for lower immobilization of NO_3^- . Lower C:N ratios are associated with higher N mineralization and nitrification, which can lead to higher NO_3^- export (Melillo et al. 1982; Lovett et al. 2004; Christopher et al. 2006). Interacting effects between DOC and NO_3^- responses to soil freezing, as well as interannual variability in C and N cycling are likely to play a role in the degree of response to soil freezing (Groffman et al. 2011).

6.4. Summary and Conclusions

Intensive sampling of streamwater revealed differences in the concentrations of NO_3^- and DOC as well as the severity of episodic acidification during snowmelt among the three watersheds. NO_3^- concentrations were the highest in W7 during each of the two years it was sampled, presumably due to higher rates of overwinter microbial N mineralization and

nitrification. NO_3^- concentrations were highest across all three watersheds during the snowmelt of 2012, a year of low snowpack with a short duration of snowmelt. Both NO_3^- and DOC concentrations varied with hydrologic flow and concentration-discharge hysteresis relationships suggest they were sourced from similar areas within the watersheds during events. While NO_3^- was flushed in high concentrations during early snowmelt, DOC was less affected by dilution throughout the snowmelt season. The DOC concentrations did not differ much among the years of study, but did vary among the watershed. DOC concentrations showed strong positive correlation with the winter climate variable of average maximum soil frost depth in each watershed, although it was not completely clear if winter climate was the driver of DOC differences or if there are other covarying factors that control DOC mobilization. Overall, the intensive sampling of streamwater during snowmelt provided valuable information regarding the dynamics of NO_3^- and DOC hydrochemistry as they vary with landscape position and between years of differing winter climate regimes.

Table 6.1. Study watershed size and topographical characteristics.

Watershed	Area (ha)	Elevation (m)	Slope (°)	Aspect
W3	42.4	527-732	12.1	S23°W
W6	13.2	549-792	15.8	S32°E
W7	77.4	619-899	12.4	N16°W

Table 6.2. Winter climatic measures for the three years of study and the mean of the years 1980-2012.

Year	¹ Mean winter daily temp – Sta. 1 (°C)	¹ Mean winter daily temp – Sta. 14 (°C)	Max. snow depth – Sta. 2 (cm)	Max. snow depth – Sta. 17 (cm)	Max. soil frost depth –Sta. 2 (cm)	Max. soil frost depth –Sta. 17 (cm)
Mean (1980-2012)	-6.22	-8.14	63.0	99.0	6.6	7.7
2010	-5.17	-8.14	48.5	65.3	7.6	5.1
2011	-8.02	-10.12	78.2	96.3	12.7	16.5
2012	-4.36	-6.67	41.4	56.4	12.7	14.0

Station 1 and Station 14 are long-term meteorological data monitoring sites in the south-facing and north-facing watersheds, respectively. Station 2 and Station 17 are long-term snow and soil frost data monitoring sites in the south-facing and north-facing watersheds, respectively

¹Mean winter daily temperature in the mean of daily values from the months December, January, and February.

Table 6.3. Pre-snowmelt and peak early (March) and late (April) snowmelt values by watershed weir sampling site.

	Site	Condition	Date	Flow	DOC	NO ₃ ⁻	SO ₄ ²⁻	Ca ²⁺	ANC
2011	W3-L	Premelt	4 Mar	0.7	119.1	3.2	74.0	28.2	16.5
		Peak-Mar	7 Mar	35.2	260.2	21.1	51.2	26.2	-1.9
		Peak-Apr	11 Apr	54.4	243.8	12.7	48.6	23.6	3.6
	W6-L	Premelt	5 Mar	0.5	155.9	2.2	76.2	25.4	5.8
		Peak-Mar	6 Mar	23.0	273.2	14.9	48.6	23.4	-6.6
		Peak-Apr	11 Apr	48.8	240.5	10.5	50.0	17.0	-15.1
	W7-L	Premelt	4 Mar	0.1	100.8	3.3	72.4	27.8	33.9
		Peak-Mar ^a	8 Mar	6.7	148.5	23.3	46.8	20.2	-6.6
		Peak-Apr	11 Apr	36.9	210.3	19.2	47.6	18.4	-11.1
2012	W3-L	Premelt	6 Mar	0.8	128.1	5.0	72.0	28.5	19.2
		Peak-Mar	19 Mar	16.1	237.8	23.5	48.6	26.0	3.4
		Peak-Apr	23 Apr	19.2	219.4	16.1	53.8	18.4	2.6
	W6-L	Premelt	6 Mar	0.5	172.6	3.8	74.2	23.8	7.0
		Peak-Mar	19 Mar	16.7	198.9	20.4	46.4	19.6	-10.2
		Peak-Apr	23 Apr	20.5	217.0	9.4	49.4	16.0	-3.4
	W7-L	Premelt	7 Mar	0.3	95.5	5.9	68.8	34.1	28.5
		Peak-Mar	20 Mar	22.2	219.0	33.0	39.8	25.8	-7.3
		Peak-Apr	23 Apr	24.7	217.2	47.2	48.2	15.0	-58.5

^aDiscrete sample not collected at W7-L associated with the hydrograph peak on 7 Mar 2011. Values presented (8 Mar 2011) are closest sampling association available.

^bUnits for flow are mm day⁻¹; units for DOC are µmol C L⁻¹; units for NO₃⁻, SO₄²⁻, Ca²⁺, and ANC are µEq L⁻¹.

Table 6.4. Summary of NO₃⁻ and DOC volume-weighted averages and total fluxes by snowmelt months March and April, and totals for the two months for each sampling year.

Site	Date	Total flow (mm)	Vol-wt NO ₃ ⁻ (μmol L ⁻¹)	NO ₃ ⁻ flux (mol ha ⁻¹)	Vol-wt DOC (μmol L ⁻¹)	DOC flux (mol ha ⁻¹)
W3-L	Mar 2010	222.3	5.4	12.0	203.3	451.9
	Apr 2010	113.1	1.7	1.9	184.2	208.3
	Total 2010	335.4	4.2	13.9	196.9	660.2
	Mar 2011	173.4	12.4	21.5	208.9	362.2
	Apr 2011	343.2	7.0	24.0	221.7	760.9
	Total 2011	516.6	8.8	45.5	217.4	1123.1
	Mar 2012	163.3	16.4	26.8	204.0	333.1
	Apr 2012	86.7	7.0	6.1	174.8	151.6
	Total 2012	250.0	13.1	32.9	193.9	484.7
W6-L	Mar 2010	187.7	3.0	5.6	177.8	333.7
	Apr 2010	120.9	0.4	0.5	166.4	201.8
	Total 2010	308.6	2.0	6.1	173.3	534.9
	Mar 2011	158.2	7.0	11.1	203.8	322.4
	Apr 2011	368.6	3.2	11.8	199.3	734.6
	Total 2011	526.8	4.3	22.9	200.7	1057.0
	Mar 2012	147.1	12.0	17.7	188.0	276.5
	Apr 2012	77.1	4.2	3.2	167.2	128.9
	Total 2012	224.2	9.3	20.9	180.8	405.4
W7-L	Mar 2011	105.7	18.4	19.4	152.6	161.3
	Apr 2011	341.9	11.3	38.6	187.4	640.7
	Total 2011	447.6	13.0	58.0	179.2	802.0
	Mar 2012	154.8	26.0	40.2	171.5	265.5
	Apr 2012	71.6	22.7	16.3	164.6	117.9
	Total 2012	226.4	25.0	56.5	169.3	383.4

Table 6.5. Concentration-discharge hysteresis loops for NO₃⁻ and DOC by sampling site and hydrologic event.

Dates	Sampling site	NO ₃ ⁻	DOC
16-21 Mar 2011	W3-L	no hysteresis	clockwise
	W6-L	clockwise	clockwise
	W7-L	^a NA	^a NA
10-16 Apr 2011	W3-L	counterclockwise	counterclockwise
	W6-L	counterclockwise	counterclockwise
	W7-L	counterclockwise	counterclockwise
16-22 Mar 2012	W3-L	counterclockwise	counterclockwise
	W6-L	counterclockwise	clockwise
	W7-L	counterclockwise	clockwise
20-26 Apr 2012	W3-L	counterclockwise	counterclockwise
	W6-L	counterclockwise	counterclockwise
	W7-L	counterclockwise	counterclockwise

^aNA = not available because of missing data

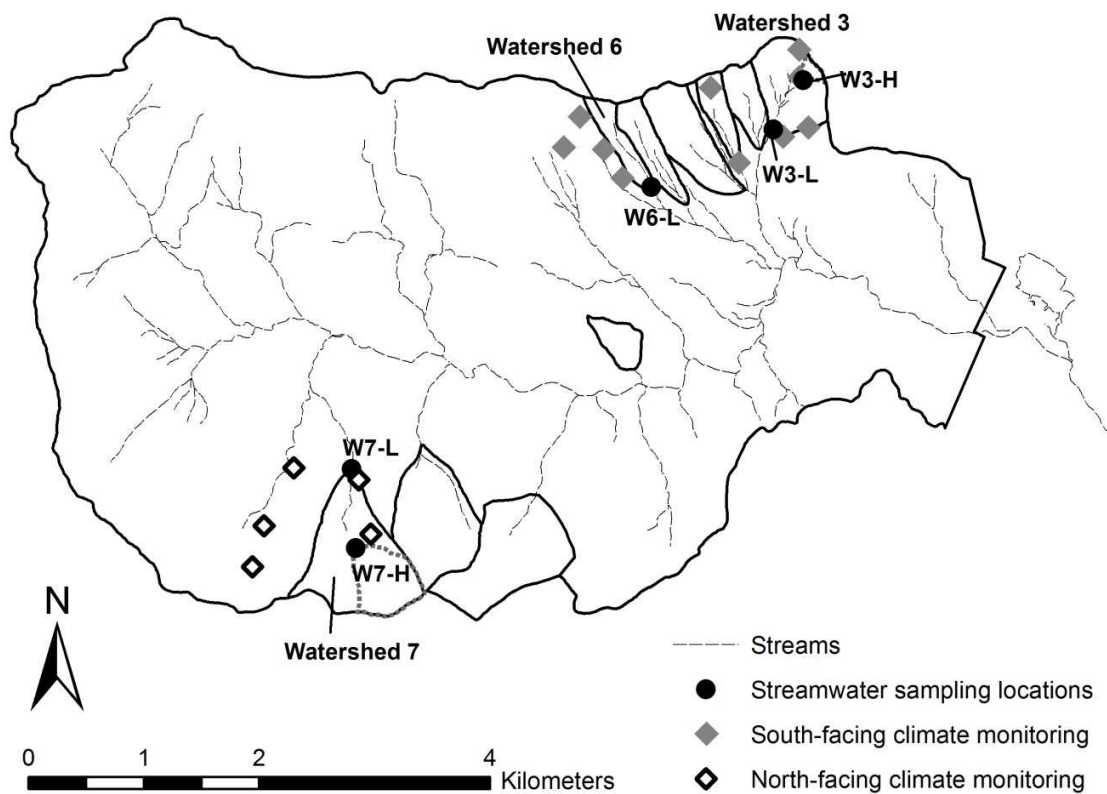


Figure 6.1. Map of Hubbard Brook Experimental Forest with study watersheds, sampling and monitoring sites indicated.

Watershed 3 - 2010

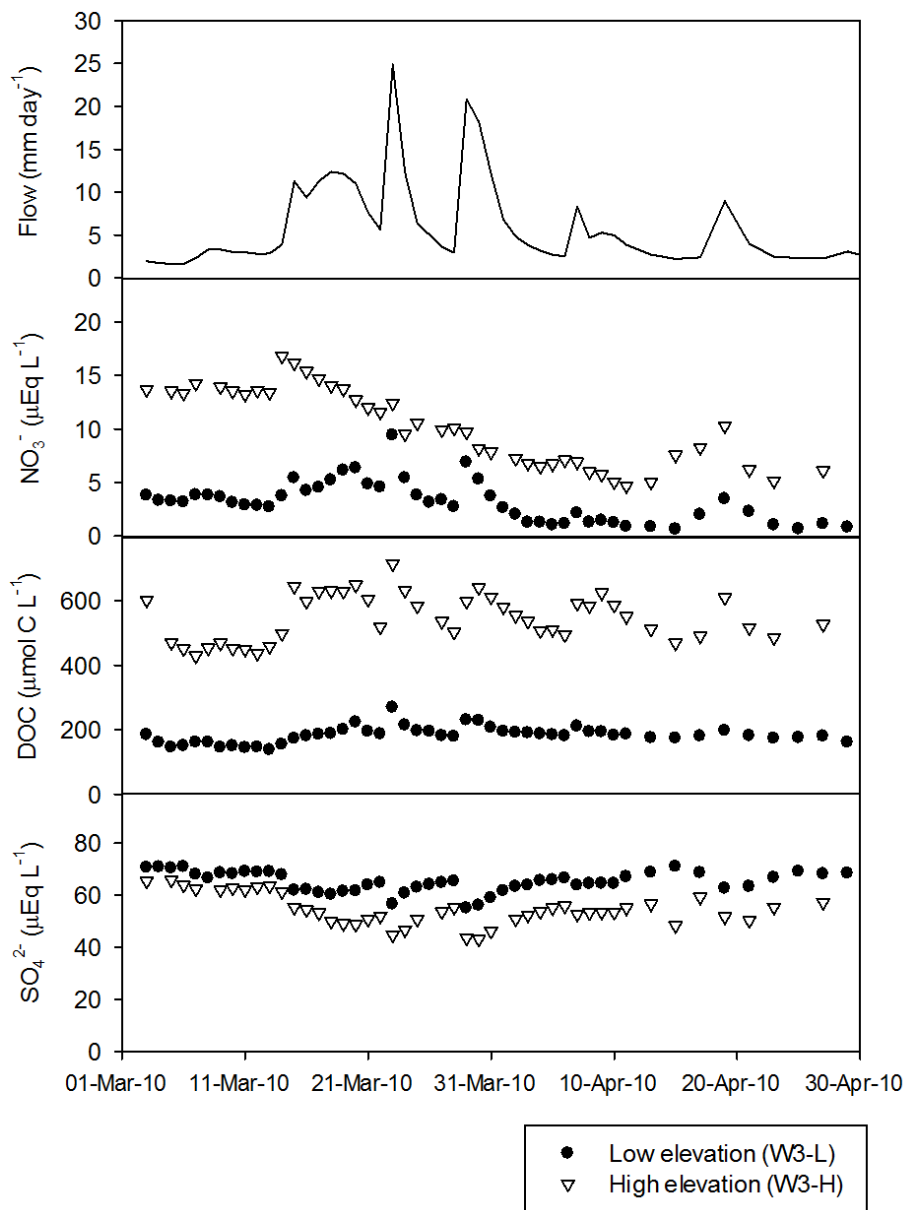


Figure 6.2. Snowmelt season hydrochemical dynamics in Watershed 3 based on discrete daily samples from 1 March 2010 to 30 April 2010, with a) stream flow, b) NO_3^- , c) DOC, d) SO_4^{2-} , and e) ANC indicated. Low elevation samples collected at the W3 weir (W3-L, 527 m). High elevation samples collected at 635 m (site W3-H).

Watershed 6 - 2010

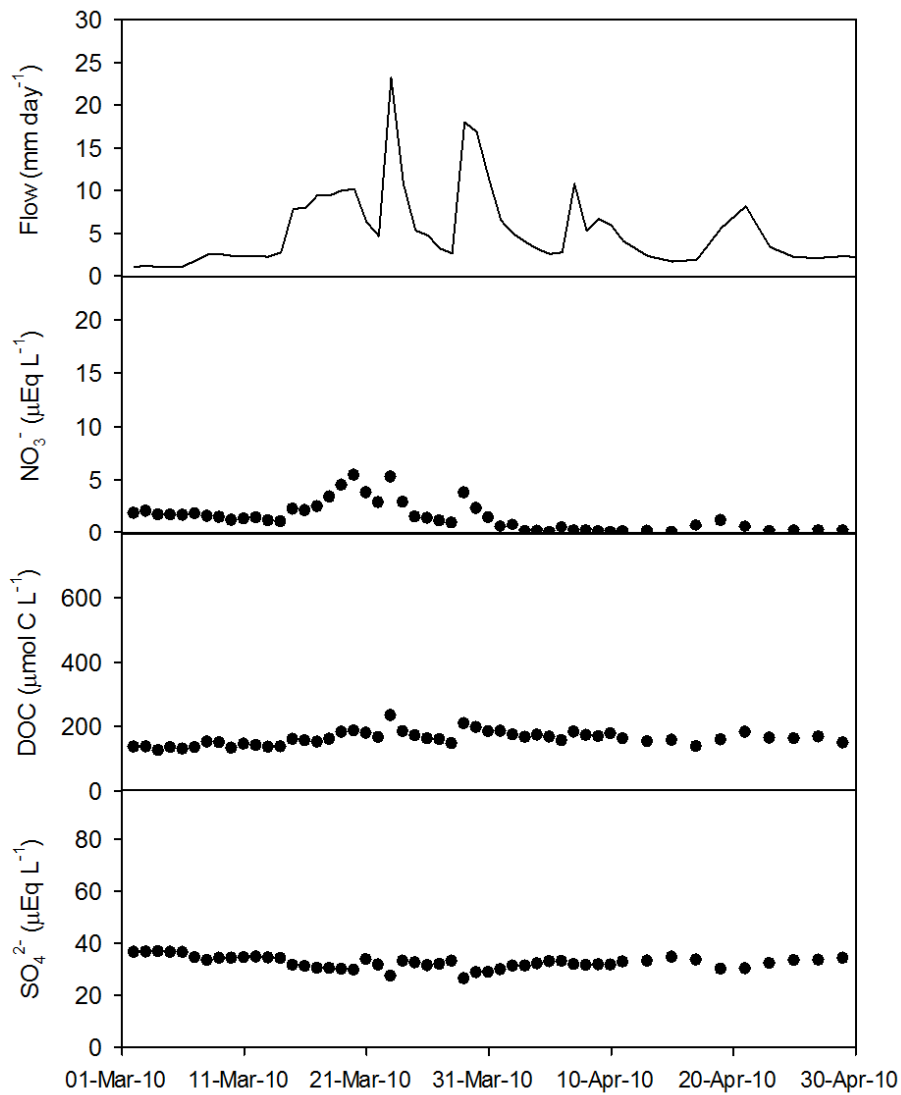


Figure 6.3. Snowmelt season hydrochemical dynamics in Watershed 6 (site W6-L) based on discrete daily samples from 1 March 2010 to 30 April 2010, with a) stream flow, b) NO₃⁻, c) DOC, d) SO₄²⁻, and e) ANC indicated.

Watershed 3 - 2011

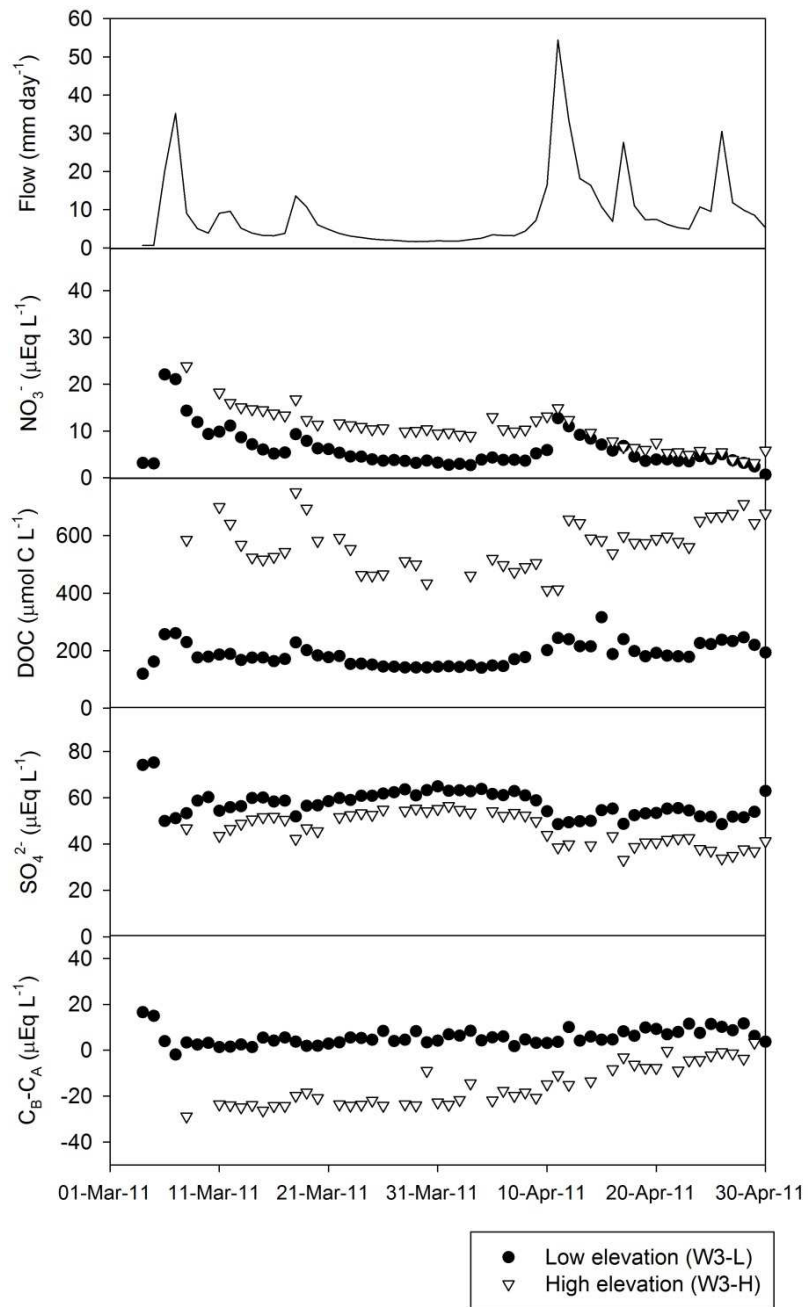


Figure 6.4. Snowmelt season hydrochemical dynamics in Watershed 3 based on discrete daily samples from 1 March 2011 to 30 April 2011, with a) stream flow, b) NO₃⁻, c) DOC, d) SO₄²⁻, and e) ANC indicated. Low elevation samples collected at the W3 weir (W3-L, 527 m). High elevation samples collected at 635 m (site W3-H).

Watershed 6 - 2011

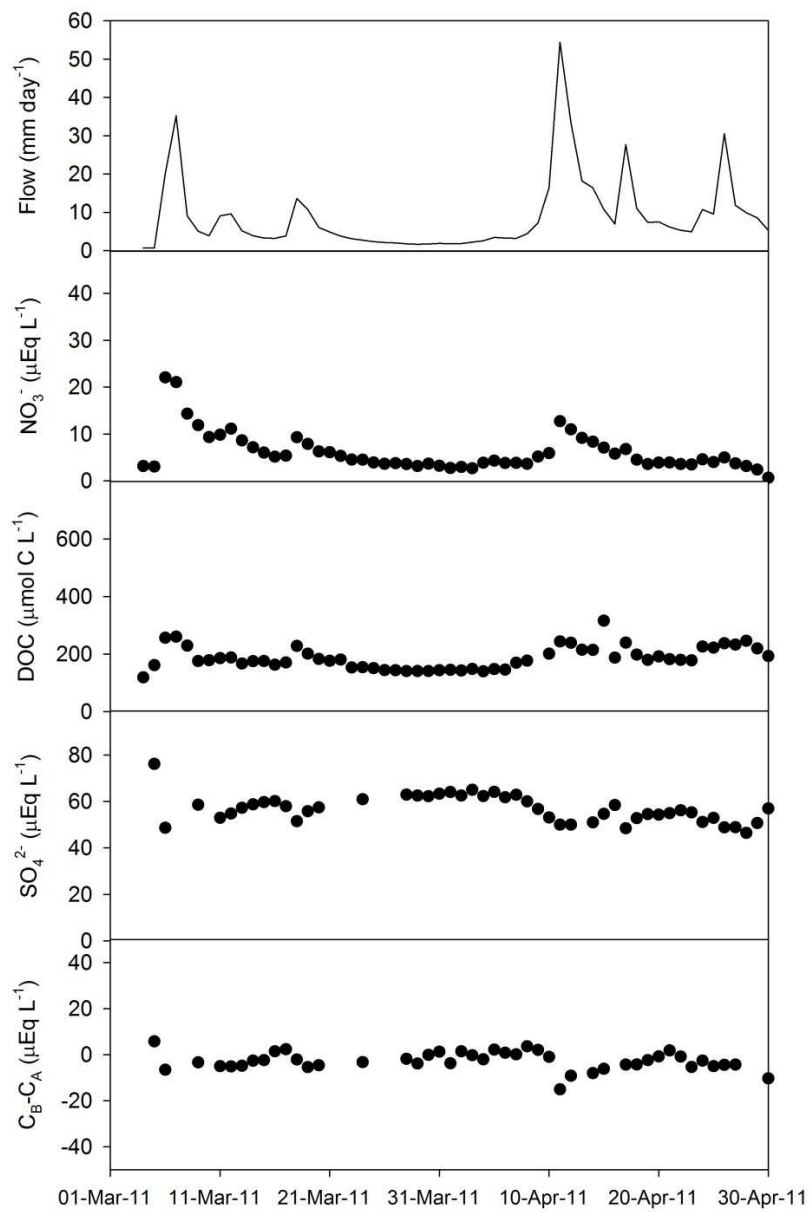


Figure 6.5. Snowmelt season hydrochemical dynamics in Watershed 6 (site W6-L) based on discrete daily samples from 1 March 2011 to 30 April 2011, with a) stream flow, b) NO₃⁻, c) DOC, d) SO₄²⁻, and e) ANC indicated.

Watershed 7 - 2011

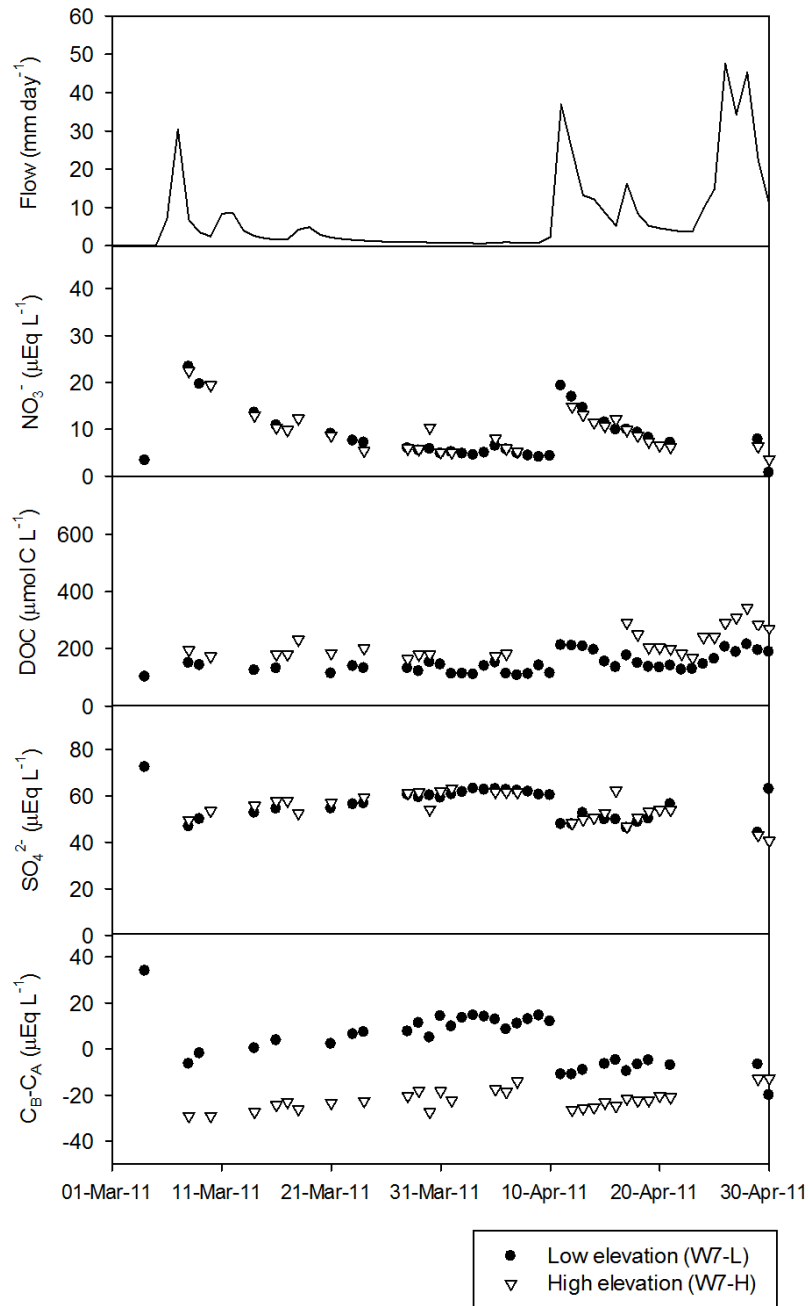


Figure 6.6. Snowmelt season hydrochemical dynamics in Watershed 3 based on discrete daily samples from 1 March 2011 to 30 April 2011, with a) stream flow, b) NO_3^- , c) DOC, d) SO_4^{2-} , and e) ANC indicated. Low elevation samples collected at the W3 weir (site W7-L, 619 m). High elevation samples collected at 720 m (site W7-H).

Watershed 3 - 2012

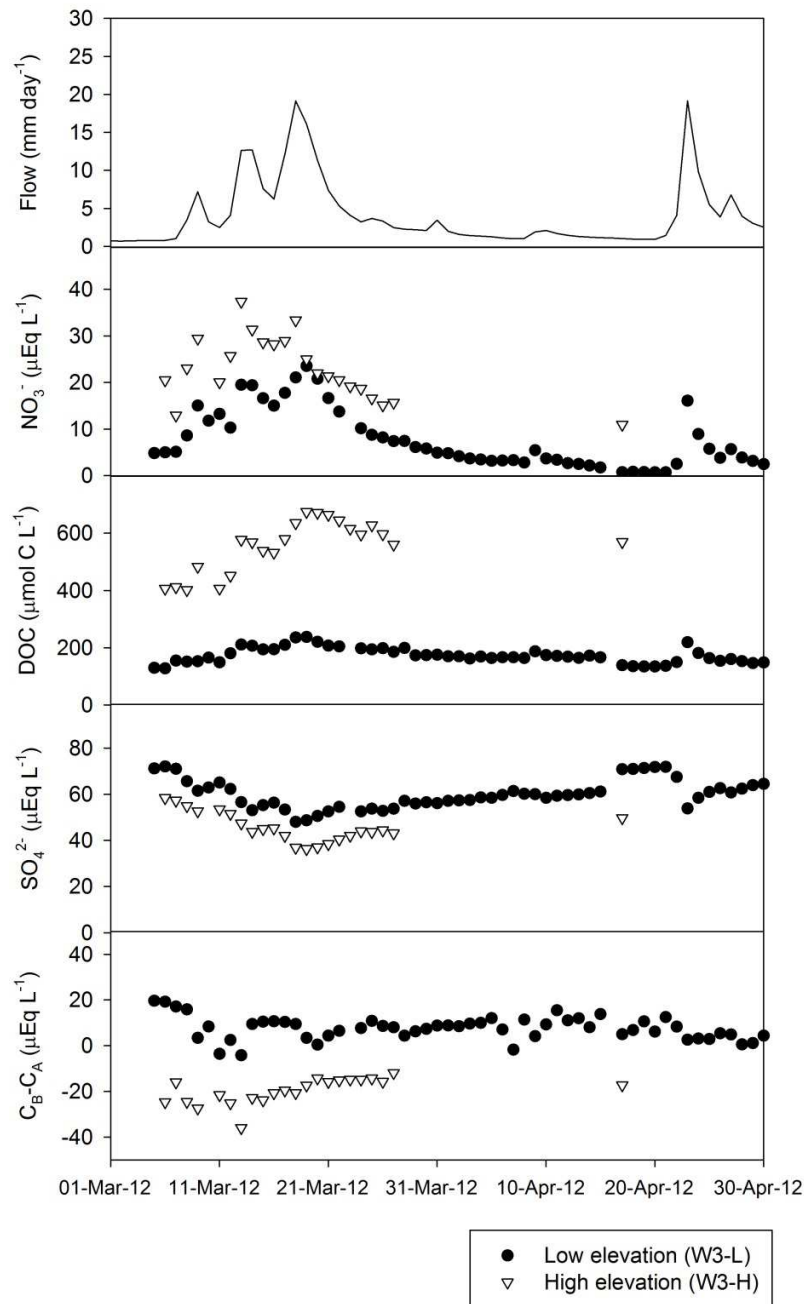


Figure 6.7. Snowmelt season hydrochemical dynamics in Watershed 3 based on discrete daily samples from 1 March 2012 to 30 April 2012, with a) stream flow, b) NO_3^- , c) DOC, d) SO_4^{2-} , and e) ANC indicated. Low elevation samples collected at the W3 weir (W3-L, 527 m). High elevation samples collected at 635 m (site W3-H).

Watershed 6 - 2012

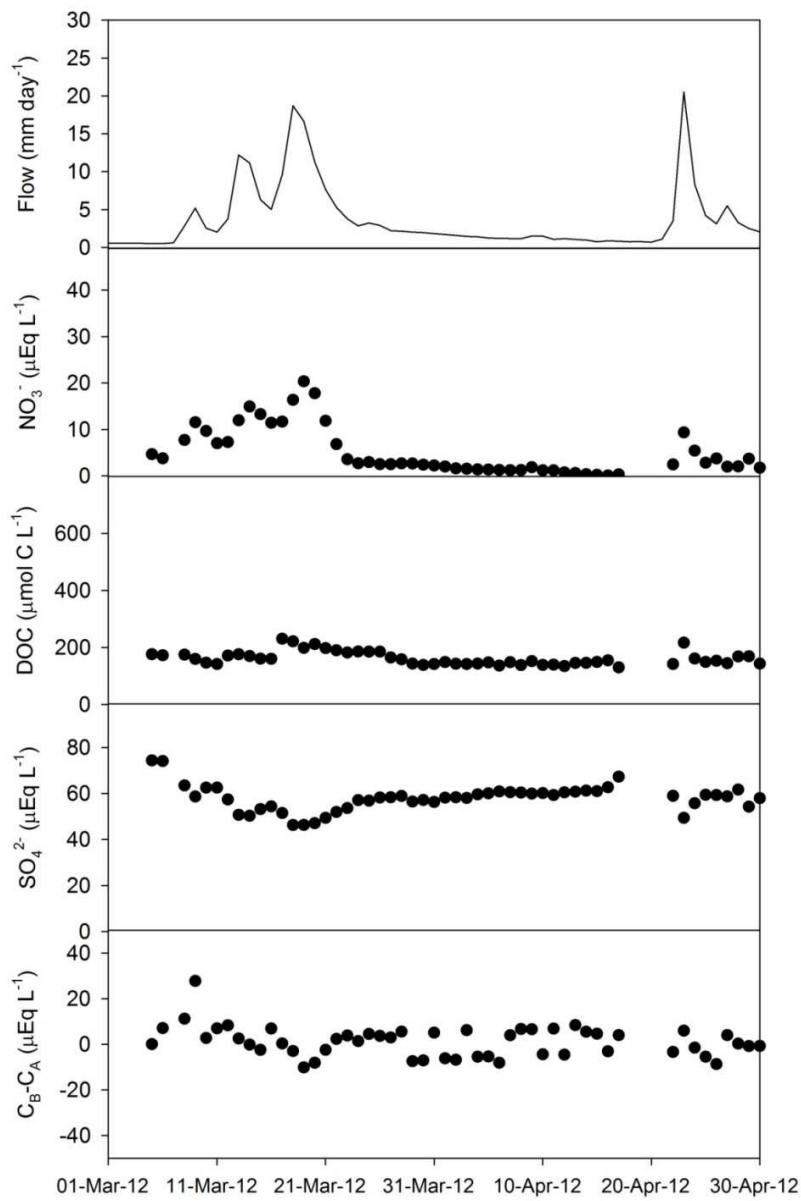


Figure 6.8. Snowmelt season hydrochemical dynamics in Watershed 6 (site W6-L) based on discrete daily samples from 1 March 2012 to 30 April 2012, with a) stream flow, b) NO_3^- , c) DOC, d) SO_4^{2-} , and e) ANC indicated.

Watershed 7 - 2012

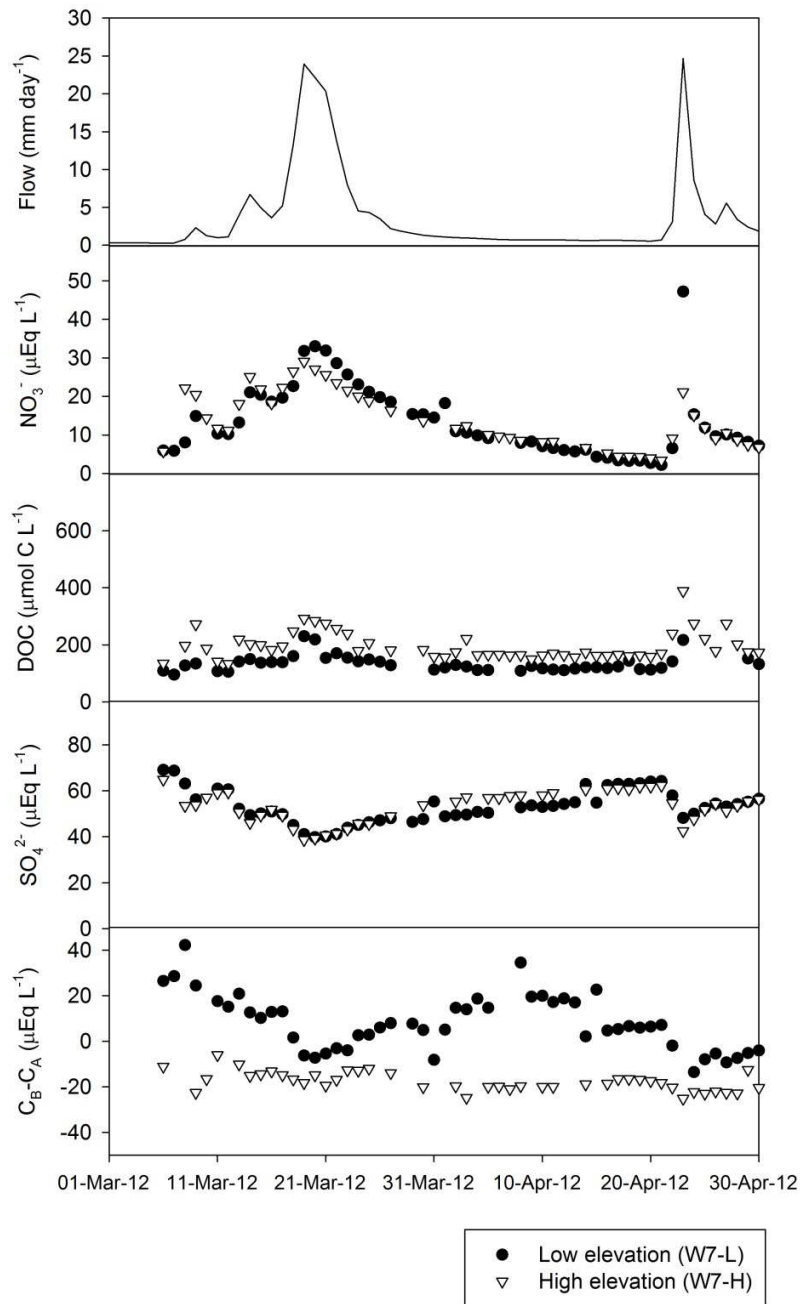


Figure 6.9. Snowmelt season hydrochemical dynamics in Watershed 3 based on discrete daily samples from 1 March 2012 to 30 April 2012, with a) stream flow, b) NO₃⁻, c) DOC, d) SO₄²⁻, and e) ANC indicated. Low elevation samples collected at the W3 weir (site W7-L, 619 m). High elevation samples collected at 720 m (site W7-H).

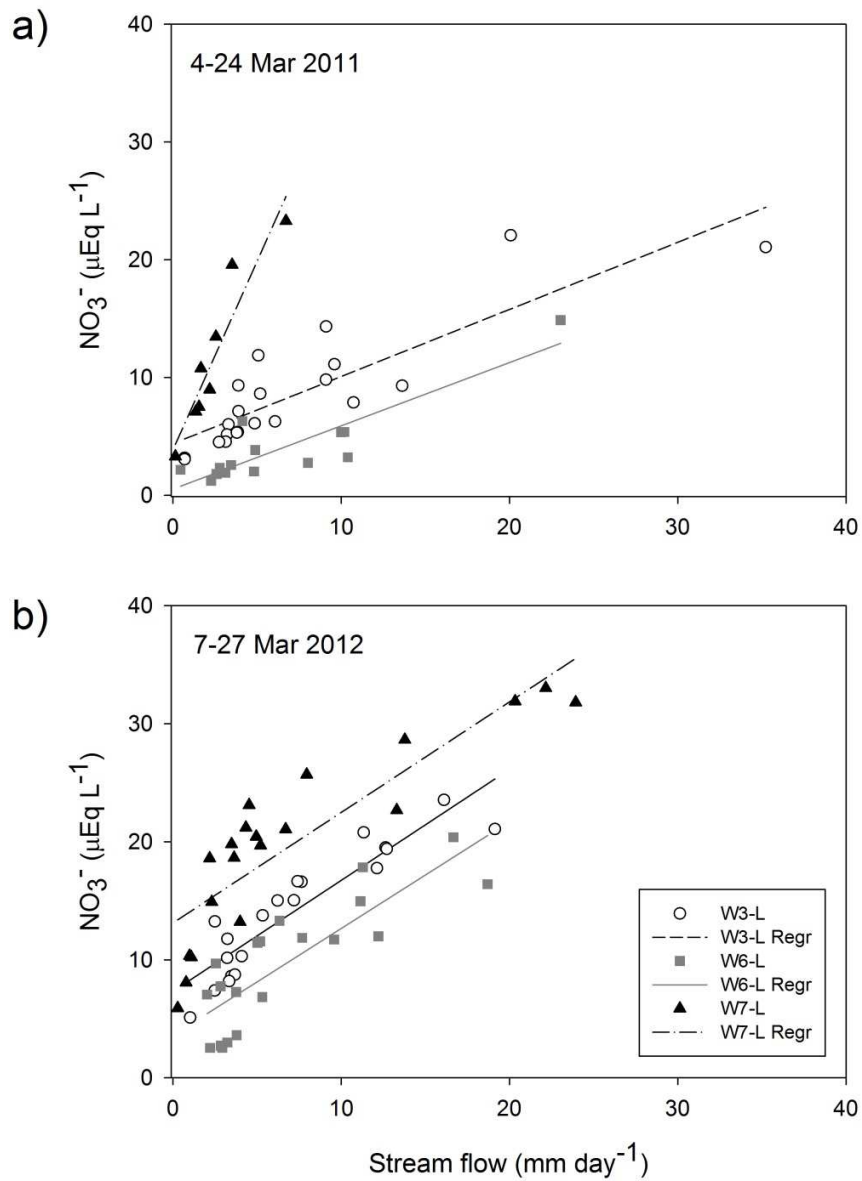


Figure 6.10. Concentration-discharge relationships for NO₃⁻ in streamwater at W3-L, W6-L, and W7-L during a) early snowmelt 2011 and b) early and peak snowmelt 2012.

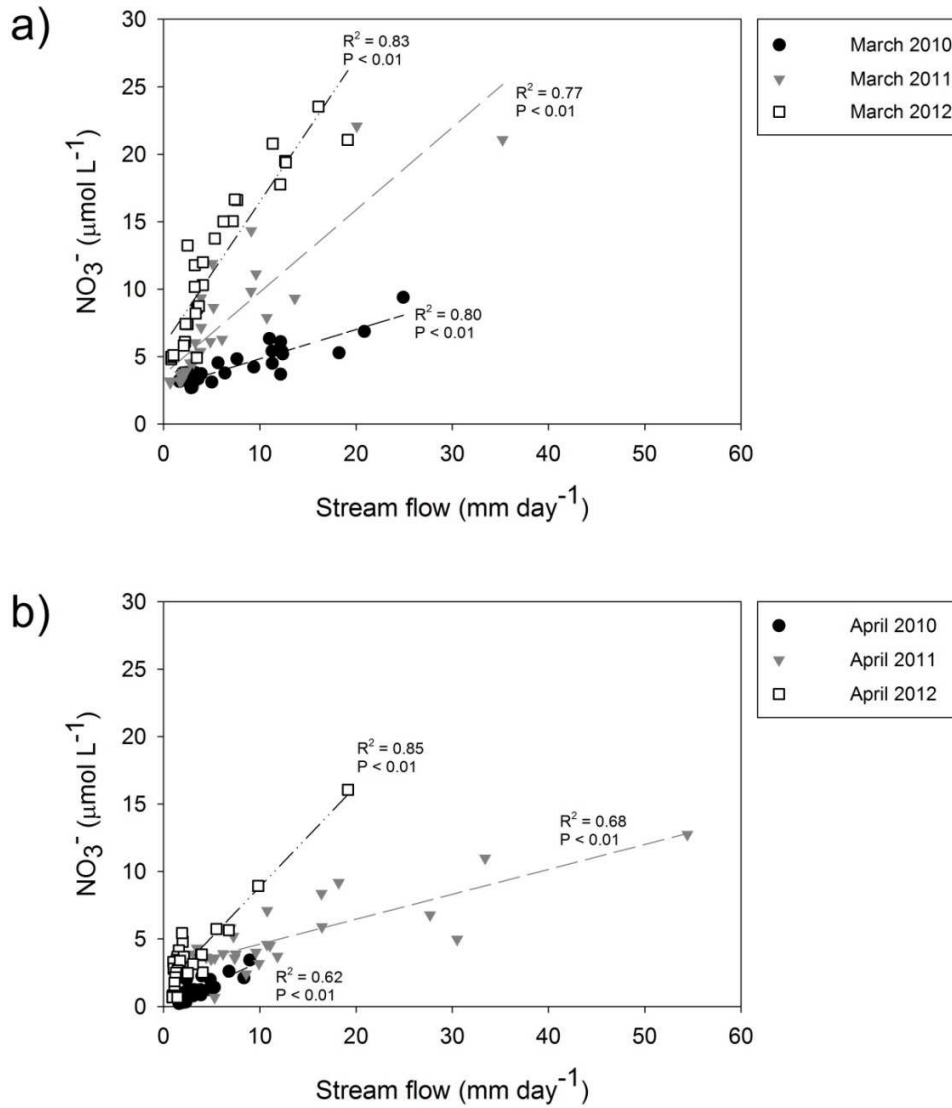


Figure 6.11. Concentration-discharge relationships for NO₃⁻ at site W3-L during a) March and b) April sampling dates of the 2010, 2011, and 2012 snowmelt seasons.

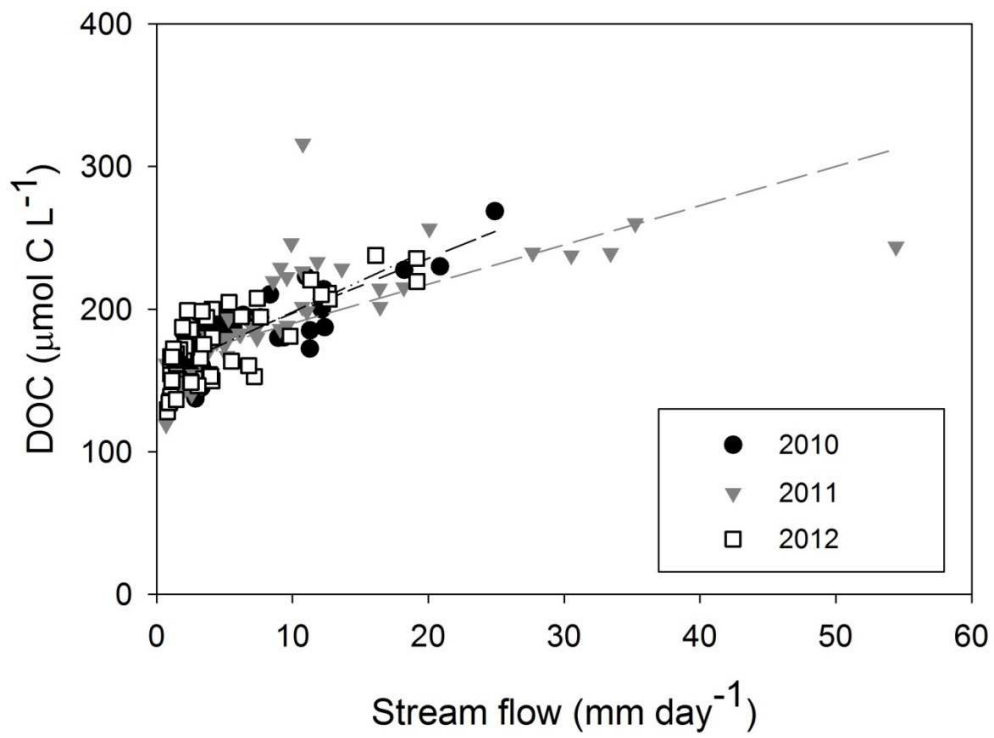


Figure 6.12. Concentration-discharge relationships for DOC at site W3-L by sampling year.

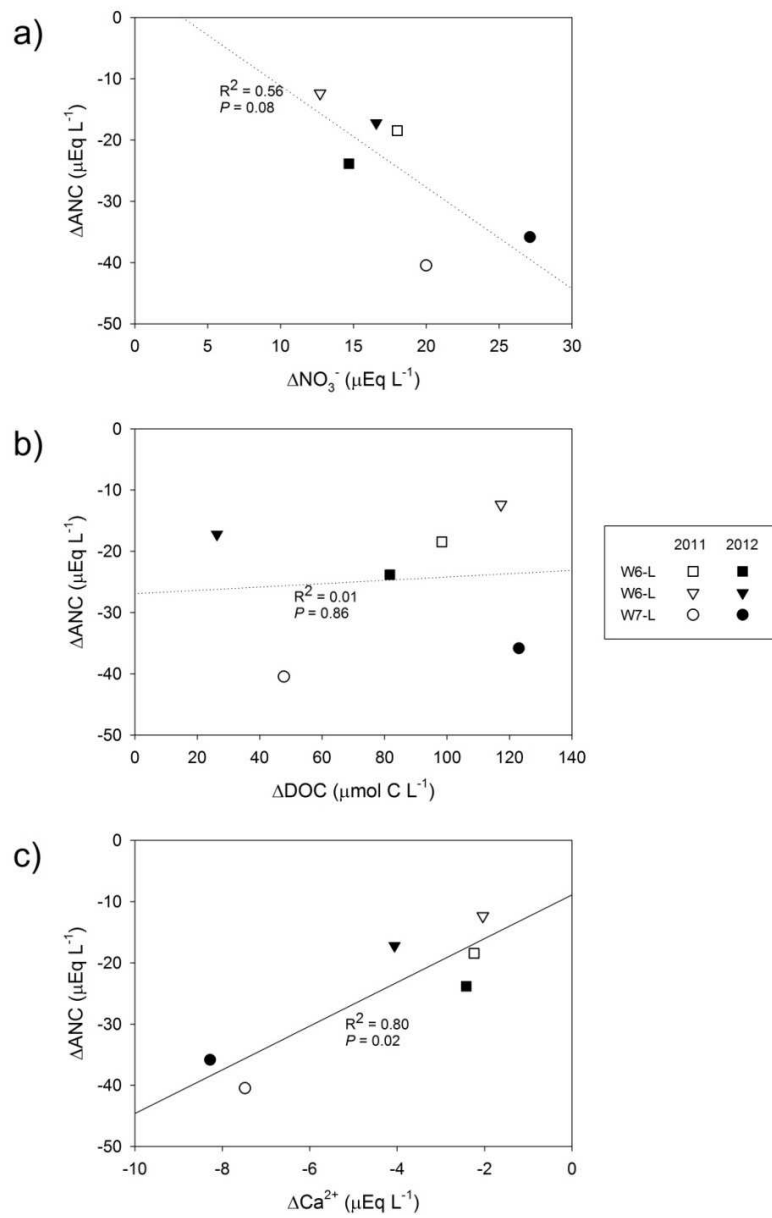


Figure 6.13. Relationship of ΔANC with a) ΔNO_3^- , b) ΔDOC , and c) ΔCa^{2+} by watershed and year.

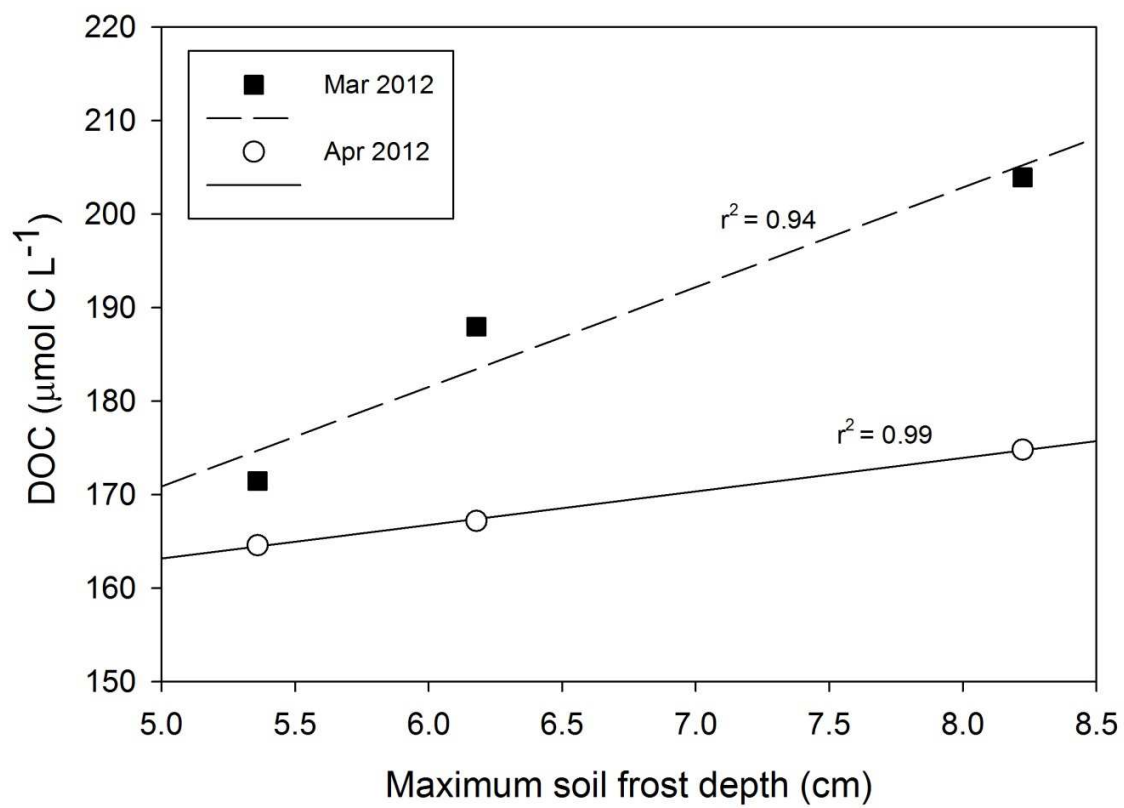


Figure 6.14. 2012 Mean volume-weighted DOC concentration by month as a function of preceding winter maximum soil frost depth.

7. Hydrological flowpaths during snowmelt in forested headwater catchments under differing winter climatic and soil frost regimes

7.1. Methods

7.1.1. Watersheds for snowmelt hydrologic flowpath study

This snowmelt hydrologic study was conducted in two gauged experimental watersheds: Watershed 3 (W3), and Watershed 6 (W6). W3 and W6 are both located on a south-facing slope of the Hubbard Brook Valley, approximately 1.1 km apart (Figure 7.1). They currently serve as reference watersheds at Hubbard Brook; W3 is the hydrologic reference watershed and W6 is the biogeochemical reference watershed. Watershed 3 is somewhat lower in elevation than W6 and is a larger catchment (Table 7.1). Both W3 and W6 have forest cover of similar age and disturbance history, having been commercially logged in the early 20th century. The vegetation composition is dominated by northern hardwood species, including American beech (*Fagus grandifolia* Ehrh.), sugar maple (*Acer saccharum* Marsh.), and yellow birch (*Betula alleghaniensis* Britt.). At higher elevations, balsam fir (*Abies balsamea* (L.) Mill), red spruce (*Picea rubens* Sarg.), and white birch (*Betula papyrifera* var. *cordifolia* Marsh.) are prominent.

Streamwater was sampled at the base of the watershed, just above the gauging station. In W3 an upstream sampling site was added in order to compare the snowmelt hydrologic flowpath dynamics of a higher elevation subcatchment with the whole watershed, capturing expected differences in winter climatic and soil frost conditions. Logistical constraints precluded an upstream site for W6. The stream flow tends to be less consistent at high elevation reaches, making the use of automated samplers less feasible.

7.1.2. Snowmelt streamwater sampling

Stream water sampling during the snowmelt period was started the first week of March each year and continued until early or mid-May, once the stream flow appeared to return to baseline conditions. Samples were collected daily using Teledyne ISCO (Lincoln, NE) 3700 or 6712 automated samplers. The samplers were programmed to collect water simultaneously from each site once per day. Collection occurred in the middle of the afternoon when stream flow and air temperature were generally highest in order to minimize the likelihood of sampling problems due to low flow or ice formation in sampling lines and/or pump mechanisms. The samples were removed from the autosamplers within 14 days from the time of collection. Samples were subsequently stored at 4°C until laboratory analysis. Prior to removal from the ISCO autosamplers, the samples were at ambient field temperatures, which were comparable to laboratory refrigeration, although it is likely that water samples did freeze and thaw during the early weeks of the sampling.

7.1.3. Stream flow measurements

Continuous stream flow measurements are made at the outlet of each watershed, by gauging stage heights with either a V notch weir (W3) or a V notch weir coupled with a San Dimas flume (W6) (Reinhart and Pierce 1964). Stream flow is expressed in millimeters per day, which is derived from integrating instantaneous measurements over time and normalizing by the watershed area.

7.1.4. Snowpack and soil frost monitoring

I utilized nine monitoring plots, each 10 m in diameter, to characterize the winter climatic conditions across the extent of the south-facing watersheds of the HBEF, with plots placed to capture the range between high and low elevation portions of the watersheds (Figure 7.1). These included four plots in W3, three plots immediately west of W6, and two plots located between W3 and W6 in Watershed 1. One plot west of W6 was relocated after the spring of 2011 to a higher elevation for the following winter. Each plot was monitored approximately biweekly. The snow depth was recorded as the mean of three locations in each plot. Snow depth and snow water equivalence were measured using Federal (Mt. Rose) snow tubes. Three replicate soil frost tubes were installed during the fall of 2010 in each plot according to the methods outlined by Hardy et al. (2001). These consisted of removable PVC tubes filled with methylene blue dye, which turns a purple color when frozen and thus allows personnel to visually measure the depth frozen water. Each monitoring plot was also equipped with replicate soil temperature probes (Decagon Model 5TM) at 5 cm depth, which recorded hourly soil temperature measurements.

7.1.5. Hydrologic flowpath determination

To quantify the sources of stream water and characterize flowpaths during snowmelt, I assumed three end-members: snowmelt (or precipitation), shallow soil water (draining the Oa horizon), and shallow groundwater (baseflow). The snow end-member was characterized for each watershed by taking the mean chemical concentrations in snow core samples from points near the weir stream sampling points (W6-L and W3-L) and the upper stream sampling point in W3 (W3-H). The forest floor soil water end-member was characterized by the mean chemical concentrations of samples collected from lysimeters representing the study watersheds during

snowmelt. For W3-L, lysimeters installed within the watersheds (Figure 7.1) were used to determine the soil water end-member, after weighting the values according to the watershed areas associated with each lysimeter elevation. For W6, lysimeters just west of the watershed which have been monitored since 1984 (see Chapter 4) were used to characterize the forest floor soil water end-member of stream water collected at site W6-L. The chemistry of pre-snowmelt baseflow stream water was assumed to be representative of the groundwater end-member at each stream sampling site.

7.1.6. *Laboratory analysis*

Concentrations of hydrologic flowpath tracers were measured in each sample of snowmelt streamwater and in each of the three proposed end-members—snow, Oa soil water, and premelt streamwater representing groundwater. The concentrations of Mg, Na, and H₄SiO₄ (as total Si) were measured with an inductively coupled plasma mass spectrometer (ICP-MS; Perkin Elmer, Waltham, MA). Chloride and SO₄²⁻ were measured using ion chromatography (Dionex, Sunnyvale, CA). Water isotopes, δ¹⁸O and δD, were analyzed with either a Los Gatos (Mountain View, CA) or a Picarro (Santa Clara, CA) liquid water isotope analyzer using cavity ring down spectroscopy (CRDS). Dissolved organic carbon and NO₃⁻ concentrations were measured as indicators of shallow soil leachate independent of the flowpath tracers. The DOC concentration was measured using persulfate oxidation followed by infrared CO₂ detection (Teledyne Tekmar, Mason, OH). Nitrate was measured with ion chromatography at the same time as Cl⁻ and SO₄²⁻.

7.1.7. End-member mixing analysis

Each end-member's contribution to daily stream water discharge was determined through end-member mixing analysis (EMMA), an approach developed by Christophersen and Hooper (1992). The approach to applying EMMA was similar to that outlined by Burns et al. (2001) and Wellington and Driscoll (2004), with modifications for the solutes used. The solutes selected— Na^+ , Mg^{2+} , H_4SiO_4 , and SO_4^{2-} —were chosen based on the appearance of conservative mixing. A correlation matrix (Table 7.2) of the potential tracers demonstrates the linear relationships among the four chosen. For the daily snowmelt stream sampling dataset, I employed the EMMA using the following steps:

- 1) A dataset of daily samples with concentrations of each tracer solute (Na^+ , Mg^{2+} , H_4SiO_4 , and SO_4^{2-}) was obtained.
- 2) The data were standardized into a correlation matrix so that solutes with a greater range of variability would not overly influence the model relative to the solutes with less variability.
- 3) A principal components analysis (PCA) was performed on the correlation matrix using all four solutes. A two principal component model was selected because it accounted for the greatest amount of variability, which confirmed three end-members.
- 4) The concentrations of the three end members were standardized and projected into the U space defined by the PCA and the extent to which they bounded the stream water data throughout the course of snowmelt was examined.
- 5) Linear regression was used to compare the solute concentrations for each sample as predicted by the model.

The EMMA model was then used to calculate the proportional contribution to stream flow of each of the three end members for each daily sample throughout the snowmelt season. The following mass balance equations were solved:

$$U1_{st} = U1_p f_p + U1_s f_s + U1_g f_g$$

$$U2_{st} = U2_p f_p + U2_s f_s + U2_g f_g$$

$$f_p + f_s + f_g = 1$$

where $U1$ and $U2$ are the first and second principal components of the PCA; the subscripts st , p , s , and g represent stream water, snow (or precipitation), forest floor soil water, and groundwater respectively.

7.2. Results

7.2.1. Interannual and elevational patterns of snow depth and soil frost

The meteorological conditions during the winters of 2011 and 2012 resulted in markedly different soil frost regimes. A much deeper snowpack during the 2011 winter relative to 2012 (80 cm and 40 cm average depth, respectively, at 600 m elevation) provided greater insulation of soil profile. The mean depth of soil frost at the beginning of March 2011 was 1 cm at 600 m elevation, while at the beginning of March 2012 the mean soil frost depth was 5 cm at the same elevation. Furthermore, in 2012 the snowpack developed relatively late and, as a result, soil frost penetrated as deep as 14.7 cm at a monitoring plot at 536 m elevation, representative of the lowest reaches of the experimental watersheds. The 2012 soil frost depths reached a maximum in January and declined only slightly over the subsequent six weeks, before rapidly decreasing during the time of peak snowmelt in mid-March. Conversely, a deeper snowpack had developed during the winter of 2011, and the soil frost that did develop reached maximums of

approximately 5 cm in January, before markedly receding in late January and February, several weeks prior to snowmelt (Figure 7.3).

7.2.2. *End-member mixing analysis*

Of the seven potential tracers investigated, Na^+ , Mg^{2+} , SO_4^{2-} , and H_4SiO_4 were chosen based on their conservative mixing properties inferred by linear relationships in streamwater (Table 7.2) and their performance in analysis across sites. The first two principal components explained 92-99% of the variation in these data across this streamwater sites during the two years. This high explanation of variance by two principal components implies a model with three end-members is sufficient to analyze the mixing data (Christophersen and Hooper 1992). The streamwater data were generally constrained by the snowpack-precipitation, forest floor soil water, and baseflow-groundwater end-members (Figure 7.4), although several data points—especially for site W3-L—fell outside of the mixing constraints.

7.2.3. *Hydrograph separation*

Snowmelt 2011

The hydrograph of the 2011 snowmelt season was characterized by low initial streamflow at the beginning of March, before melt commenced. This premelt streamwater was defined, for purposes of the EMMA, as consisting of exclusively baseflow (groundwater), which was routed via deep flowpaths. A large rain-on-snow event (9.9 cm rain over 36 h) occurred March 6-7, 2011. This event produced a marked peak in the stream hydrographs (Figure 7.5). EMMA analysis revealed that under the high flows associated with this event, W6 streamwater was derived primarily from baseflow (groundwater), with a marked contribution of water derived

from the precipitation or snowpack. In W6, the mean contribution of the precipitation or snowpack water to the stream flow was 35% during the rain-on-snow event. Conversely, the contribution of water from shallow flowpaths through Oa soil horizon was small, ranging from 0-10% of total flow (Figure 7.5). Two smaller peaks in the hydrograph between the 10th and 20th of March—which comprised the early period of the 2011 snowmelt—had Oa soil flowpath contributions to stream flow ranging from 15-25%, with a mean of 17%. The mean contribution during this time of the snow end-member was 28%, while baseflow made up the remaining 55%. Following these early snowmelt events, the hydrograph returned to low flows (generally < 2 mm day⁻¹) dominated by baseflow from groundwater during a period of extended cold temperatures through late March into early April. This period was followed by several marked peaks in the hydrograph as snowmelt accelerated until concluding by the beginning of May, when streamflow again declined toward baseline conditions. During this high flow period of peak snowmelt (10-27 April) the contribution of the forest floor end-member in W6, the portion of stream flow derived from shallow soil flowpaths, ranged from approximately 20-44%, with a mean contribution of 33%. The W6 stream flow during this high flow final snowmelt period was roughly evenly divided between the three end members.

The 2011 Watershed 3 hydrograph, as measured at site W3-L, was very similar in flow magnitude and timing as the hydrograph observed in W6. The separation of the W3 hydrograph by EMMA revealed that the streamwater at W3-L was generally derived more from baseflow groundwater compared to W6, while the snow and forest floor soil water end-members contributed relatively less. During the early 2011 snowmelt peaks (10-20 March) the mean snow end-member contribution to stream flow was 23%, the forest floor contribution was 7%, and the remaining 70% consisted of baseflow. During the late season peak snowmelt (10-27 April), W3-

L streamwater was derived from a mean of 33% from the snow end-member, 8% from the forest floor soil water, and 59% from baseflow. During the largest hydrograph peaks in the late snowmelt (the 11th, 17th, and 26th of April), the stream water at W3-L was comprised of approximately 41% from the snow end-member on each date.

At the W3 higher elevation site (W3-H) the flowpath analysis through EMMA for spring 2011 was similar to what was observed at W3-L, although baseflow from groundwater contributed less to overall stream flow. During the early season snowmelt event (10-20 March) the mean contributions to W3-H stream water were: 23% from the snow end-member, 12% from forest floor soil water, and 65% from baseflow. The late season peak snowmelt from 10-27 April was characterized by higher contributions from the snow end-member. The EMMA revealed a mean of 40% from snow, 7% from forest floor soil water, and 53% from baseflow.

Snowmelt 2012

The 2012 snowmelt period, as marked by initial elevated stream flow above the winter baseline, commenced at a similar calendar date as in 2011 (8 March and 6 March, respectively). The 2012 spring snowmelt proceeded much faster overall than the previous year, and the snowpack completely disappeared in two weeks. During the winter of 2012 a substantially smaller snowpack developed compared with 2011. Consequently, the melting of the snowpack produced considerably lower stream flows than were observed during the spring of 2011. The results of the EMMA for the 2012 showed distinctly different patterns of flowpaths during early snowmelt from 2011 observations. During the earliest peak (max. flow = 12 mm day⁻¹) in the W6 snowmelt hydrograph (10-15 March 2012), almost no contribution of water from shallow soil (forest floor) flowpaths to the W6-L streamwater was observed. A second, larger (19 mm day⁻¹),

snowmelt peak occurred several days later, with maximum flow on 18 March 2012. The EMMA revealed modest contribution from the forest floor soil flowpaths of approximately 9% during the rising limb of the hydrograph peak, with marked increases in forest floor flow reaching a maximum of 60% during the receding limb (Figure 7.5). The rapid increase in forest floor soil flowpath contributions to W6-L streamwater coincided with the thawing of relatively deep soil frost (Table 7.4; Figure 7.5) during the mid-March snowmelt.

The pattern of minimal forest floor flowpath contributions to streamwater at W3-L was generally similar during the early 2012 snowmelt when soil frost was deep and widespread. Upon the thawing of soil frost, however, only a small increase was observed in streamwater derived from the shallow forest floor soil water end-member (Figure 7.6), especially compared to W6-L (Table 7.4). At the W3-H stream site, which drains a high elevation subcatchment that developed much shallower soil frost than the lower reaches of W3, the forest floor soil water end-member comprised a substantial portion of streamwater throughout both the early and late periods of the 2012 snowmelt (mean of 19.5% between 8-15 March and 12.1% between 16-23 March).

Late in the month of April 2012, several weeks after the snowpack had disappeared, high flow peaks in the hydrograph occurred as a result of rainfall events (8.6 cm total precipitation in W6 from 21-27 April). The results of the EMMA showed a relatively consistent flowpath distribution, with a mean of 32.1% of W6 runoff traveling via forest floor shallow soil flowpaths between 20-30 April 2012. The groundwater baseflow inputs comprised a mean of 52.7% of W6-L stream flow, and the remaining flow was characterized as the precipitation end-member, either rain falling directly into the stream channel or overland flow. The W3-L streamwater again had a markedly higher contribution from baseflow (80%) during the late April rain-on-bare ground

event, and the forest floor soil water end-member input was 9.0%. No information was available for the W3-H stream site due to failure of the automatic sampler prior to the event dates.

7.3. Discussion

The meteorological conditions during the winters of 2010-2011 and 2011-12 were distinctly different, which provided a unique opportunity to study the influence of the differing snowpack and soil frost development on runoff dynamics during snowmelt. A much deeper snowpack developed during the winter of 2010-2011 compared to the winter of 2011-2012. The deep snowpack developed relatively early in the winter across the entire elevation range of the Hubbard Brook experimental watersheds. Thus, the deep snowpack provided insulation of the forest floor and soil frost development was minimal and weakly correlated with elevation (Figure 7.2). The winter of 2011-2012, by contrast, was characterized by a later developing snowpack with maximal depths markedly shallower than the previous winter. The late-developing, shallow snowpack led to relatively deep soil frost, which persisted from early in the winter through the beginning stages of snowmelt (Figure 7.3). This markedly greater development of soil frost during the winter of 2011-2012 occurred despite higher mean air temperatures. The mean daily air temperature (at the Hubbard Brook weather station #1) from December through February was -8.1°C during the winter of 2010-2011, compared to -4.3°C during the winter of 2011-2012. Additionally, a much stronger relationship between soil frost depth and elevation was observed throughout the winter of 2011-2012 (Figure 7.2), with little or no soil frost occurring at the higher elevation portions of the south-facing watersheds, and extensive, relatively deep (10-15 cm) frost occurring at the lower elevation zones.

7.3.1. Influence of soil frost on infiltration

There was no indication that soil frost significantly reduced infiltration of melt waters into the soil profile and promoted surface runoff. The flow proportions derived from the snow (or precipitation) end-member were relatively similar across all hydrologic events related to snowmelt sampled during the 2 years (27.0-33.6% at W6-L, Table 7.4). The highest contribution to flow from the snow-precipitation end-member (33.6%) was observed during the heavy rain-on-snow event of 6-7 March 2011, a time when soil frost was minimal. During that event nearly 10 cm of precipitation fell in a 36-hour period on top of a deep snowpack. The relatively high amount of streamflow derived from the snow-precipitation end-member for that event can be attributed to a high proportion of lateral flow directly through the snowpack. The streamflow produced by the rain-on-snow event during the two days was considerably smaller than the total precipitation, 56.8 mm vs. 99 mm at W6. The low overall runoff ratio suggests that the rainfall caused little melting of the snowpack. Indeed, the mean daily temperatures at the weather station #1 were 2°C on 6 March 2011 and -5°C on 7 March 2011, indicating rainwater was only slightly above freezing temperature. It is likely that much of the rain water was retained in the snowpack or beneath the soil profile, recharging groundwater levels.

Lower percentages of streamflow were derived from precipitation that did not connect to soil water or groundwater during the 20-30 April 2012 rain-on-bare ground hydrologic event (15.1% at W6-L and 11.0% at W3-L, Table 7.4). This event was the result of several rainy days during which 8.6 cm of precipitation fell over the course of one week. The lower contribution from the precipitation end-member is not surprising given the lower intensity of rain spread out over several days and the lack of snowpack through which additional flowpaths could form.

The lack of increased runoff of snowmelt disconnected from soil water or groundwater flowpaths found during a time period of superficial soil frost indicates that the soil retained its permeability despite being frozen. Previous studies which have found significantly reduced infiltration into frozen soils (Kane and Stein 1983; Thunholm et al. 1989; Stähli et al. 1996) have often concentrated on agricultural soils. The results observed in the forested catchments at Hubbard Brook are comparable to other studies where forest soils retained permeability despite frozen conditions (Shanley and Chalmers 1999; Nyberg et al. 2001; Lindström et al. 2002). Lindström et al. (2002) analyzed long-term data at the Nyänget catchment, a boreal forest site in northern Sweden, and found no clear connection between the extent of soil frost and the timing or magnitude of snowmelt runoff. The authors attributed this lack of a relationship to the fact that soils typically thawed prior to peak snowmelt. Nyberg et al. (2001), conducting hydrometric studies at the same Swedish catchment, could not find any definite evidence of flowpaths being affected by soil frost. Laudon et al. (2004), on the other hand, reported shifting flowpaths due to soil frost in an analysis using water isotope tracers at the Svartberget Research Station, a nearby Swedish boreal forest catchment. They found increased overland flow during the early portion of spring snowmelt. Shanley and Chalmers (1999) used time-series data at the Sleepers River Watershed in northern Vermont and found significantly increased runoff over frozen soils only in an agricultural catchment, and not in the mesoscale catchment containing forested lands. They attributed this to differences in soil frost development and infiltration characteristics between agricultural and forested soils and the muting of effects at larger scales. They observed that the forested areas developed shallower and more irregular frost compared to the relatively deep impermeable frost in the open fields. Shanley et al. (2002) found that during snowmelt when

ground frost was widespread, the percentage of new water in runoff increased with increasing percentage of open land in the drainage area.

7.3.2. Development of different types of soil frost

Differences in infiltration into frozen soil are likely due to the occurrence of concrete versus granular frost. Soils that are partially saturated at the onset of freezing are likely to develop concrete frost which is impermeable (Granger et al. 1984; Johnsson and Lundin 1991). This relationship was demonstrated by Zhao and Gray (1999), who developed a model for infiltration into soils based on an analysis of different studies showing that infiltration is inversely related to the soil water content at the time of freezing. By contrast, unsaturated soils that freeze tend to retain their permeability. Trimble et al. (1958) found that forested soils developed granular frost, which retained a high infiltration capacity, as opposed to concrete frost found in open areas. Upland soils at Hubbard Brook are generally well-drained (Bailey et al. 2014) and it would be expected that they would develop granular soil frost and retain capacity for infiltration.

While the results presented here are consistent with other studies that show that forested soils tend to develop granular frost that does not significantly reduce permeability, there are no known comparable studies that investigate the influence of granular frost on subsurface flowpaths following meltwater infiltration into the soil profile. These results indicate that the granular frost presumably found in Hubbard Brook soils has the capacity to reduce the flow of runoff through the shallow forest floor flowpaths to zero or near-zero during a period of relatively deep frost. The typical organic horizon depth at Hubbard Brook is approximately 6.9 cm (Johnson et al. 1991). The data reported here indicate that soil frost depths in early and mid-

March 2012 would have extended to that depth and often deeper throughout much of the experimental watersheds, especially at the lower elevation sites where snowpack melting began earlier. As evidenced in the 2012 W6-L hydrograph separation (Figure 7.5), the contribution to streamwater from the Oa soil shallow flowpaths increased dramatically approximately 17-18 March 2012 as snowmelt approached its peak and final stage. Prior to this period the forest floor contribution to streamflow had been zero or nearly zero. The markedly increased contribution from forest floor flowpaths coincides with a rapid melting of the soil frost. While this rapid melting is not evident from the frost depth monitoring data alone (Figure 7.3), the soil temperature monitoring probes at 5 cm depth recorded an abrupt increase around 17-20 March 2012, depending on the elevation (Figure 7.7).

7.3.3. Variability of forest floor preferential flowpaths related to soil frost depth

The hydrograph separation through EMMA revealed interesting differences in flowpath utilization during the various hydrologic events over the course of the two snowmelt seasons of sampling, which corresponded to differences in the presence and severity of soil frost in the study watersheds. Because of the marked difference in soil frost magnitude—especially at lower elevations—between the two winters, I was able to conduct an interannual comparison to relate how the presence of soil frost affected flowpaths through the upper soil as the catchment hydrology transitioned from winter baseflow to the high-flow snowmelt period.

The soil frost that extended to depths greater than 10 cm at the beginning of snowmelt in 2012 appears to have led to reduced flow through shallow soil (forest floor) flowpaths during early melt. A period of early snowmelt of 7-10 days in mid-March was defined for both 2011 and 2012, which were similar in magnitude of total flow (at W6-L, 63.3 mm from 10-20 March 2011,

46.0 mm from 8-15 March 2012). The EMMA results indicated that W6-L streamwater during the early snowmelt period of 2012 contained a much smaller contribution from forest floor soil flowpaths than was observed in 2011, thus supporting the hypothesis that preferential lateral flowpaths in the forest floor are closed or constricted when soil frost penetrates the entire depth of the organic horizon. During the early snowmelt period in 2012, W6 had soil frost depth estimated, based on linear regressions of frost depth with elevation (Figure 7.2), to be up to 8.1 cm. in depth, with even deeper values in localized areas.

It is difficult to make direct comparisons of flowpath usage between watersheds (W6-L vs. W3-L) in this study. W3 is substantially larger than W6 and the watersheds differ in slope and aspect as well. Nonetheless, the interannual patterns of the forest floor flowpath contribution for streamwater at W3-L are largely consistent with what was observed at W6-L, with lower forest floor flowpath contributions under the high frost conditions early during the 2012 snowmelt relative to the minimal soil frost conditions throughout the 2011 snowmelt. Lower overall forest floor flowpath contributions at W3-L compared to W6-L are also consistent with the less “flashy” nature of the gentler-sloping watershed, as well as the deeper glacial till underlying W3, which would allow for more deep groundwater flowpaths.

The strong relationship of soil frost depth with elevation (Figure 7.2; Figure 7.3) observed through late winter and early spring 2012 provided the opportunity to compare the flowpaths to streamwater at low elevation with significant soil frost with those in a higher elevation subcatchment with less soil frost development. At the higher elevation site (W3-H), the contribution of forest floor soil water was markedly higher than at the base of the watershed (W3-L) throughout the peak of the 2012 snowmelt. Additionally, the thickness of the forest floor is typically less at lower elevation (Johnson et al. 2000). At the higher elevation sites the total

soil depth is shallower and the organic horizon comprises a greater percentage of the total soil profile. Consequently, hydrologic flow is more likely to be routed through this soil horizon during events. Soil frost depth was relatively shallow and variable in the upper reaches of W3 (mean of approximately 3 cm) at the initiation of snowmelt. Because several centimeters of frost is unlikely to penetrate the entire depth the organic soil horizon at high elevation, it is not surprising that a substantial contribution of runoff was derived from forest floor soil water during peak snowmelt at the upper stream sampling site. Conversely, the lower reaches of the watershed have shallower depths of the organic horizon—which constitute a smaller relative portion of the total soil profile—and had markedly deeper penetration of soil frost. The data indicate that the soil frost extended through the depth of the organic soil horizon during the early days of peak snowmelt, limiting the contribution of forest floor soil water to stream runoff.

7.3.4. Dissolved organic carbon and nitrate as indicators of shifting flowpaths

Examining solutes in streamwater other than the tracers used in the hydrograph separation can provide independent evidence for flowpath shifts. When high flow event water is routed through shallow hydrologic flowpaths in the organic soil, increased mobilization of DOC and NO_3^- are typical responses (Sebestyen et al. 2008; Pellerin et al. 2012). Thus the DOC or NO_3^- concentrations in streamwater can provide an indication of flowpaths through organic soil independent of the conservative tracers in the EMMA analysis. During the low-flow premelt period through the earliest snowmelt peak in the W6 hydrograph (5-15 March 2012), when substantial soil frost was present in the Oa horizon, no relationship between stream discharge and DOC concentration was evident ($p = 0.53$; Figure 7.8). In contrast, the relationship between flow and DOC concentration became significantly positive following the melting of the soil frost (18-

26 March 2012, slope = $1.94 \mu\text{mol C L}^{-1}/\text{mm day}^{-1}$, $p < 0.01$). This relationship change does not appear to be simply a result of increased subsurface flow concurrent with lower flow through an ablating snowpack. During the previous year's early snowmelt period (5-20 March 2011)—when a deeper snowpack had developed and the presence of soil frost was minimal—the relationship between W6 stream discharge and DOC concentration was strongly positive (slope = $5.00 \mu\text{mol C L}^{-1}/\text{mm day}^{-1}$, $p < 0.01$; Figure 7.8). The early snowmelt data from 2012 in W3 provide similar evidence for frost-reduced shallow soil flowpath utilization and associated DOC mobilization. From premelt baseflow through the rising limb of the initial snowmelt hydrograph peak (6-12 March 2012), when soil frost extended beyond the depth of the Oa horizon through the lower elevation reaches of the watershed, no significant relationship was found between stream flow and DOC concentration measured at site W3-L ($p = 0.37$). Conversely, during the same sampling dates at the higher elevation site (W3-H), the stream DOC concentration was significantly correlated with the discharge measured at the base of the watershed (slope = $12.0 \mu\text{mol C L}^{-1}/\text{mm day}^{-1}$, $p = 0.03$).

The relationship between discharge and NO_3^- under differing frost conditions is less clear than for DOC (Figure 7.8). NO_3^- concentrations were significantly positively correlated to discharge in each circumstance. This is not entirely surprising, given that NO_3^- is sourced not only from the forest floor (as the product of soil nitrogen mineralization and nitrification), but also from atmospheric deposition and therefore from the snowpack as well. On the other hand, the data shown in Figure 7.8 indicate that the slope of the relationship between NO_3^- and discharge is lower under the condition of extensive soil frost in 2012 compared to the minimal soil frost condition several days later. The opposite relationship would normally be expected given that NO_3^- is typically flushed in highest concentrations at the onset of snowmelt with

progressive dilution through the course of season. These differing relationships seem to indicate a reduced contribution of forest floor-derived NO_3^- during the time of extensive soil frost.

7.3.5. Proposed mechanism of soil frost effect on organic soil flowpaths

The data presented here indicate reduced flow through the shallow soil forest floor flowpaths—as detected by EMMA—under conditions of extensive soil frost through the depth of the Oa horizon. The soil frost appears to have formed in granular form under unsaturated conditions as there was no evidence of significantly reduced infiltration into the soil profile. Two proposed conceptual models explain how the granular frost prohibits the movement of meltwater (or its detection) through Oa preferential flowpaths (Figure 7.9). One possible mechanism is that granules of ice fill many of the Oa soil pore spaces, especially in the preferential flowpaths. While these are not of sufficient size and quantity to prevent infiltration into the soil from above, they appear to have the net effect of lessening flow through preferential flowpaths and effectively forcing water to use deeper mineral soil flowpaths, where the chemical signature more resembles baseflow. An alternative model would leave open the possibility that a substantial portion of flow still is routed through the Oa preferential flowpaths, but because of the frozen condition of the soil, possibly because of ice coatings on the soil matrix, the water does not undergo normal chemical exchange with the horizon and therefore does not take on the chemical signature that would be detected through EMMA.

7.3.6. Implications of climate change for flowpaths and stream chemistry

The long-term record at Hubbard Brook indicates decreased snowpacks (Campbell et al. 2010) and earlier snowmelts (Campbell et al. 2011) due to winter climate change. Model

projections indicate greater warming over the next 50-100 years (Hayhoe et al. 2007), which would lead to shallower and later developing snowpacks, thus more often exposing the soil more often to freezing during cold spells. My results only showed a relatively short duration of soil frost affecting hydrologic flowpaths. However, it is within reason that greater development of frost, coupled with a rapid snowmelt, such as those driven by large rain-on-snow events, could have marked effects on hydrologic flowpaths and consequently runoff chemistry. Moreover, more frequent mid-winter melt events could potentially saturate the soil leading to more concrete frost upon refreezing. In a Swiss forest site with Spodosol soils, Stadler et al. (1996) found that surface runoff was greatly increased during a second melt event relative to the first, due to greater ice content in the soil following the first melt event. This scenario would be expected to result in markedly different hydrological dynamics and resulting stream chemistry in headwater catchments during early snowmelt, with strong implications for runoff quantity and water quality downstream.

7.4. Summary and Conclusions

The results presented in this chapter indicate that development of soil frost varies across the landscape and is inversely related to snow depth. Development of granular frost in the soils of the HBEF appears to maintain the infiltration capacity of the soils, thus not appreciably increasing surface runoff. I observed a decreased contribution of forest floor flowpaths to stream flow during snowmelt at a time when soil frost was extensive and relatively deep. These results indicate that the granular soil frost can effectively block flow through the most preferential of the forest floor flowpaths thereby promoting deeper infiltration and longer flowpaths. While the effect of reduced forest floor flowpaths was only noted for a relatively short period before it

thawed, it has the potential to alter the chemistry of streamwater runoff. Analysis of concentration-discharge relationships indicated that DOC and NO_3^- concentrations would be reduced as soil frost prevents flow through the forest floor, although they would be available to be leached during high flow after the soil thaws.

Table 7.1. Catchment and subcatchment information for each snowmelt stream sampling site at the Hubbard Brook Experimental Forest, NH.

Stream sampling site name	Sampling site elevation (m)	Catchment area (ha)	Catchment elevation range (m)	Catchment mean elevation (m)	Catchment slope (°)
W6-L	549	13.2	549-792	679	15.8
W3-L	527	42.4	527-732	631	12.1
W3-H	635	2.8	635-693	660	13.5

Table 7.2. Correlation matrix of potential hydrologic flowpath tracers.

	Cl ⁻	SO ₄ ²⁻	Na ⁺	Mg ²⁺	H ₄ SiO ₄	δD	δ ¹⁸ O
Cl ⁻	1.00	0.45	0.26	0.10	0.08	0.21	-0.38
SO ₄ ²⁻	0.45	1.00	0.82	0.50	0.57	0.59	-0.08
Na ⁺	0.26	0.82	1.00	0.65	0.71	0.49	0.00
Mg ²⁺	0.10	0.50	0.65	1.00	0.35	0.46	0.08
H ₄ SiO ₄	0.08	0.57	0.71	0.35	1.00	0.41	0.41
δD	0.21	0.59	0.49	0.46	0.41	1.00	0.21
δ ¹⁸ O	-0.38	-0.08	0.00	0.08	0.41	0.21	1.00

Table 7.3. Mean concentration values of potential hydrologic flowpath tracers in each end-member. Units for Cl⁻, SO₄²⁻, Na⁺, Mg²⁺, and H₄SiO₄ are μmol L⁻¹. Units for δD and δ¹⁸O are ‰. Standard deviations are indicated in parentheses.

	Cl ⁻	SO ₄ ²⁻	Na ⁺	Mg ²⁺	H ₄ SiO ₄	δD	δ ¹⁸ O
Snow	6.1 (1.9)	3.2 (1.5)	7.2 (2.5)	1.0 (1.3)	3.0 (1.9)	-130.7 (15.9)	-17.9 (2.5)
Forest floor	9.6 (2.5)	24.6 (8.7)	32.1 (8.6)	4.8 (2.5)	72.0 (32.0)	-75.8 (4.3)	-12.3 (1.0)
Baseflow	12.1 (0.4)	38.1 (1.6)	44.4 (1.4)	12.1 (1.0)	90.5 (2.3)	-63.3 (0.2)	-9.8 (0.1)

Table 7.4. Hydrological events during the spring of 2011 and 2012. End-member flow contributions for snow-precipitation, forest floor (FF) soil water, and baseflow-groundwater are estimated through EMMA. Values in parentheses are standard deviations. Soil frost depths are estimated through the linear regression model of soil frost and elevation.

a) 6-7 Mar 2011 - Rain-on-snow					
	Total flow (mm)	Snow-precip (%)	FF (%)	Baseflow (%)	Soil frost (cm)
W6-L	56.8	33.6 (9.1)	6.1 (8.7)	60.3 (0.4)	0-2.0
W3-L	55.3	30.8 (0.9)	0 (0)	69.1 (0.9)	0-2.2
W3-H	NA	NA	NA	NA	0-1.3
b) 10-20 Mar 2011 - Early snowmelt					
	Total flow (mm)	Snow-precip (%)	FF (%)	Baseflow (%)	Soil frost (cm)
W6-L	63.3	28.0 (5.6)	17.0 (8.4)	55.0 (6.4)	0-1.4
W3-L	72.4	23.6 (5.0)	6.8 (6.1)	69.6 (4.4)	0-1.6
W3-H	NA	23.1 (5.2)	12.3 (7.7)	64.6 (6.5)	0-0.6
c) 10-27 Apr 2011 - Peak snowmelt					
	Total flow (mm)	Snow-precip (%)	FF (%)	Baseflow (%)	Soil frost (cm)
W6-L	306.3	32.2 (4.1)	32.9 (10.2)	34.9 (10.7)	Negligible*
W3-L	289.3	33.6 (5.5)	7.8 (8.0)	58.6 (4.1)	Negligible*
W3-H	NA	40.5 (6.5)	6.7 (6.7)	52.7 (6.9)	Negligible*
d) 8-15 Mar 2012 - Early snowmelt					
	Total flow (mm)	Snow-precip (%)	FF (%)	Baseflow (%)	Soil frost (cm)
W6-L	46.0	27.0 (7.6)	1.8 (4.5)	71.2 (9.4)	0-8.1
W3-L	53.4	20.0 (4.7)	1.3 (2.9)	78.6 (3.9)	0-9.0
W3-H	NA	12.0 (5.2)	19.5 (9.8)	68.5 (5.7)	0-4.6
e) 16-23 Mar 2012 - Late snowmelt					
	Total flow (mm)	Snow-precip (%)	FF (%)	Baseflow (%)	Soil frost (cm)
W6-L	78.0	28.0 (8.5)	24.9 (19.4)	47.1 (13.9)	Negligible*
W3-L	81.7	23.9 (4.9)	3.6 (6.2)	72.5 (5.5)	Negligible*
W3-H	NA	26.1 (6.8)	12.1 (7.8)	61.8 (9.3)	Negligible*
f) 20-30 Apr 2012 - Rain-on-bare ground					
	Total flow (mm)	Snow-precip (%)	FF (%)	Baseflow (%)	Soil frost (cm)
W6-L	54.8	15.1 (7.3)	32.1 (13.7)	52.7 (7.9)	0
W3-L	61.1	11.0 (6.8)	9.0 (6.9)	80.0 (6.7)	0
W3-H	NA	NA	NA	NA	0

*Assumed based on soil temperature increases since prior frost measurement

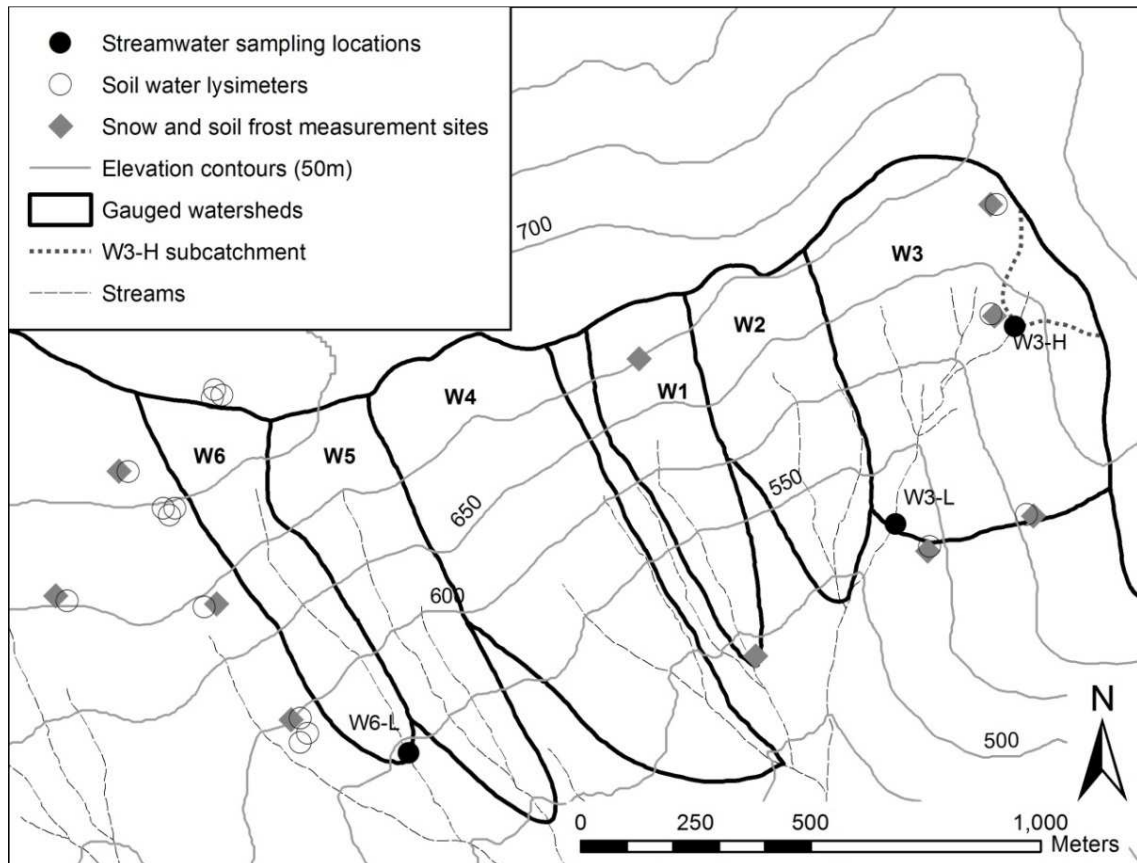


Figure 7.1. Map of Hubbard Brook's south-facing experimental watersheds, indicating locations of stream sampling sites, soil water lysimeters, and snow and soil frost monitoring sites.

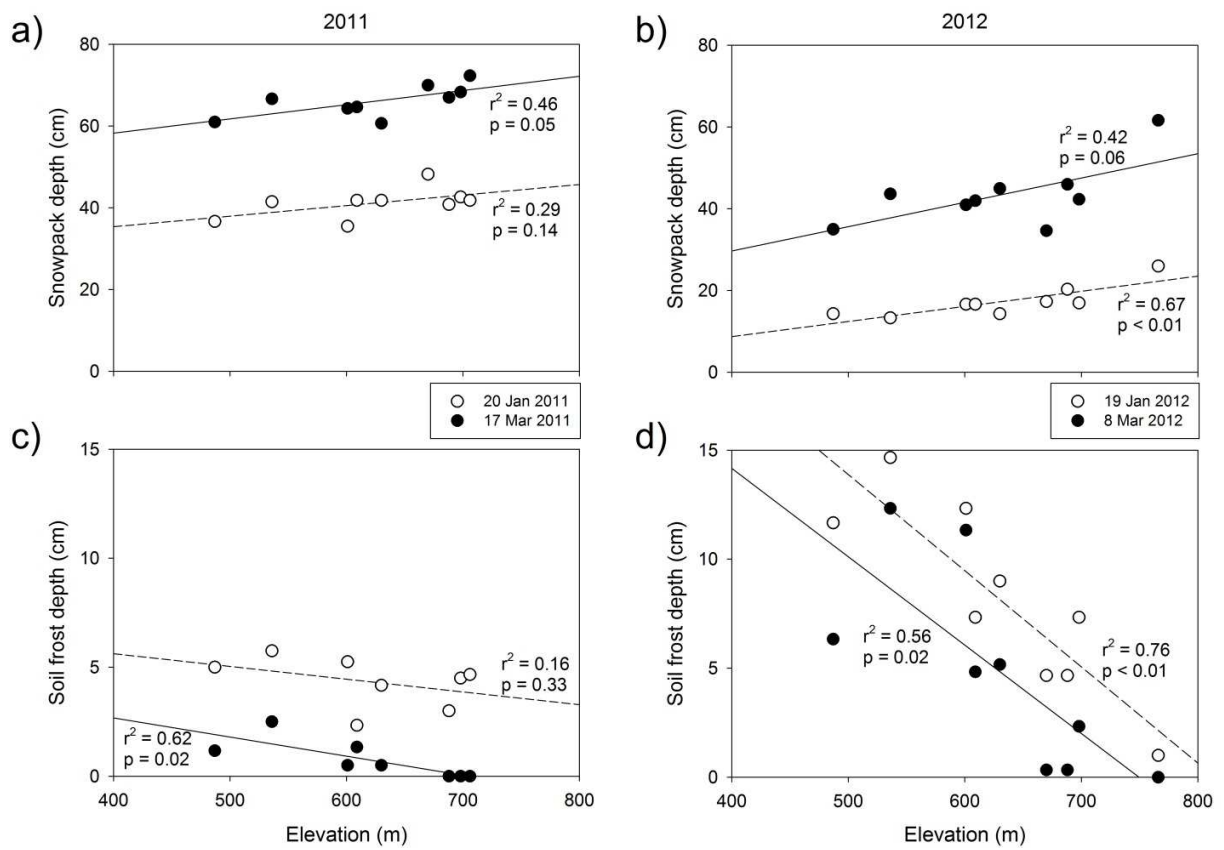


Figure 7.2. Relationship of snowpack (a,b) and soil frost depth (c,d) with elevation for each of the two study winters. Regression statistics shown for mid-winter (open circles) and early snowmelt (closed circles).

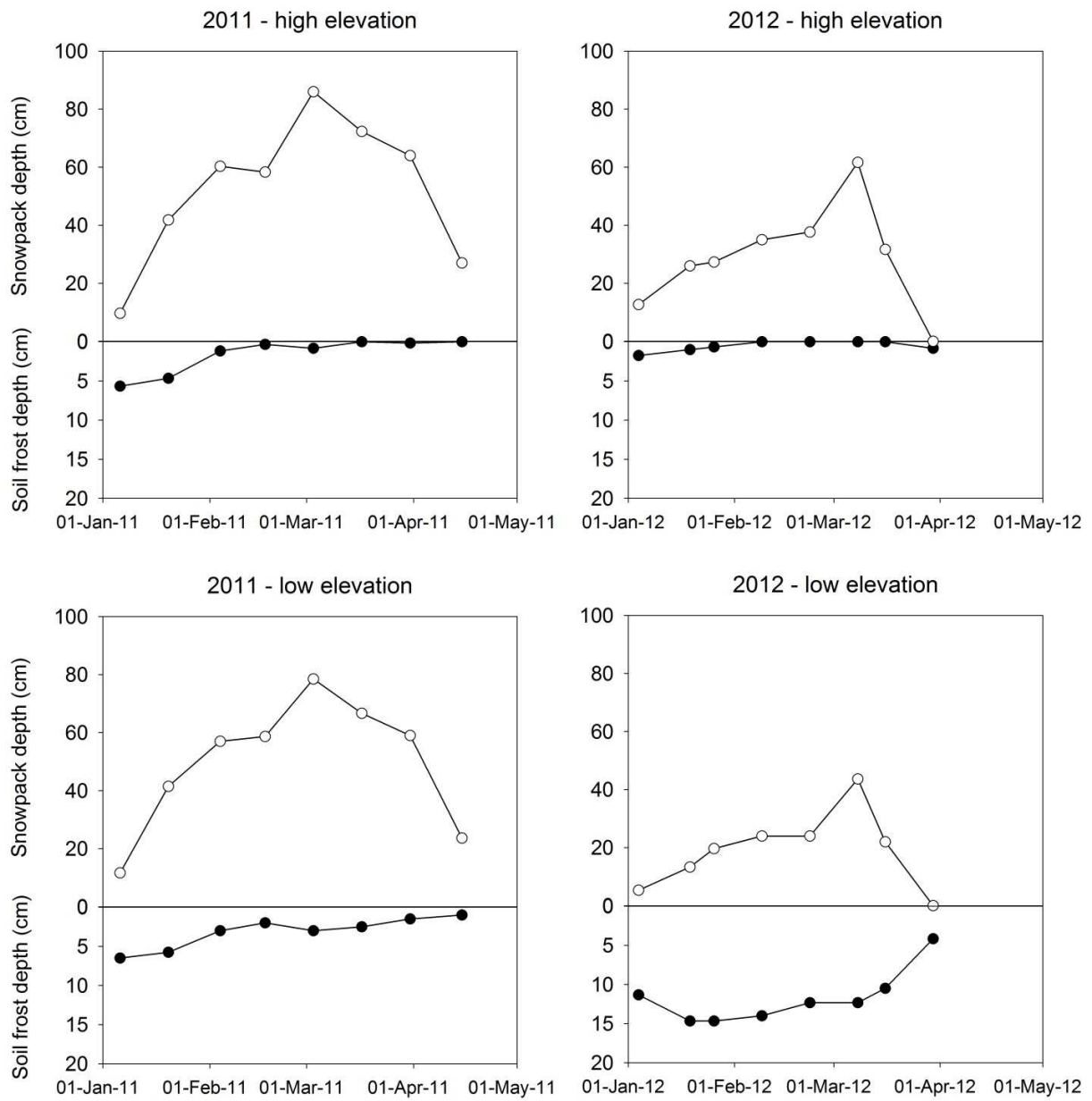


Figure 7.3. Snowpack and soil frost evolution during the winters of 2011 and 2012 at high elevation (766 m) and low elevation (536 m) monitoring sites.

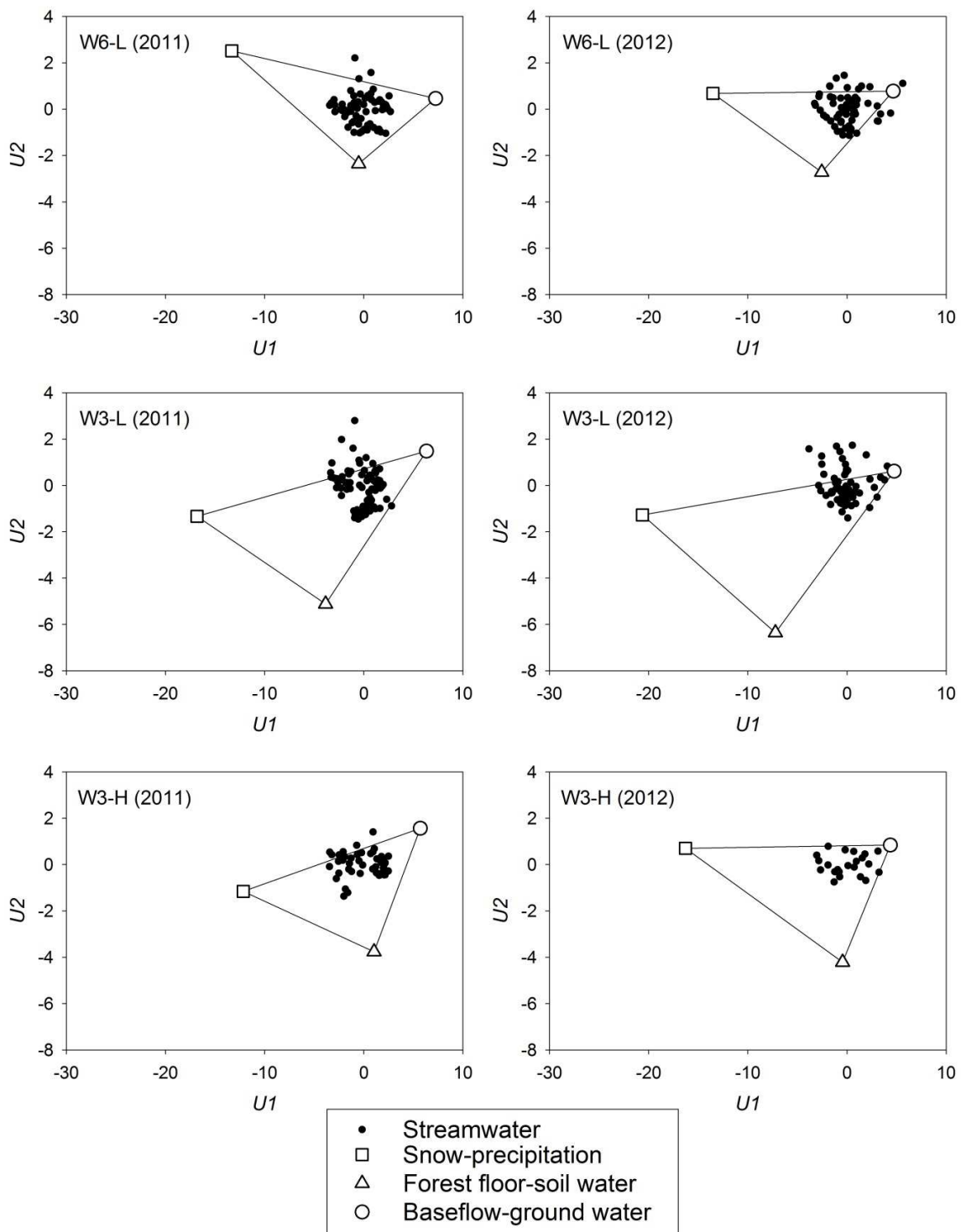


Figure 7.4. Mixing diagrams generated with principal component analysis for streamwater collected at the three sampling sites during the winters of 2011 and 2012.

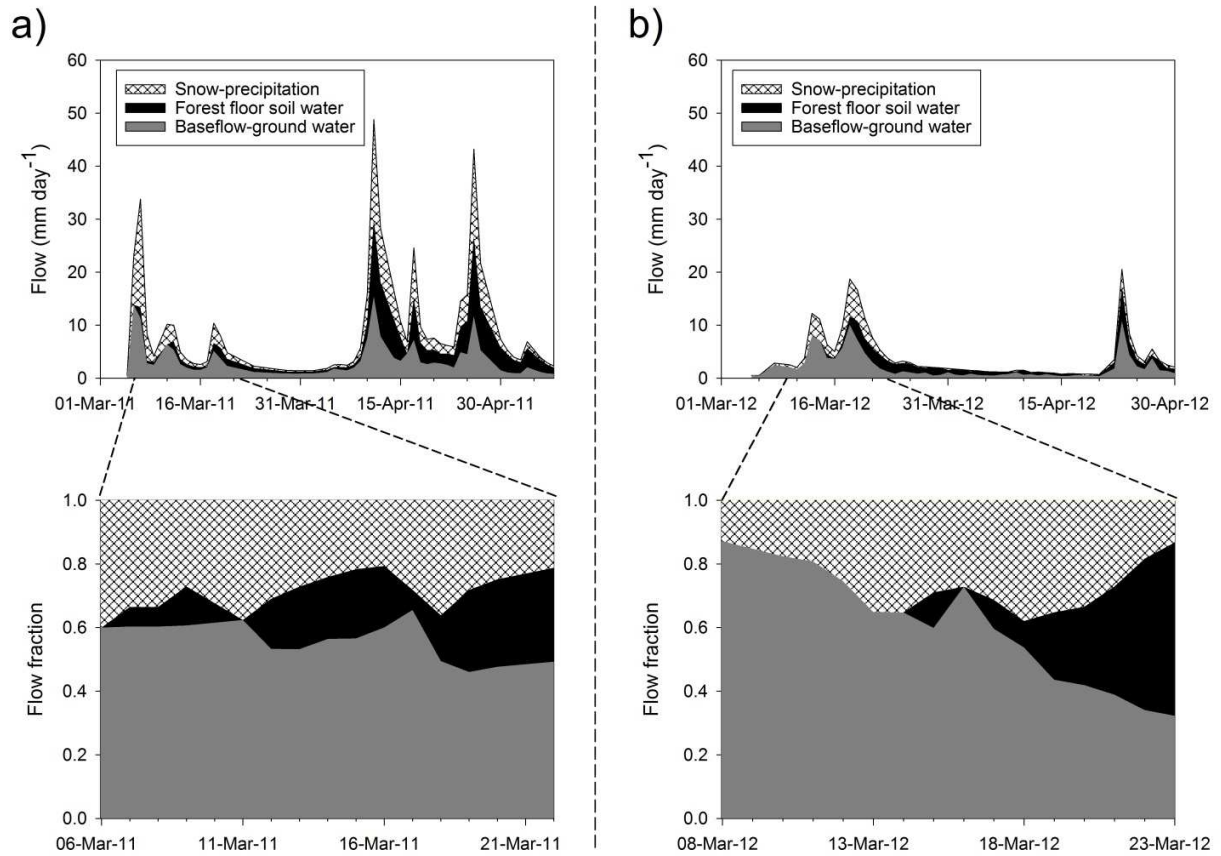


Figure 7.5. Watershed 6 hydrograph separation (W6-L) with EMMA for snowmelt during a two month period in a) 2011 and b) 2012. Lower panels indicate fraction of flow through flowpaths during an approximately two week period of early season snowmelt.

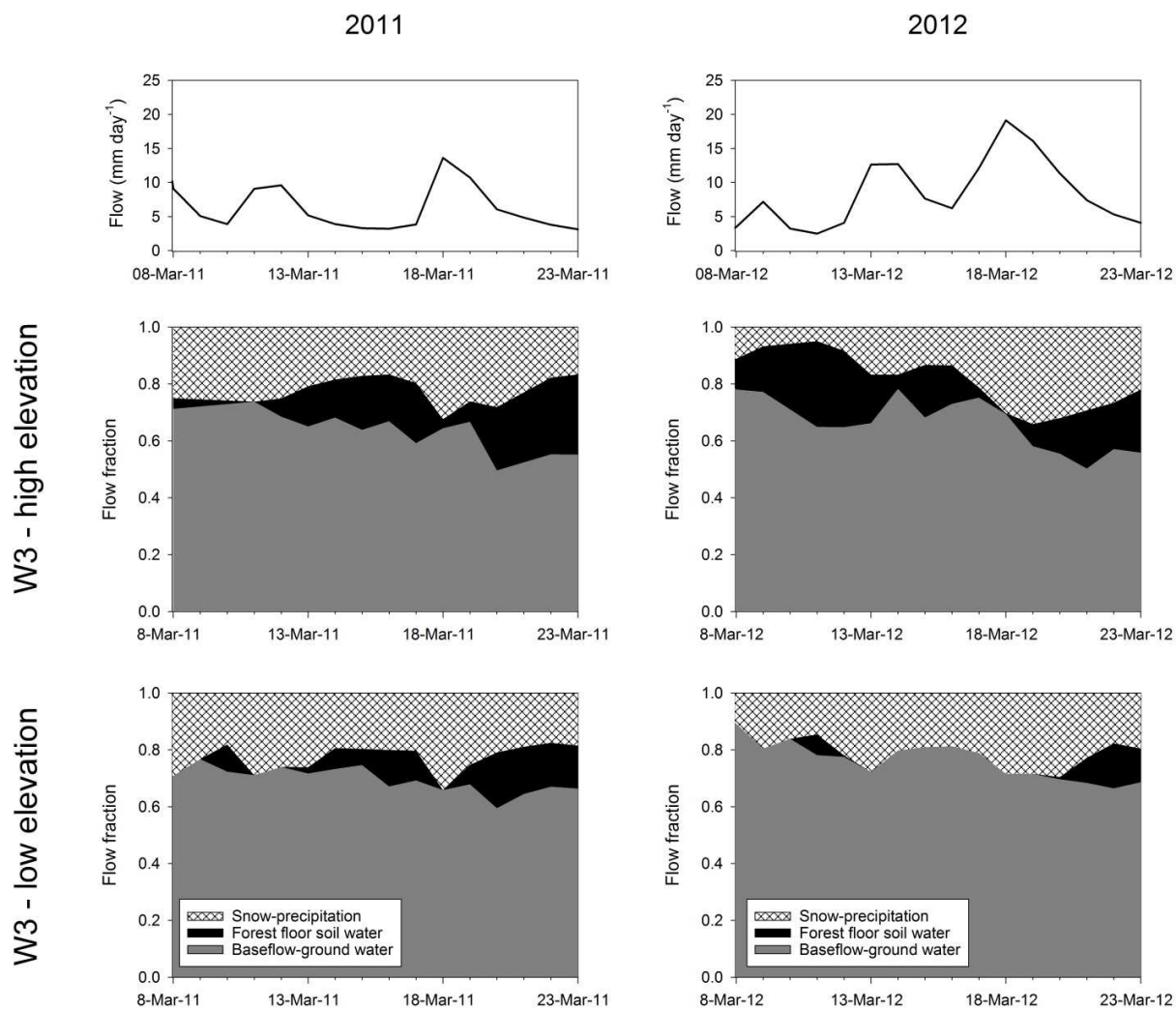


Figure 7.6. Watershed 3 fractional separation of flowpaths from EMMA for a two week period early in the snowmelt season in 2011 (left column) and 2012 (right column). The top panels of each column show the W3 hydrograph. The proportional flow at the W3-H site is indicated in the middle set of panels and the lower panels show the proportional flow at the W3-L site.

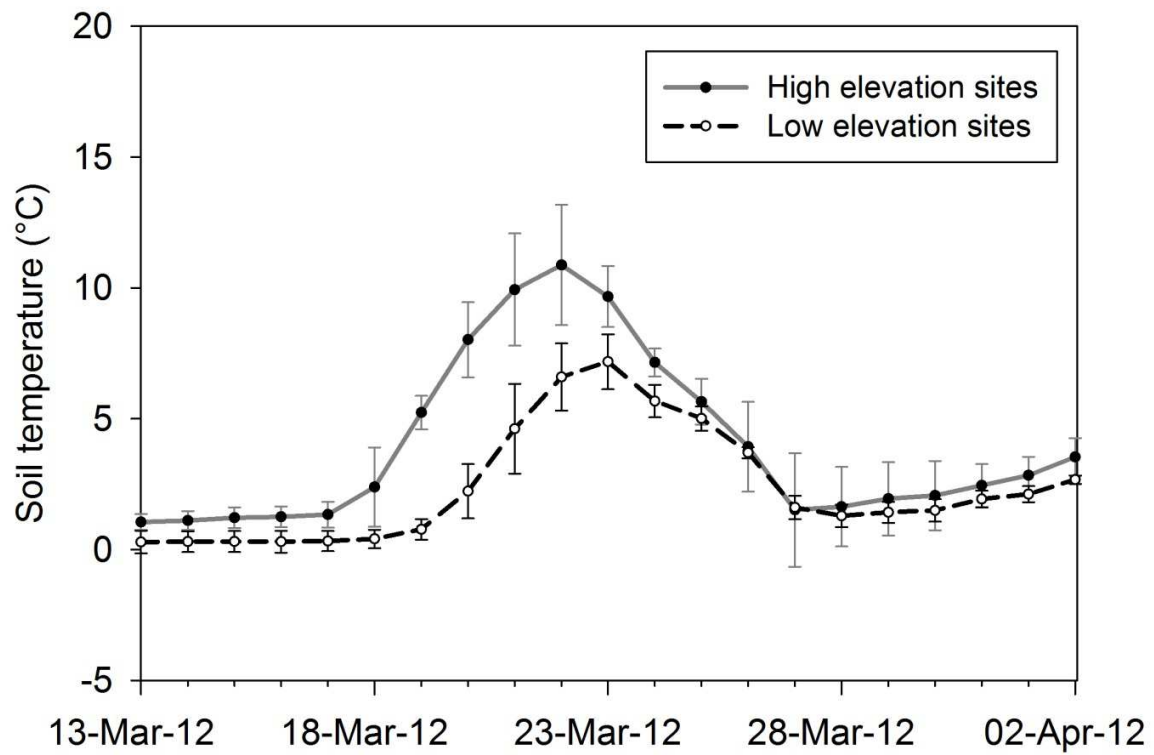


Figure 7.7. Detail of mean daily soil temperatures at 5 cm depth for three high elevation sites (688 m, 698 m, and 766 m) and three low elevation sites (487 m, 536 m, and 601 m) during peak snowmelt in March 2012. Error bars represent standard deviations.

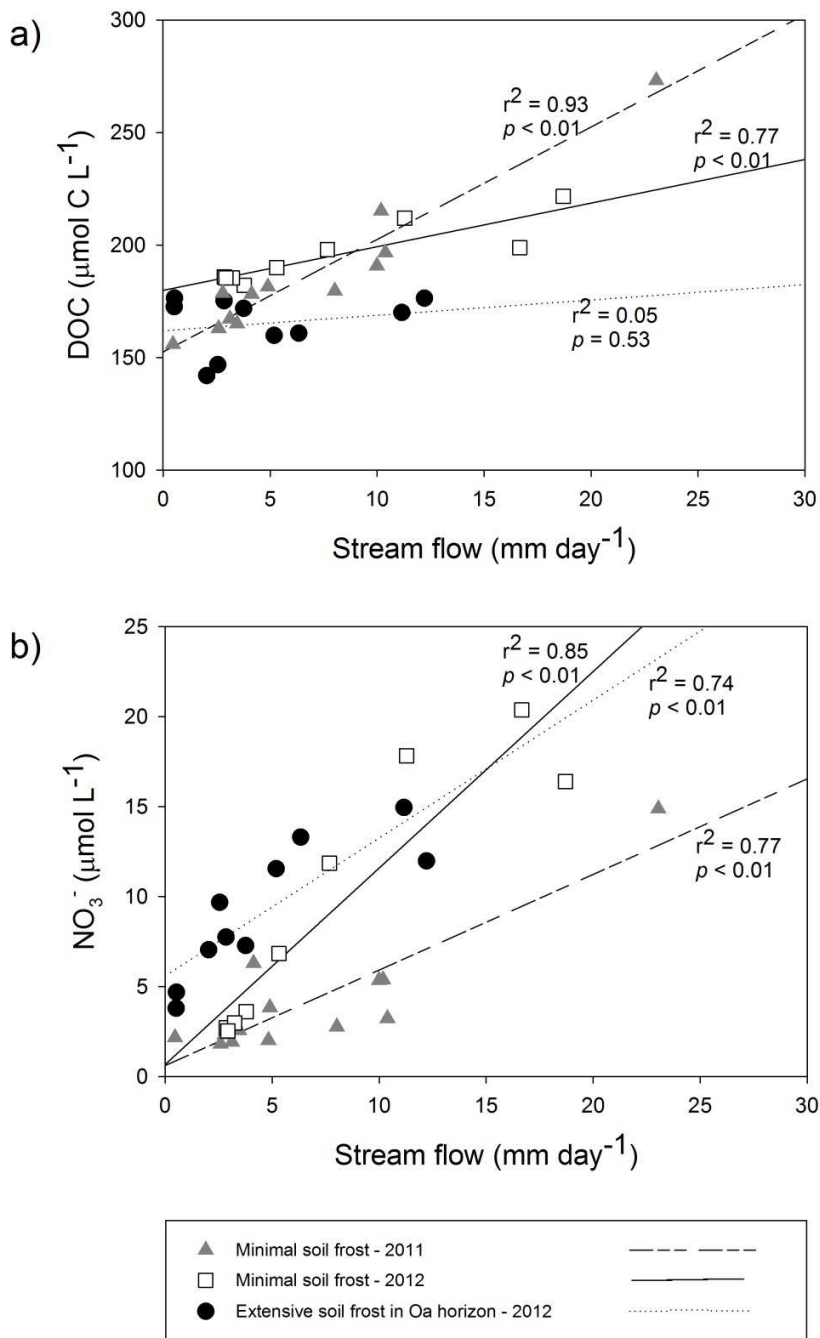


Figure 7.8. Concentration-discharge relationships in W6 for a) DOC, and b) NO_3^- during early snowmelt periods of minimal soil frost and extensive soil frost to the depth of the Oa horizon. Dates for 2011 data are 5-20 March 2011. The 2012 dates with soil frost are 5-15 March, and without soil frost are 18-26 March.

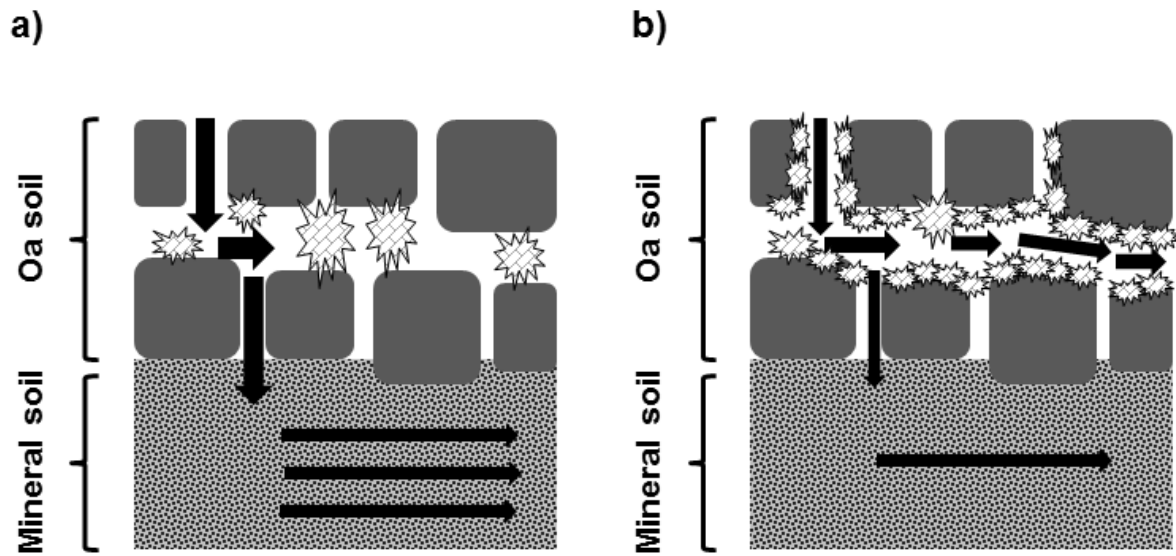


Figure 7.9. Conceptual model of potential granular soil frost effects on Oa soil horizon preferential flowpaths, in which a) frost granules block preferential flowpaths, slowing flow and promoting deeper percolation into mineral soil, and b) preferential flowpaths are maintained but frost presence prevent chemical exchange with soil matrix.

8. Synthesis and Integration

8.1. Overall summary of results

I used a two phase approach to study the hydrochemical dynamics of stream and soil water at Hubbard Brook. Phase I was an evaluation of hydrochemical trends over 30 years to characterize the changes in the chemistry of stream and soil water in response to continued decreases in atmospheric acid deposition to the forest. I included an analysis of the trends during snowmelt because it is the most important period in terms of annual hydrologic flow and solute losses from the watershed. Historically the snowmelt period is among the most acute times for episodic acidification, so an evaluation of the trends during this time was critical for a more comprehensive understanding of changing water quality patterns. Phase II was a series of field investigations with the goal of better understanding the variation in hydrological and biogeochemical dynamics as related to differences in winter climate. These experiments were conducted using the natural gradient of winter climate across the Hubbard Brook valley.

The results of Phase I, presented in Chapter 4, showed that drainage waters at Hubbard Brook are slowly but steadily recovering from chronic acidification, with measurable increases in ANC and pH, and reduced leaching of base cations and mobilization of Al_i . The trends assessed during the snowmelt periods of the record showed that snowmelt waters, while still more acidic than the whole-year baseline, are recovering at a very similar rate as noted in the overall trends. This finding was contrary to my original hypothesis that snowmelt acidification would be more marked relative to the overall trend due to a cumulative depletion of base cations from the forest floor resulting from long-term acid deposition, where snowmelt runoff is often routed. Additionally, I hypothesized that because NO_3^- deposition had not declined to the extent

that SO_4^{2-} had over the 30 year record, that snowmelt acidification would be relatively more severe because NO_3^- is flushed in high concentrations during snowmelt. In fact, the trend analysis showed that NO_3^- concentrations in stream and soil water declined throughout the entire record, prior to deposition decreases. Moreover, the decreases in stream NO_3^- during the snowmelt period were more rapid than observations for the whole-year record. This highlights the importance of better understanding controls on nitrogen cycling during the winter preceding snowmelt.

The results of the Phase II winter climate field experiments are presented in Chapters 5-7. Chapter 5 was an investigation of how soil water chemistry may change under differing winter climate regimes. I used a set of 20 plots to capture the range of winter climate conditions experienced across the Hubbard Brook valley. This range is also analogous to projections of future scenarios of continued winter warming. I evaluated patterns of NO_3^- and DOC leaching in soil solutions as they related to winter climate factors that are hypothesized to be sensitive to climate change, increases in soil freezing intensity, and freeze/thaw cycles due to reduced snowpack insulation. Two years of data at these sites showed that DOC responses appear to be particularly sensitive to soil freezing. I observed increased DOC leaching from spring through July, primarily in the Oa soil horizons, following soil freezing that occurred during the preceding winter. This effect was more prominent during the second year of my study, when the preceding winter was characterized by a lower snowpack that exposed the soil at many plots to greater soil frost development and more freeze/thaw cycles. I did not observe a consistent NO_3^- leaching response, which was contrary to my original hypothesis that NO_3^- leaching in soil solutions would increase along the gradient where soil frost development was greater. This expectation was based on earlier soil freezing experiments conducted at Hubbard Brook (Fitzhugh et al.

2001) and elsewhere, which showed sugar maple plots having high NO_3^- losses following soil freezing events. The response of DOC but not NO_3^- to increased soil freezing is consistent with other studies (Groffman et al. 2011) and may indicate that mobilization of DOC can effectively inhibit a NO_3^- response.

In Chapter 6 I assessed the dynamics of NO_3^- and DOC in streamwater during snowmelt, using an intensive sampling regime across differing watersheds and at differing elevations to capture the variation in winter climate and relate it to watershed export patterns. I found higher NO_3^- concentrations and fluxes and lower concentrations and fluxes of DOC in the stream water of W7 relative to the W3 and W6. W7 is the north-facing watershed, and it experienced generally higher snow accumulations and lower intensities of soil frost. While it is difficult to elucidate the precise effects of winter climate variations with only two years of snowmelt for all the sites, and limitations in long-term datasets that could be used for comparison, the results match the basic patterns implied by the soil solution analysis of Chapter 5. Dissolved organic carbon was leached at higher concentrations at the sites with less protection from a deep snowpack, and NO_3^- concentrations were not correlated with the soil freezing parameters investigated.

The final research component of the Phase II field studies was the hydrological flowpath analysis presented in Chapter 7. This work was motivated by concern that soil frost present at the time of snowmelt may alter the hydrologic flowpaths in the soil and may help to resolve inconsistencies between soil freezing effects on solute leaching observed at the plot scale (e.g. Fitzhugh et al. 2001) and those observed at the catchment scale (e.g. Judd et al. 2011). I hypothesized that soil frost presence in the forest floor during snowmelt would decrease the contributions of shallow soil flowpaths to total stream runoff due to the constricting effects of granular frost in the preferential flowpaths. The results I observed support this hypothesis. The

analysis showed a distinct lack of forest floor flowpath contribution to streamwater in locations and times with deeper penetration of soil frost. The effect was most pronounced during the early snowmelt of 2012 when soil frost was relatively widespread. After several days of reduced flow through the forest floor preferential flowpaths, melting snow and rising soil temperatures thawed the remaining soil frost and I observed marked increases in streamwater derived from these shallow soil flowpaths. While the altered flowpaths did appear to have an effect on concentrations of stream NO_3^- and DOC it is difficult to determine to what extent soil frost-induced changes in hydrologic flowpaths would have on overall watershed export during snowmelt. This effect would be expected to be small if the soil frost persisted for a short time during snowmelt. On the other hand, effects could be more pronounced if frost persisted longer or more concrete frost developed which could limit infiltration of melt waters into the soil profile to a greater degree than granular frost.

The set of studies I presented highlight the complex relationship between winter climate variability and drainage water hydrochemistry. Overwinter biogeochemical processes are an important component of the annual cycle (Campbell et al. 2005) and winter climate change is an important factor influencing these cycles in ways not completely understood. Because snowmelt is such an important hydrological event of the annual cycle in upland watersheds, understanding controls on runoff chemistry is critical to water quality concerns downstream. My studies emphasize the importance long-term trends which reflect changes in water quality, as well as the influence of interannual climate variations.

8.2. Recommendations for future studies

Based on the results I found in this dissertation, I can recommend several important research priorities.

- Soil freezing disturbance effects are not well understood in soils. Despite unclear results from past experiments, controlled laboratory investigations can provide insight into the dynamics of hydrochemical responses to soil freezing. Specific experiments should be designed to evaluate the DOC response varying intensities and frequencies of freeze/thaw cycles.
- The interaction of DOC and NO_3^- responses to winter climate and soil freezing variability needs further investigation. Controlled additions of NO_3^- and DOC of differing quality could help to determine the mechanisms promoting NO_3^- loss responses or immobilization.
- DOC is an important factor in biogeochemical cycling and water quality. More monitoring of DOC should be conducted to better understand the variation in headwater catchments. *In situ* sensors provide a great opportunity to learn more about DOC as it varies with hydrology.
- Increases in DOC concentrations are a widespread phenomenon in surface waters and have implications for water quality. Conducting long-term sampling from various watersheds and including analysis of DOC quality—such as fluorescence spectra—can provide insight about sources of DOC is derived and consequently the controls on its mobilization.

9. References

- Aber JD, Driscoll CT (1997) Effects of land use, climate variation, and N deposition on N cycling and C storage in northern hardwood forests. *Global Biogeochemical Cycles* 11:639–648. doi:10.1029/97GB01366
- Aber JD, Nadelhoffer KJ, Steudler P, Melillo JM (1989) Nitrogen Saturation in Northern Forest Ecosystems. *BioScience* 39:378–386. doi:10.2307/1311067
- Ågren A, Haei M, Köhler SJ, Bishop K, Laudon H (2010) Regulation of stream water dissolved organic carbon (DOC) concentrations during snowmelt; the role of discharge, winter climate and memory effects. *Biogeosciences* 7:2901–2913. doi:10.5194/bg-7-2901-2010
- Akselsson C, Hultberg H, Karlsson PE, Pihl Karlsson G, Hellsten S (2013) Acidification trends in south Swedish forest soils 1986–2008 — Slow recovery and high sensitivity to sea-salt episodes. *Science of the Total Environment* 444:271–287. doi:10.1016/j.scitotenv.2012.11.106
- Austnes K, Vestgarden LS (2008) Prolonged frost increases release of C and N from a montane heathland soil in southern Norway. *Soil Biology and Biochemistry* 40:2540–2546. doi:10.1016/j.soilbio.2008.06.014
- Austnes K, Kaste Ø, Vestgarden LS, Mulder J (2008) Manipulation of snow in small headwater catchments at Storgama, Norway: Effects on leaching of total organic carbon and total organic nitrogen. *Ambio* 37:38–47. doi:10.1579/0044-7447(2008)37[38:MOSISH]2.0.CO;2
- Bailey SW, Brousseau PA, McGuire KJ, Ross DS (2014) Influence of landscape position and transient water table on soil development and carbon distribution in a steep, headwater catchment. *Geoderma*. doi:10.1016/j.geoderma.2014.02.017
- Baker J, Schofield C (1982) Aluminum Toxicity to Fish in Acidic Waters. *Water Air and Soil Pollution* 18:289–309. doi:10.1007/BF02419419
- Baker JP, Sickie JV, Gagen CJ, DeWalle DR, Sharpe WE, Carline RF, Baldigo BP, Murdoch PS, Bath DW, Krester WA, Simonin HA, Wigington PJ (1996) Episodic acidification of small streams in the Northeastern United States: Effects on fish populations. *Ecological Applications* 6:422–437. doi:10.2307/2269380
- Battles JJ, Fahey TJ, Driscoll CT, Blum JD, Johnson CE (2014) Restoring soil calcium reverses forest decline. *Environmental Science & Technology Letters*. doi:10.1021/ez400033d
- Baumgardner, Lavery TF, Rogers CM, Isil SS (2002) Estimates of the atmospheric deposition of sulfur and nitrogen species: Clean Air Status and Trends Network, 1990–2000. *Environmental Science & Technology* 36:2614–2629. doi:10.1021/es011146g

- Bayard D, Stähli M, Parriaux A, Flühler H (2005) The influence of seasonally frozen soil on the snowmelt runoff at two Alpine sites in southern Switzerland. *Journal of Hydrology* 309:66–84. doi:10.1016/j.jhydrol.2004.11.012
- Berggren D, Mulder J (1995) The role of organic matter in controlling aluminum solubility in acidic mineral soil horizons. *Geochimica et Cosmochimica Acta* 59:4167–4180. doi:10.1016/0016-7037(95)94443-J
- Bernal S, Hedin LO, Likens GE, Gerber S, Buso DC (2012) Complex response of the forest nitrogen cycle to climate change. *Proceedings of the National Academy of Sciences* 109:3406–3411. doi:10.1073/pnas.1121448109
- Bernhardt ES, Likens GE (2002) Dissolved organic carbon enrichment alters nitrogen dynamics in a forest stream. *Ecology* 83:1689–1700. doi:10.1890/0012-9658(2002)083[1689:DOCEAN]2.0.CO;2
- Bernhardt ES, Likens GE, Hall RO, Buso DC, Fisher SG, Burton TM, Meyer JL, McDowell WH, Mayer MS, Bowden WB (2005) Can't see the forest for the stream? In-stream processing and terrestrial nitrogen exports. *Bioscience* 55:219–230
- Boutin R, Robitaille G (1995) Increased soil nitrate losses under mature sugar maple trees affected by experimentally induced deep frost. *Canadian Journal of Forest Research* 25:588–602. doi:10.1139/x95-066
- Boyer EW, Hornberger GM, Bencala KE, McKnight DM (1997) Response characteristics of DOC flushing in an alpine catchment. *Hydrological Processes* 11:1635–1647. doi:10.1002/(SICI)1099-1085(19971015)11:12<1635::AID-HYP494>3.0.CO;2-H
- Boyer EW, Hornberger GM, Bencala KE, McKnight DM (2000) Effects of asynchronous snowmelt on flushing of dissolved organic carbon: a mixing model approach. *Hydrological Processes* 14:3291–3308. doi:10.1002/1099-1085(20001230)14:18<3291::AID-HYP202>3.0.CO;2-2
- Brooks PD, Williams MW, Schmidt SK (1998) Inorganic nitrogen and microbial biomass dynamics before and during spring snowmelt. *Biogeochemistry* 43:1–15. doi:10.1023/A:1005947511910
- Burakowski EA, Wake CP, Braswell B, Brown DP (2008) Trends in wintertime climate in the northeastern United States: 1965–2005. *Journal of Geophysical Research: Atmospheres* 113:n/a–n/a. doi:10.1029/2008JD009870
- Burns DA, McDonnell JJ, Hooper RP, Peters NE, Freer JE, Kendall C, Beven K (2001) Quantifying contributions to storm runoff through end-member mixing analysis and hydrologic measurements at the Panola Mountain Research Watershed (Georgia, USA). *Hydrological Processes* 15:1903–1924. doi:10.1002/hyp.246

- Burns DA, McHale MR, Driscoll CT, Roy KM (2006) Response of surface water chemistry to reduced levels of acid precipitation: comparison of trends in two regions of New York, USA. *Hydrological Processes* 20:1611–1627. doi:10.1002/hyp.5961
- Callesen I, Borken W, Kalbitz K, Matzner E (2007) Long-term development of nitrogen fluxes in a coniferous ecosystem: Does soil freezing trigger nitrate leaching? *Journal of Plant Nutrition and Soil Science* 170:189–196. doi:10.1002/jpln.200622034
- Campbell JL, Mitchell MJ, Groffman PM, Christenson LM, Hardy JP (2005) Winter in northeastern North America: a critical period for ecological processes. *Frontiers in Ecology and the Environment* 3:314–322. doi:10.1890/1540-9295(2005)003[0314:WINNAA]2.0.CO;2
- Campbell JL, Mitchell MJ, Mayer B (2006) Isotopic assessment of NO₃⁻ and SO₄²⁻ mobility during winter in two adjacent watersheds in the Adirondack Mountains, New York. *Journal of Geophysical Research: Biogeosciences* 111:n/a–n/a. doi:10.1029/2006JG000208
- Campbell JL, Driscoll CT, Eagar C, Likens GE, Siccama TG, Johnson CE, Fahey TJ, Hamburg SP, Holmes RT, Bailey AS, Buso DC (2007) Long-term trends from ecosystem research at the Hubbard Brook Experimental Forest. Gen Tech Rep NRS-17 Newtown Square, PA: US Dept Agriculture, Forest Service, Northern Research Station:41
- Campbell JL, Rustad LE, Boyer EW, Christopher SF, Driscoll CT, Fernandez IJ, Groffman PM, Houle D, Kiekbusch J, Magill AH, Mitchell MJ, Ollinger SV (2009) Consequences of climate change for biogeochemical cycling in forests of northeastern North America. *Canadian Journal of Forest Research-Revue Canadienne De Recherche Forestiere* 39:264–284. doi:10.1139/X08-104
- Campbell JL, Ollinger SV, Flerchinger GN, Wicklein H, Hayhoe K, Bailey AS (2010) Past and projected future changes in snowpack and soil frost at the Hubbard Brook Experimental Forest, New Hampshire, USA. *Hydrological Processes* 24:2465–2480. doi:10.1002/hyp.7666
- Campbell JL, Driscoll CT, Pourmokhtarian A, Hayhoe K (2011) Streamflow responses to past and projected future changes in climate at the Hubbard Brook Experimental Forest, New Hampshire, United States. *Water Resources Research* 47. doi:10.1029/2010WR009438
- Campbell JL, Reinmann AB, Templer PH (2014) Soil Freezing Effects on Sources of Nitrogen and Carbon Leached During Snowmelt. *Soil Science Society of America Journal* 78:297. doi:10.2136/sssaj2013.06.0218
- Chen CW, Gherini SA, Peters NE, Murdoch PS, Newton RM, Goldstein RA (1984) Hydrologic analyses of acidic and alkaline lakes. *Water Resources Research* 20:1875–1882. doi:10.1029/WR020i012p01875

- Cho Y, Driscoll CT, Johnson CE, Blum JD, Fahey TJ (2012) Watershed-Level Responses to Calcium Silicate Treatment in a Northern Hardwood Forest. *Ecosystems* 15:416–434. doi:10.1007/s10021-012-9518-2
- Christopher SF, Page BD, Campbell JL, Mitchell MJ (2006) Contrasting stream water NO₃⁻ and Ca²⁺ in two nearly adjacent catchments: the role of soil Ca and forest vegetation. *Global Change Biology* 12:364–381. doi:10.1111/j.1365-2486.2005.01084.x
- Christopher SF, Mitchell MJ, McHale MR, Boyer EW, Burns DA, Kendall C (2008) Factors controlling nitrogen release from two forested catchments with contrasting hydrochemical responses. *Hydrological Processes* 22:46–62. doi:10.1002/hyp.6632
- Christophersen N, Hooper RP (1992) Multivariate analysis of stream water chemical data: The use of principal components analysis for the end-member mixing problem. *Water Resources Research* 28:99–107. doi:10.1029/91WR02518
- Clair TA, Dennis IF, Vet R, Laudon H (2008) Long-term trends in catchment organic carbon and nitrogen exports from three acidified catchments in Nova Scotia, Canada. *Biogeochemistry* 87:83–97. doi:10.1007/s10533-007-9170-7
- Clark JM, Bottrell SH, Evans CD, Monteith DT, Bartlett R, Rose R, Newton RJ, Chapman PJ (2010) The importance of the relationship between scale and process in understanding long-term DOC dynamics. *Science of the Total Environment* 408:2768–2775. doi:10.1016/j.scitotenv.2010.02.046
- Cleavitt NL, Fahey TJ, Groffman PM, Hardy JP, Henry KS, Driscoll CT (2008) Effects of soil freezing on fine roots in a northern hardwood forest. *Canadian Journal of Forest Research-Revue Canadienne De Recherche Forestiere* 38:82–91
- Craig BW, Friedland AJ (1991) Spatial patterns in forest composition and standing dead red spruce in montane forests of the Adirondacks and northern Appalachians. *Environmental Monitoring and Assessment* 18:129–143. doi:10.1007/BF00394975
- Cronan CS, Grigal DF (1995) Use of Calcium/Aluminum Ratios as Indicators of Stress in Forest Ecosystems. *Journal of Environmental Quality* 24:209–226. doi:10.2134/jeq1995.00472425002400020002x
- Cronan CS, Schofield CL (1990) Relationships between aqueous aluminum and acidic deposition in forested watersheds of North America and northern Europe. *Environmental Science Technology* 24:1100–1105. doi:10.1021/es00077a022
- Decker KLM, Wang D, Waite C, Scherbatskoy T (2003) Snow removal and ambient air temperature effects on forest soil temperatures in Northern Vermont. *Soil Science Society of America Journal* 67:1234–1234
- DeHayes DH, Schaberg PG, Hawley GJ, Strimbeck GR (1999) Acid Rain Impacts on Calcium Nutrition and Forest Health. *BioScience* 49:789–800. doi:10.1525/bisi.1999.49.10.789

- DeWalle DR, Swistock BR (1994) Causes of episodic acidification in five Pennsylvania streams on the Northern Appalachian Plateau. *Water Resources Research* 30:1955–1963. doi:10.1029/94WR00758
- Diebold CH (1938) The effect of vegetation upon snow cover and frost penetration during the March 1936 floods. *Journal of Forestry* 36:1131–1137
- Dittman JA, Driscoll CT, Groffman PM, Fahey TJ (2007) Dynamics of Nitrogen and Dissolved Organic Carbon at the Hubbard Brook Experimental Forest. *Ecology* 88:1153–1166. doi:10.2307/27651215
- Driscoll CT, Fuller RD, Schecher WD (1989) The role of organic acids in the acidification of surface waters in the Eastern U.S. *Water, Air, and Soil Pollution* 43:21–40. doi:10.1007/BF00175580
- Driscoll CT, Yan C, Schofield CL, Munson R, Holsapple J (1994) The mercury cycle and fish in the Adirondack lakes. *Environmental Science & Technology* 28:136A–143A. doi:10.1021/es00052a003
- Driscoll CT, Lawrence GB, Bulger AJ, Butler TJ, Cronan CS, Eagar C, Lambert KF, Likens GE, Stoddard JL, Weathers KC (2001) Acidic deposition in the northeastern United States: Sources and inputs, ecosystem effects, and management strategies. *Bioscience* 51:180–198. doi:10.1641/0006-3568(2001)051[0180:ADITNU]2.0.CO;2
- Driscoll CT, Driscoll KM, Roy KM, Mitchell MJ (2003) Chemical response of lakes in the Adirondack region of New York to declines in acidic deposition. *Environmental Science & Technology* 37:2036–2042. doi:10.1021/es020924h
- Driscoll CT, Driscoll KM, Roy KM, Dukett J (2007) Changes in the chemistry of lakes in the Adirondack region of New York following declines in acidic deposition. *Applied Geochemistry* 22:1181–1188. doi:10.1016/j.apgeochem.2007.03.009
- Duchesne L, Ouimet R, Houle D (2002) Basal area growth of sugar maple in relation to acid deposition, stand health, and soil nutrients. *Journal of Environmental Quality* 31:1676–1683. doi:10.2134/jeq2002.1676
- Dunne T, Black RD (1971) Runoff processes during snowmelt. *Water Resources Research* 7:1160–1172. doi:10.1029/WR007i005p01160
- Evans CD, Monteith DT, Cooper DM (2005) Long-term increases in surface water dissolved organic carbon: Observations, possible causes and environmental impacts. *Environmental Pollution* 137:55–71. doi:10.1016/j.envpol.2004.12.031
- Evans CD, Chapman PJ, Clark JM, Monteith DT, Cresser MS (2006) Alternative explanations for rising dissolved organic carbon export from organic soils. *Global Change Biology* 12:2044–2053. doi:10.1111/j.1365-2486.2006.01241.x

- Fahey TJ, Lang GE (1975) Concrete Frost along an Elevational Gradient in New Hampshire. *Canadian Journal of Forest Research* 5:700–705. doi:10.1139/x75-096
- Federer CA, Hornbeck JW, Tritton LM, Martin CW, Pierce RS, Smith CT (1989) Long-term depletion of calcium and other nutrients in eastern US forests. *Environmental Management* 13:593–601. doi:10.1007/BF01874965
- Fitzhugh RD, Driscoll CT, Groffman PM, Tierney GL, Fahey TJ, Hardy JP (2001) Effects of soil freezing disturbance on soil solution nitrogen, phosphorus, and carbon chemistry in a northern hardwood ecosystem. *Biogeochemistry* 56:215–238. doi:10.1023/A:1013076609950
- Fitzhugh RD, Likens GE, Driscoll CT, Mitchell MJ, Groffman PM, Fahey TJ, Hardy JP (2003) Role of soil freezing events in interannual patterns of stream chemistry at the Hubbard Brook experimental forest, New Hampshire. *Environmental Science & Technology* 37:1575–1580. doi:10.1021/es026189r
- Galloway JN, Hendrey GR, Schofield CL, Peters NE, Johannes AH (1987) Processes and Causes of Lake Acidification during Spring Snowmelt in the West-Central Adirondack Mountains, New York. *Canadian Journal of Fisheries and Aquatic Sciences* 44:1595–1602. doi:10.1139/f87-193
- Gbondo-Tugbawa SS, Driscoll CT, Aber JD, Likens GE (2001) Evaluation of an integrated biogeochemical model (PnET-BGC) at a northern hardwood forest ecosystem. *Water Resources Research* 37:1057–1070. doi:10.1029/2000WR900375
- Gbondo-Tugbawa SS, Driscoll CT, Mitchell MJ, Aber JD, Likens GE (2002) A model to simulate the response of a northern hardwood forest ecosystem to changes in S deposition. *Ecological Applications* 12:8–23. doi:10.1890/1051-0761(2002)012[0008:AMTSTR]2.0.CO;2
- Goodale CL, Aber JD, Vitousek PM, McDowell WH (2005) Long-Term Decreases in Stream Nitrate: Successional Causes Unlikely; Possible Links to DOC? *Ecosystems* 8:334–337. doi:10.2307/25053830
- Granger RJ, Gray DM, Dyck GE (1984) Snowmelt infiltration to frozen Prairie soils. *Canadian Journal of Earth Sciences* 21:669–677. doi:10.1139/e84-073
- Greaver TL, Sullivan TJ, Herrick JD, Barber MC, Baron JS, Cosby BJ, Deerhake ME, Dennis RL, Dubois J-JB, Goodale CL, Herlihy AT, Lawrence GB, Liu L, Lynch JA, Novak KJ (2012) Ecological effects of nitrogen and sulfur air pollution in the US: what do we know? *Frontiers in Ecology and the Environment* 10:365–372. doi:10.1890/110049
- Groffman, Hardy JP, Fisk MC, Fahey TJ, Driscoll CT (2009) Climate Variation and Soil Carbon and Nitrogen Cycling Processes in a Northern Hardwood Forest. *Ecosystems* 12:927–943. doi:10.1007/s10021-009-9268-y

- Groffman PM, Driscoll CT, Fahey TJ, Hardy JP, Fitzhugh RD, Tierney GL (2001a) Colder soils in a warmer world: A snow manipulation study in a northern hardwood forest ecosystem. *Biogeochemistry* 56:135–150. doi:10.1023/A:1013039830323
- Groffman PM, Driscoll CT, Fahey TJ, Hardy JP, Fitzhugh RD, Tierney GL (2001b) Effects of mild winter freezing on soil nitrogen and carbon dynamics in a northern hardwood forest. *Biogeochemistry* 56:191–213. doi:10.1023/A:1013024603959
- Groffman PM, Hardy JP, Fashu-Kanu S, Driscoll CT, Cleavitt NL, Fahey TJ, Fisk MC (2011) Snow depth, soil freezing and nitrogen cycling in a northern hardwood forest landscape. *Biogeochemistry* 102:223–238. doi:10.1007/s10533-010-9436-3
- Groffman PM, Rustad LE, Templer PH, Campbell JL, Christenson LM, Lany NK, Soggi AM, Vadeboncoeur MA, Schaberg PG, Wilson GF, Driscoll CT, Fahey TJ, Fisk MC, Goodale CL, Green MB, Hamburg SP, Johnson CE, Mitchell MJ, Morse JL, et al. (2012) Long-Term Integrated Studies Show Complex and Surprising Effects of Climate Change in the Northern Hardwood Forest. *BioScience* 62:1056–1066. doi:10.1525/bio.2012.62.12.7
- Grogan P, Michelsen A, Ambus P, Jonasson S (2004) Freeze–thaw regime effects on carbon and nitrogen dynamics in sub-arctic heath tundra mesocosms. *Soil Biology and Biochemistry* 36:641–654. doi:10.1016/j.soilbio.2003.12.007
- Haei M, Öquist MG, Buffam I, Ågren A, Blomkvist P, Bishop K, Ottosson Löfvenius M, Laudon H (2010) Cold winter soils enhance dissolved organic carbon concentrations in soil and stream water. *Geophysical Research Letters* 37:n/a–n/a. doi:10.1029/2010GL042821
- Haei M, Öquist MG, Ilstedt U, Laudon H (2012) The influence of soil frost on the quality of dissolved organic carbon in a boreal forest soil: combining field and laboratory experiments. *Biogeochemistry* 107:95–106. doi:10.1007/s10533-010-9534-2
- Hamburg SP, Vadeboncoeur MA, Richardson AD, Bailey AS (2013) Climate change at the ecosystem scale: a 50-year record in New Hampshire. *Climatic Change* 116:457–477. doi:10.1007/s10584-012-0517-2
- Hardy JP, Groffman PM, Fitzhugh RD, Henry KS, Welman AT, Demers JD, Fahey TJ, Driscoll CT, Tierney GL, Nolan S (2001) Snow depth manipulation and its influence on soil frost and water dynamics in a northern hardwood forest. *Biogeochemistry* 56:151–174. doi:10.1023/A:1013036803050
- Hart G, Leonard RE, Pierce RS (1962) Leaf fall, humus depth, and soil frost in a northern hardwood forest. USDA Forest Service, Northeastern Experiment Station, Upper Darby, PA
- Haupt HF (1967) Infiltration, overland flow, and soil movement on frozen and snow-covered plots. *Water Resources Research* 3:145–161. doi:10.1029/WR003i001p00145
- Hayhoe K, Wake CP, Huntington TG, Luo L, Schwartz MD, Sheffield J, Wood E, Anderson B, Bradbury J, DeGaetano A, Troy TJ, Wolfe D (2007) Past and future changes in climate

- and hydrological indicators in the US Northeast. *Climate Dynamics* 28:381–407. doi:10.1007/s00382-006-0187-8
- Hayhoe K, Wake C, Anderson B, Liang X-Z, Maurer E, Zhu J, Bradbury J, DeGaetano A, Stoner AM, Wuebbles D (2008) Regional climate change projections for the Northeast USA. *Mitigation and Adaptation Strategies for Global Change* 13:425–436. doi:10.1007/s11027-007-9133-2
- Hentschel K, Borken W, Matzner E (2008) Repeated freeze–thaw events affect leaching losses of nitrogen and dissolved organic matter in a forest soil. *Journal of Plant Nutrition and Soil Science* 171:699–706. doi:10.1002/jpln.200700154
- Hentschel K, Borken W, Zuber T, Bogner C, Huwe B, Matzner E (2009) Effects of soil frost on nitrogen net mineralization, soil solution chemistry and seepage losses in a temperate forest soil. *Global Change Biology* 15:825–836. doi:10.1111/j.1365-2486.2008.01753.x
- Herrmann A, Witter E (2002) Sources of C and N contributing to the flush in mineralization upon freeze–thaw cycles in soils. *Soil Biology and Biochemistry* 34:1495–1505. doi:10.1016/S0038-0717(02)00121-9
- Hinton MJ, Schiff SL, English MC (1998) Sources and flowpaths of dissolved organic carbon during storms in two forested watersheds of the Precambrian Shield. *Biogeochemistry* 41:175–197. doi:10.1023/A:1005903428956
- Hirsch RM, Slack JR (1984) A nonparametric trend test for seasonal data with serial dependence. *Water Resources Research* 20:727–732. doi:10.1029/WR020i006p00727
- Hirsch RM, Slack JR, Smith RA (1982) Techniques of trend analysis for monthly water quality data. *Water Resources Research* 18:107–121. doi:10.1029/WR018i001p00107
- Hongve D, Riise G, Kristiansen JF (2004) Increased colour and organic acid concentrations in Norwegian forest lakes and drinking water – a result of increased precipitation? *Aquatic Sciences* 66:231–238. doi:10.1007/s00027-004-0708-7
- Hornberger GM, Bencala KE, McKnight DM (1994) Hydrological Controls on Dissolved Organic Carbon during Snowmelt in the Snake River near Montezuma, Colorado. *Biogeochemistry* 25:147–165. doi:10.2307/1469014
- Horsley SB, Long RP, Bailey SW, Hallett RA, Hall TJ (2000) Factors associated with the decline disease of sugar maple on the Allegheny Plateau. *Canadian Journal of Forest Research* 30:1365–1378. doi:10.1139/x00-057
- Hruška J, Krám P, McDowell WH, Oulehle F (2009) Increased dissolved organic carbon (DOC) in central European streams is driven by reductions in ionic strength rather than climate change or decreasing acidity. *Environmental Science & Technology* 43:4320–4326. doi:10.1021/es803645w

- Huntington TG, Hodgkins GA, Keim BD, Dudley RW (2004) Changes in the proportion of precipitation occurring as snow in New England (1949–2000). *Journal of Climate* 17:2626–2636. doi:10.1175/1520-0442(2004)017<2626:CITPOP>2.0.CO;2
- Isard SA, Schaetzl RJ (1998) Effects of winter weather conditions on soil freezing in Southern Michigan. *Physical Geography* 19:71–94. doi:10.1080/02723646.1998.10642641
- Jaworski NA, Howarth RW, Hetling LJ (1997) Atmospheric Deposition of Nitrogen Oxides onto the Landscape Contributes to Coastal Eutrophication in the Northeast United States. *Environmental Science & Technology* 31:1995–2004. doi:10.1021/es960803f
- Johnson CE, Johnson AH, Huntington TG, Siccama TG (1991) Whole-Tree Clear-Cutting Effects on Soil Horizons and Organic-Matter Pools. *Soil Science Society of America Journal* 55:497–502. doi:10.2136/sssaj1991.03615995005500020034x
- Johnson CE, Driscoll CT, Siccama TG, Likens GE (2000) Element fluxes and landscape position in a northern hardwood forest watershed ecosystem. *Ecosystems* 3:159–184. doi:10.1007/s100210000017
- Johnsson H, Lundin L-C (1991) Surface runoff and soil water percolation as affected by snow and soil frost. *Journal of Hydrology* 122:141–159. doi:10.1016/0022-1694(91)90177-J
- Judd KE, Likens GE, Buso DC, Bailey AS (2011) Minimal response in watershed nitrate export to severe soil frost raises questions about nutrient dynamics in the Hubbard Brook experimental forest. *Biogeochemistry* 106:443–459. doi:10.1007/s10533-010-9524-4
- Juice SM, Fahey TJ, Siccama TG, Driscoll CT, Denny EG, Eagar C, Cleavitt NL, Minocha R, Richardson AD (2006) Response of sugar maple to calcium addition to northern hardwood forest. *Ecology* 87:1267–1280. doi:10.1890/0012-9658(2006)87[1267:ROSMTC]2.0.CO;2
- Kahl JS, Norton SA, Haines TA, Rochette EA, Heath RH, Nodvin SC (1992) Mechanisms of episodic acidification in low-order streams in Maine, USA. *Environmental Pollution* 78:37–44. doi:10.1016/0269-7491(92)90007-W
- Kalbitz K, Solinger S, Park JH, Michalzik B, Matzner E (2000) Controls on the dynamics of dissolved organic matter in soils: a review. *Soil Science* 165:277–304. doi:10.1097/00010694-200004000-00001
- Kane DL, Stein J (1983) Water movement into seasonally frozen soils. *Water Resources Research* 19:1547–1557. doi:10.1029/WR019i006p01547
- Kaste Ø, Austnes K, Vestgarden LS, Wright RF (2008) Manipulation of snow in small headwater catchments at Storgama, Norway: effects on leaching of inorganic nitrogen. *Ambio* 37:29–37. doi:10.1579/0044-7447(2008)37[29:MOSISH]2.0.CO;2

- Kendall KA, Shanley JB, McDonnell JJ (1999) A hydrometric and geochemical approach to test the transmissivity feedback hypothesis during snowmelt. *Journal of Hydrology* 219:188–205. doi:10.1016/S0022-1694(99)00059-1
- Kennedy J, Billett M f., Duthie D, Fraser A r., Harrison A f. (1996) Organic matter retention in an upland humic podzol; the effects of pH and solute type. *European Journal of Soil Science* 47:615–625. doi:10.1111/j.1365-2389.1996.tb01860.x
- Kramer JR, Broussard P, Collins P, Clair TA, Takats P (1990) Variability of organic acids in watersheds. In: Purdue EM, Gjessing ET (eds) *Organic Acids in Aquatic Ecosystems*. John Wiley, New York, pp 127–139
- Laudon H, Seibert J, Köhler S, Bishop K (2004) Hydrological flow paths during snowmelt: Congruence between hydrometric measurements and oxygen 18 in meltwater, soil water, and runoff. *Water Resources Research* 40:n/a–n/a. doi:10.1029/2003WR002455
- Lawrence GB, Fuller RD, Driscoll CT (1986) Spatial Relationships of Aluminum Chemistry in the Streams of the Hubbard Brook Experimental Forest, New Hampshire. *Biogeochemistry* 2:115–135. doi:10.2307/1468730
- Lawrence GB, David MB, Lovett GM, Murdoch PS, Burns DA, Stoddard JL, Baldigo BP, Porter JH, Thompson AW (1999) Soil calcium status and the response of stream chemistry to changing acidic deposition rates. *Ecological Applications* 9:1059–1072. doi:10.1890/1051-0761(1999)009[1059:SCSATR]2.0.CO;2
- Lehmann CMB, Bowersox VC, Larson SM (2005) Spatial and temporal trends of precipitation chemistry in the United States, 1985–2002. *Environmental Pollution* 135:347–361. doi:10.1016/j.envpol.2004.11.016
- Lepistö A, Kortelainen P, Mattsson T (2008) Increased organic C and N leaching in a northern boreal river basin in Finland. *Global Biogeochemical Cycles* 22:n/a–n/a. doi:10.1029/2007GB003175
- Likens G, Bormann F, Johnson N (1972) Acid Rain. *Environment* 14:33–40
- Likens GE (2000) A long-term record of ice-cover for Mirror Lake, NH: effects of global warming? *Verhandlungen Internationale Vereinigung für theoretische und angewandte Limnologie* 27:2765–2769
- Likens GE, Bormann FH (1995) *Biogeochemistry of a forested ecosystem.*, 2nd edn.
- Likens GE, Buso DC (2012) Dilution and the Elusive Baseline. *Environmental Science & Technology* 46:4382–4387. doi:10.1021/es3000189
- Likens GE, Bormann FH, Pierce RS, Eaton JS, Johnson NM (1977) *Biogeochemistry of a Forested Ecosystem*. Springer-Verlag, New York

- Likens GE, Driscoll CT, Buso DC (1996) Long-Term Effects of Acid Rain: Response and Recovery of a Forest Ecosystem. *Science* 272:244–246.
doi:10.1126/science.272.5259.244
- Likens GE, Butler TJ, Buso DC (2001) Long- and short-term changes in sulfate deposition: Effects of the 1990 Clean Air Act Amendments. *Biogeochemistry* 52:1–11.
doi:10.1023/A:1026563400336
- Likens GE, Driscoll CT, Buso DC, Mitchell MJ, Lovett GM, Bailey SW, Siccama TG, Reiners WA, Alewell C (2002) The Biogeochemistry of Sulfur at Hubbard Brook. *Biogeochemistry* 60:235–315. doi:10.2307/1469763
- Likens GE, Buso DC, Butler TJ (2005) Long-term relationships between SO₂ and NO_x emissions and SO₄²⁻ and NO₃⁻ concentration in bulk deposition at the Hubbard Brook Experimental Forest, NH. *Journal of Environmental Monitoring* 7:964.
doi:10.1039/b506370a
- Lindström G, Bishop K, Löfvenius MO (2002) Soil frost and runoff at Svartberget, northern Sweden—measurements and model analysis. *Hydrological Processes* 16:3379–3392.
doi:10.1002/hyp.1106
- Löfgren S, Zetterberg T (2011) Decreased DOC concentrations in soil water in forested areas in southern Sweden during 1987–2008. *Science of The Total Environment* 409:1916–1926.
doi:10.1016/j.scitotenv.2011.02.017
- Löfgren S, Gustafsson JP, Bringmark L (2010) Decreasing DOC trends in soil solution along the hillslopes at two IM sites in southern Sweden—geochemical modeling of organic matter solubility during acidification recovery. *The Science of the total environment* 409:201–210. doi:10.1016/j.scitotenv.2010.09.023
- Lovett GM, Weathers KC, Arthur MA, Schultz JC (2004) Nitrogen cycling in a northern hardwood forest: Do species matter? *Biogeochemistry* 67:289–308.
doi:10.1023/B: BIOG.0000015786.65466.f5
- Maclean RA, English MC, Schiff SL (1995) Hydrological and hydrochemical response of a small canadian shield catchment to late winter rain-on-snow events. *Hydrological Processes* 9:845–863. doi:10.1002/hyp.3360090803
- McDowell WH (1982) Mechanisms controlling the organic chemistry of Bear Brook New Hampshire.
- McGlynn BL, McDonnell JJ (2003) Role of discrete landscape units in controlling catchment dissolved organic carbon dynamics. *Water Resources Research* 39:n/a–n/a.
doi:10.1029/2002WR001525
- Melillo JM, Aber JD, Muratore JF (1982) Nitrogen and lignin control of hardwood leaf litter decomposition dynamics. *Ecology* 63:621–626. doi:10.2307/1936780

- Mitchell MJ, Likens GE (2011) Watershed Sulfur Biogeochemistry: Shift from Atmospheric Deposition Dominance to Climatic Regulation. *Environmental Science & Technology* 45:5267–5271. doi:10.1021/es200844n
- Mitchell MJ, Driscoll CT, Kahl JS, Murdoch PS, Pardo LH (1996) Climatic Control of Nitrate Loss from Forested Watersheds in the Northeast United States. *Environmental Science & Technology* 30:2609–2612. doi:10.1021/es9600237
- Mitchell MJ, Piatek KB, Christopher S, Mayer B, Kendall C, Mchale P (2006) Solute sources in stream water during consecutive fall storms in a northern hardwood forest watershed: A combined hydrological, chemical and isotopic approach. *Biogeochemistry* 78:217–246. doi:10.1007/s10533-005-4277-1
- Mitchell MJ, Lovett G, Bailey S, Beall F, Burns D, Buso D, Clair TA, Courchesne F, Duchesne L, Eimers C, Fernandez I, Houle D, Jeffries DS, Likens GE, Moran MD, Rogers C, Schwede D, Shanley J, Weathers KC, et al. (2011) Comparisons of watershed sulfur budgets in southeast Canada and northeast US: new approaches and implications. *Biogeochemistry* 103:181–207. doi:10.1007/s10533-010-9455-0
- Monteith DT, Stoddard JL, Evans CD, Wit HA de, Forsius M, Høgåsen T, Wilander A, Skjelkvåle BL, Jeffries DS, Vuorenmaa J, Keller B, Kopáček J, Vesely J (2007) Dissolved organic carbon trends resulting from changes in atmospheric deposition chemistry. *Nature* 450:537–540. doi:10.1038/nature06316
- Mørkved PT, Dörsch P, Henriksen TM, Bakken LR (2006) N₂O emissions and product ratios of nitrification and denitrification as affected by freezing and thawing. *Soil Biology and Biochemistry* 38:3411–3420. doi:10.1016/j.soilbio.2006.05.015
- Munter JA (1986) Evidence of groundwater recharge through frozen soils at Anchorage, Alaska. In: Kane DL (ed) *Proceedings of the Symposium: Cold Regions Hydrology*. American Water Resources Association, Fairbanks, AK, pp 245–252
- NADP (2013) National Atmospheric Deposition Program/National Trends Network, University of Illinois
- Nyberg L, Stähli M, Mellander P-E, Bishop KH (2001) Soil frost effects on soil water and runoff dynamics along a boreal forest transect: 1. Field investigations. *Hydrological Processes* 15:909–926. doi:10.1002/hyp.256
- O'Brien AK, Rice KC, Kennedy MM, Bricker OP (1993) Comparison of episodic acidification of Mid-Atlantic Upland and Coastal Plain streams. *Water Resources Research* 29:3029–3039. doi:10.1029/93WR01408
- Oden S (1968) The acidification of air precipitation and its consequences in the natural environment. *Bulletin of Ecological Research Communications NFR*. Translation Consultants Ltd., Arlington, VA

- Ohte N, Sebestyén SD, Shanley JB, Doctor DH, Kendall C, Wankel SD, Boyer EW (2004) Tracing sources of nitrate in snowmelt runoff using a high-resolution isotopic technique. *Geophysical Research Letters* 31:n/a–n/a. doi:10.1029/2004GL020908
- Palmer SM, Driscoll CT, Johnson CE (2004) Long-term trends in soil solution and stream water chemistry at the Hubbard Brook Experimental Forest: relationship with landscape position. *Biogeochemistry* 68:51–70. doi:10.1023/B:BIOG.0000025741.88474.0d
- Pellerin BA, Saraceno JF, Shanley JB, Sebestyén SD, Aiken GR, Wollheim WM, Bergamaschi BA (2012) Taking the pulse of snowmelt: in situ sensors reveal seasonal, event and diurnal patterns of nitrate and dissolved organic matter variability in an upland forest stream. *Biogeochemistry* 108:183–198. doi:10.1007/s10533-011-9589-8
- Piatek KB, Mitchell MJ, Silva SR, Kendall C (2005) Sources of nitrate in snowmelt discharge: evidence from water chemistry and stable isotopes of nitrate. *Water, Air, and Soil Pollution* 165:13–35. doi:10.1007/s11270-005-4641-8
- Pierce RS, Lull HW, Storey HC (1958) Influence of land use and forest condition on soil freezing and snow depth. *Forest Science* 4:246–263
- Pihl Karlsson G, Akselsson C, Hellsten S, Karlsson PE (2011) Reduced European emissions of S and N – Effects on air concentrations, deposition and soil water chemistry in Swedish forests. *Environmental Pollution* 159:3571–3582. doi:10.1016/j.envpol.2011.08.007
- Potter FI, Lynch JA, Corbett ES (1988) Source areas contributing to the episodic acidification of a forested headwater stream. *Journal of Contaminant Hydrology* 3:293–305. doi:10.1016/0169-7722(88)90037-X
- Pourmogharian A, Driscoll CT, Campbell JL, Hayhoe K (2012) Modeling potential hydrochemical responses to climate change and increasing CO₂ at the Hubbard Brook Experimental Forest using a dynamic biogeochemical model (PnET-BGC). *Water Resources Research* 48. doi:10.1029/2011WR011228
- Reinhart KG, Pierce RS (1964) Stream-gaging stations for research on small watersheds. U.S. Dept. of Agriculture, Forest Service, Washington, D.C.
- Reinmann AB, Templer PH, Campbell JL (2012) Severe soil frost reduces losses of carbon and nitrogen from the forest floor during simulated snowmelt: A laboratory experiment. *Soil Biology and Biochemistry* 44:65–74. doi:10.1016/j.soilbio.2011.08.018
- Sarkkola S, Koivusalo H, Laurén A, Kortelainen P, Mattsson T, Palviainen M, Piirainen S, Starr M, Finér L (2009) Trends in hydrometeorological conditions and stream water organic carbon in boreal forested catchments. *Science of The Total Environment* 408:92–101. doi:10.1016/j.scitotenv.2009.09.008
- Sartz RS (1957) Influence of land use on time of soil freezing and thawing in the Northeast. *Journal of Forestry* 55:716–718

- Schaefer DA, Driscoll CT, Van Dreason R, Yatsko CP (1990) The episodic acidification of Adirondack Lakes during snowmelt. *Water Resources Research* 26:1639–1647. doi:10.1029/WR026i007p01639
- Schwarz PA, Fahey TJ, McCulloch CE (2003) Factors controlling spatial variation of tree species abundance in a forested landscape. *Ecology* 84:1862–1878. doi:10.1890/0012-9658(2003)084[1862:FCSVOT]2.0.CO;2
- Sebestyen SD, Boyer EW, Shanley JB, Kendall C, Doctor DH, Aiken GR, Ohte N (2008) Sources, transformations, and hydrological processes that control stream nitrate and dissolved organic matter concentrations during snowmelt in an upland forest. *Water Resources Research* 44. doi:10.1029/2008WR006983
- Shanley JB, Chalmers A (1999) The effect of frozen soil on snowmelt runoff at Sleepers River, Vermont. *Hydrological Processes* 13:1843–1857. doi:10.1002/(SICI)1099-1085(199909)13:12/13<1843::AID-HYP879>3.0.CO;2-G
- Shanley JB, Kendall C, Smith TE, Wolock DM, McDonnell JJ (2002) Controls on old and new water contributions to stream flow at some nested catchments in Vermont, USA. *Hydrological Processes* 16:589–609. doi:10.1002/hyp.312
- Skjelkvåle BL, Stoddard JL, Jeffries DS, Tørseth K, Høgåsen T, Bowman J, Mannio J, Monteith DT, Mosello R, Rogora M, Rzychon D, Vesely J, Wieting J, Wilander A, Worsztynowicz A (2005) Regional scale evidence for improvements in surface water chemistry 1990–2001. *Environmental Pollution* 137:165–176. doi:10.1016/j.envpol.2004.12.023
- Skyllberg U (1999) pH and solubility of aluminium in acidic forest soils: a consequence of reactions between organic acidity and aluminium alkalinity. *European Journal of Soil Science* 50:95–106. doi:10.1046/j.1365-2389.1999.00205.x
- Sobczak WV, Findlay S, Dye S (2003) Relationships between DOC bioavailability and nitrate removal in an upland stream: An experimental approach. *Biogeochemistry* 62:309–327. doi:10.1023/A:1021192631423
- Stadler D, Wunderli H, Auckenthaler A, Flüeler H, Bründl M (1996) Measurement of frost-induced snowmelt runoff in a forest soil. *Hydrological Processes* 10:1293–1304. doi:10.1002/(SICI)1099-1085(199610)10:10<1293::AID-HYP461>3.0.CO;2-I
- Stähli M, Jansson P-E, Lundin L-C (1996) Preferential Water Flow in a Frozen Soil — a Two-Domain Model Approach. *Hydrological Processes* 10:1305–1316. doi:10.1002/(SICI)1099-1085(199610)10:10<1305::AID-HYP462>3.0.CO;2-F
- Stoddard JL, Jeffries DS, Lükewille A, Clair TA, Dillon PJ, Driscoll CT, Forsius M, Johannessen M, Kahl JS, Kellogg JH, Kemp A, Mannio J, Monteith DT, Murdoch PS, Patrick S, Rebsdorf A, Skjelkvåle BL, Stainton MP, Traaen T, et al. (1999) Regional trends in aquatic recovery from acidification in North America and Europe. *Nature* 401:575–578. doi:10.1038/44114

- Sullivan TJ, Eilers JM, Cosby BJ, Vaché KB (1997) Increasing role of nitrogen in the acidification of surface waters in the Adirondack Mountains, New York. *Water, Air, and Soil Pollution* 95:313–336. doi:10.1007/BF02406172
- Tebaldi C, Hayhoe K, Arblaster JM, Meehl GA (2006) Going to the Extremes. *Climatic Change* 79:185–211. doi:10.1007/s10584-006-9051-4
- Thunholm B, Lundin L-C, Lindell S (1989) Infiltration into a frozen heavy clay soil. *Nordic Hydrology* 20:153–166. doi:10.2166/nh.1989.012
- Tierney GL, Fahey TJ, Groffman PM, Hardy JP, Fitzhugh RD, Driscoll CT (2001) Soil freezing alters fine root dynamics in a northern hardwood forest. *Biogeochemistry* 56:175–190. doi:10.1023/A:1013072519889
- Tipping E, Hurley MA (1988) A model of solid-solution interactions in acid organic soils, based on the complexation properties of humic substances. *Journal of Soil Science* 39:505–519. doi:10.1111/j.1365-2389.1988.tb01235.x
- Trimble GR, Sartz RS, Pierce RS (1958) How type of soil frost affects infiltration. *Journal of Soil and Water Conservation* 13:81–82
- USDA NRCS (2009) Soil Quality: Managing Cool, Wet Soils. *Soil Quality - Agronomy Technical Note 20*
- Vitousek PM, Reiners WA (1975) Ecosystem Succession and Nutrient Retention: A Hypothesis. *BioScience* 25:376–381. doi:10.2307/1297148
- Warby RAF, Johnson CE, Driscoll CT (2005) Chemical recovery of surface waters across the northeastern United States from reduced inputs of acidic deposition: 1984–2001. *Environmental Science & Technology* 39:6548–6554. doi:10.1021/es048553n
- Watmough SA, Eimers MC, Aherne J, Dillon PJ (2004) Climate effects on stream nitrate concentrations at 16 forested catchments in South Central Ontario. *Environmental Science & Technology* 38:2383–2388. doi:10.1021/es035126l
- Wellington BI, Driscoll CT (2004) The episodic acidification of a stream with elevated concentrations of dissolved organic carbon. *Hydrological Processes* 18:2663–2680
- Wigington P, Davis T, Tranter M, Eshleman K (1990) Episodic acidification of surface waters due to acidic deposition, NAPAP Report 12.
- Wigington PJ, DeWalle DR, Murdoch PS, Kretser WA, Simonin HA, Sickie JV, Baker JP (1996) Episodic acidification of small streams in the Northeastern United States: ionic controls of episodes. *Ecological Applications* 6:389–407. doi:10.2307/2269378
- Worrall F, Burt TP (2007) Trends in DOC concentration in Great Britain. *Journal of Hydrology* 346:81–92. doi:10.1016/j.jhydrol.2007.08.021

- Worrall F, Harriman R, Evans CD, Watts CD, Adamson J, Neal C, Tipping E, Burt T, Grieve I, Monteith D, Naden PS, Nisbet T, Reynolds B, Stevens P (2004) Trends in Dissolved Organic Carbon in UK Rivers and Lakes. *Biogeochemistry* 70:369–402. doi:10.1007/s10533-004-8131-7
- Wu Y, Clarke N, Mulder J (2010) Dissolved organic carbon concentrations in throughfall and soil waters at level II monitoring plots in Norway: short- and long-term variations. *Water, Air, and Soil Pollution* 205:273–288. doi:10.1007/s11270-009-0073-1
- Yallop AR, Clutterbuck B (2009) Land management as a factor controlling dissolved organic carbon release from upland peat soils 1: Spatial variation in DOC productivity. *Science of the Total Environment* 407:3803–3813. doi:10.1016/j.scitotenv.2009.03.012
- Yanai RD, Vadeboncoeur MA, Hamburg SP, Arthur MA, Fuss CB, Groffman PM, Siccama TG, Driscoll CT (2013) From Missing Source to Missing Sink: Long-Term Changes in the Nitrogen Budget of a Northern Hardwood Forest. *Environmental Science & Technology* 47:11440–11448. doi:10.1021/es4025723
- Zhao L, Gray DM (1999) Estimating snowmelt infiltration into frozen soils. *Hydrological Processes* 13:1827–1842. doi:10.1002/(SICI)1099-1085(199909)13:12/13<1827::AID-HYP896>3.0.CO;2-D

10. Vita

NAME OF AUTHOR: Colin B. Fuss

PLACE OF BIRTH: Omaha, NE

DATE OF BIRTH: 2 June 1981

EDUCATION: Bachelor of Arts in Biology, 2004
Cornell University, Ithaca, NY

Master of Science in Environmental Engineering Science, 2009
Syracuse University, Syracuse, NY